# INFLUENCE OF COARSE AGGREGATE ON THE SHEAR STRENGTH OF REINFORCED CONCRETE BEAMS

by

Hoosen Ahmed Jajbhay

A dissertation submitted in fulfilment of the academic requirements for the degree of

Master of Engineering

in the

Department of Civil Engineering and Geomatics

Faculty of Engineering and the Built Environment

at the Durban University of Technology

December 2020

**DECLARATION**

I, Hoosen Ahmed Jajbhay, hereby declare that this dissertation, except where indicated in the text, is my work and has not been submitted in part, or in whole, at any other University or University of Technology.

This research was conducted at the Durban University of Technology under the supervision of Professor Dhiren Allopi.

17 December 2020

---

Hoosen Ahmed Jajbhay Date

APPROVED FOR FINAL SUBMISSION

---

Prof. Dhiren Allopi: Supervisor

DTech (Civil Eng) (MLST); MDT (Civil Eng) (TN);

Postgrad Dip Eng (Natal); Dip Datametrics (cum laude) (UNISA);

PrTech Eng; FMSAICE; MIPET; MSAT; MCILT

## ABSTRACT

Research to accurately predict the shear capacity of reinforced concrete beams without shear reinforcement has been ongoing since the early 20th century. Aggregate interlock of the coarse aggregates at the shear crack interface is one of the internal mechanisms of shear transfer and a major contributor to the shear capacity of slender beams. It is plausible, therefore, to investigate if the coarse aggregate itself influences the shear capacity of a concrete beam. The influence of the type of coarse aggregate on the shear capacity of beams without shear reinforcement was investigated in this study.

From the literature study an understanding of the properties of coarse aggregates was gained, the internal mechanisms of shear transfer in reinforced concrete beams without shear reinforcement were determined, and the parameters influencing shear strength were identified. Based on this information an experimental program was designed.

Eighteen reinforced concrete beams without shear reinforcement were cast. The beams were cast from three different types of coarse aggregates commonly used in the Durban area, i.e., dolerite, quartzite and tillite. For each type of coarse aggregate two variations were tested, i.e., 13 mm and 19 mm maximum aggregate sizes. For each size of coarse aggregate, three concrete strengths were tested. The beams were loaded in a beam press, by applying an increasing point load offset from midspan to induce cracking on the shorter side, until shear failure of the beam occurred.

For the three concrete strengths, beams cast from dolerite had the highest shear capacity while beams cast from tillite had less shear capacity than beams cast from quartzite coarse aggregate. Furthermore, beams cast from 13 mm maximum size coarse aggregate had higher shear capacity than beams cast from 19 mm aggregate. The conclusion may be drawn that the type and size of coarse aggregate does influence the shear strength of a reinforced concrete beam without shear reinforcement.

## ACKNOWLEDGEMENTS

In the name of God, the most Gracious, the most Merciful.

I express my profound gratitude and thanks to my mother Hawa Bibi Chupty, my wife and companion Zulaikha, and our children Fathimah, Abdullah, Ibraheem, Umm-Kulsoom, Zaynub and Ruqayyah for their love, encouragement and enduring patience while I completed this dissertation.

I am most grateful to my supervisor, Professor Dhiren Allopi, for securing me a research grant, and for his comments, patience, encouragement and technical and editorial guidance. Thank you.

I acknowledge with thanks the generous grant bestowed on me by the National Department of Transport to complete this research.

Concrete beams for the experimental program in this dissertation were cast and cured at Geosure laboratories. I am deeply grateful to Bradley Harriram and Braydon Govender – without their kind assistance, facilitation and patience I would not have been able to cast the beams. Load testing of the beams was done at the heavy structures laboratory of the University of KwaZulu-Natal with the kind permission of Christina Mcleod and assistance from Ishaan Ramlakan. I thank you all.

I am thankful to Goolam Hoosen the Head of Department of Civil Engineering & Geomatics for his persistence in ensuring I complete my dissertation, and to my past teachers and lecturers from whom I have learned much.

Thanks also to Professor David Root, from the University of Witwatersrand, who lectured me in research methodology and gave me my first insights into academic research.

# TABLE OF CONTENTS

**Declaration ii**

**Abstract iii**

**Acknowledgements ..... iv**

**Table of Contents ..... v**

**List of Tables ..... x**

**List of Figures ..... xii**

**List of Symbols ..... xviii**

**List of Abbreviations ..... xix**

**CHAPTER 1: INTRODUCTION ..... 1**

1.1 Background and Context to the Study ..... 1

1.1.1 Reinforced Concrete Beam Without Transverse Shear Reinforcement ..... 1

1.1.2 Shear Strength of a Reinforced Concrete Beam ..... 2

1.1.3 Aggregate Interlock as a Contributory Mechanism of Shear Strength ..... 3

1.2 What is Aggregate Interlock? ..... 4

1.3 Significance of Aggregate Interlock at the Crack Interface ..... 6

1.4 The Rationale for the Study ..... 6

1.5 Statement of the Problem ..... 6

1.6 Research Problem and Aims ..... 7

1.7 Scope of the Study ..... 7

1.8 Methodology ..... 8

1.9 Overview of Chapters ..... 8

1.10 Conclusion ..... 9

**CHAPTER 2: LITERATURE REVIEW ..... 10**

2.1 Purpose of the Literature Review ..... 10

2.2 Brief Description of Concrete ..... 10

2.2.1 Classification of Concrete Aggregates ..... 11

2.2.2 Strength Characteristics of Concrete ..... 11

2.2.3 Tensile Cracking of Concrete Beams ..... 12

2.2.4 Shear Transfer at the Crack Interface ..... 12

2.3 Concrete Aggregates ..... 13

2.3.1 Strength of Aggregates ..... 13

2.3.2 Sampling of Aggregates ..... 13

2.3.3 Geometrical Characteristics of Aggregate Particles ..... 13

2.3.4 Particle Shape ..... 14

2.3.5 Roundness ..... 15

2.3.6 Angularity Number ..... 15

2.3.7 Angularity Factor ..... 15

2.3.8 Sphericity ..... 15

2.3.9 Flakiness and Elongation ..... 15

2.3.10 Surface Texture of Aggregate ..... 16

2.3.11 Bond of Aggregate ..... 17

2.3.12 Strength of Aggregate ..... 17

2.3.13 Coarse Aggregates (Stone) Used in Durban ..... 17

2.3.14 Fine Aggregates (Sand) Used in Durban ..... 17

2.4 Shear Resistance Theories on Reinforced Concrete Beams Without Transverse Shear Reinforcement ..... 18

2.5 Influence of Coarse Aggregate Type on Aggregate Interlock ..... 32

2.6 Influence of Fine Aggregate on Aggregate Interlock ..... 34

2.7 Influence of Aggregate Size on Aggregate Interlock ..... 35

2.8 Influence of the Type of Concrete on Aggregate Interlock ..... 36

2.9 Influence of Beam Longitudinal Steel Reinforcement on Aggregate Interlock ..... 37
2.10 Size Effect on the Shear Capacity of Concrete ..... 38
2.11 Models (Theoretical Framework) of Aggregate Interlock ..... 40
2.12 Incorporation of Aggregate Properties into Codes of Practice Clauses on Shear Strength of Beams Without Shear Reinforcement ..... 41
2.12.1 South African Code SANS10100-1 (2000) ..... 41
2.12.2 American Code ACI 318-19 (2019) ..... 42
2.12.3 Eurocode EN 1992-1-1: (2004) (E) ..... 43
2.12.4 Canadian Code CSA A23.3 (2004) ..... 44
2.12.5 fib Model Code for Concrete Structures 2010 (2013) ..... 45
2.12.6 Swiss Codes SIA 262 (2003), SIA 262 (2013 - corrigenda 2017) ..... 46
2.13 Discussion and Conclusion ..... 47
**CHAPTER 3: EXPERIMENTAL PROGRAM ..... 48**
3.1 Introduction ..... 48
3.2 Methods of Experimentally Determining the Shear Strength of Reinforced Concrete Beams ..... 48
3.2.1 Push-off Test ..... 49
3.2.2 Shear Panel (Membrane Element) Test ..... 50
3.2.3 Beam Press Test ..... 51
3.3 Selection of an Experimental Test Method ..... 52
3.3.1 Suitability Assessment of a Beam Press Test for this Study ..... 54
3.3.2 Suitability Assessment of a Push-off Test for this Study ..... 54
3.3.3 Suitability Assessment of a Shear Panel (Membrane Element) Test for this Study ..... 55
3.3.4 Adoption of a Test Method for this Study ..... 55
3.4 The Shear Strength Parameters Varied in this Experimental Investigation (the Independent Variables) ..... 55

3.4.1 Concrete Strength ..... 55
3.4.2 Coarse Aggregate Size ..... 56
3.4.3 Coarse Aggregate Type ..... 56
3.5 The Shear Strength Parameter Measured in this Experimental Investigation (the Dependent Variable) ..... 56
3.6 The Shear Parameters Controlled in this Experimental Investigation (Variables Kept Constant) ..... 57
3.7 Description of the Experimental Program to Study the Influence of Coarse Aggregate Type and Size on the Shear Strength ..... 58
3.7.1 Trial Beam ..... 58
3.7.2 Concrete Moulds ..... 59
3.7.3 Concrete Cubes ..... 60
3.7.4 Reinforcing Steel ..... 61
3.7.5 Concrete Materials ..... 63
3.7.6 Mixing, Casting and Curing of the Concrete ..... 66
3.7.7 Dimensional Details of Concrete Beam Specimens ..... 72
3.7.8 Loading Arrangement ..... 73
3.7.9 Testing Equipment, Setup and Testing Procedure ..... 74
**CHAPTER 4: EXPERIMENTAL RESULTS ..... 78**
**CHAPTER 5: STATISTICAL ANALYSIS, INTERPRETATION AND DISCUSSION OF THE RESULTS ..... 80**
5.1 Introduction ..... 80
5.2 The Sample ..... 80
5.3 Data Analysis ..... 81
5.4 Normality Test Results ..... 81
5.5 28-Day Concrete Cube Strength (MPa) ..... 82
5.5.1 Coarse Aggregate Size (mm) = 13.2 mm ..... 83
5.5.2 Coarse Aggregate Size (mm) = 19.0 mm ..... 85

5.5.3 Coarse Aggregate Type – Tillite ..... 87
5.5.4 Coarse Aggregate Type – Quartzite ..... 88
5.5.5 Coarse Aggregate Type – Dolerite ..... 88
5.5.6 Summary ..... 89
5.6 Shear Force $V_L$ at Failure and at Scaled Shear Force (kN) ..... 89
5.6.1 Descriptive Statistics ..... 91
5.6.2 Coarse Aggregate Size (mm) = 13.2 mm ..... 93
5.6.3 Coarse Aggregate Size (mm) = 19.0 mm ..... 96
5.6.4 Coarse Aggregate Type – Tillite ..... 99
5.6.5 Coarse Aggregate Type – Q uartzite ..... 100
5.6.6 Coarse Aggregate Type – Dolerite ..... 101
5.6.7 Mean ±1 Standard Deviation (SD) Shear Force ..... 102
5.7 Regression Analysis Based on Shear Force at Failure ..... 103
5.8 Analysis of Shear Failure Loads Based on Aggregate Size and Aggregate Type ..... 108
5.8.1 All Aggregates ..... 108
5.8.2 Coarse Aggregate Size (mm) = 13.2 mm ..... 110
5.8.3 Coarse Aggregate Size (mm) = 19.0 mm ..... 111
5.8.4 Coarse Aggregate Type – Tillite ..... 113
5.8.5 Coarse Aggregate Type – Quartzite ..... 114
5.8.6 Coarse Aggregate Type – Dolerite ..... 116
5.9 Interpretation and Discussion of Results ..... 117
5.10 Conclusions from Statistical Analysis ..... 118
**CHAPTER 6: CONCLUSION, RECOMMENDATIONS AND FUTURE RESEARCH ..... 119**
**CHAPTER 7: REFERENCES ..... 120**

# LIST OF TABLES

Table 2-1: Particle shape classification (BS 812: Part 1: 1975) with examples ..... 14

Table 2-2: Surface texture of aggregates (BS 812: Part 1: 1975) with examples .. 16

Table 3-1: Types of shear tests conducted in some of the experimental programs referenced in the literature review ..... 52

Table 4-1: Tabulated results of point load P at failure and shear force VL at failure ..... 79

Table 5-1: One-sample Kolmogorov-Smirnov test ..... 81

Table 5-2: 28-day concrete cube strengths – descriptive statistics for the different aggregates ..... 82

Table 5-3: 28-day concrete cube strength – ANOVA test results for 13.2 mm aggregate ..... 83

Table 5-4: 28-day cube strength – multiple comparisons for 13.2 mm coarse aggregate ..... 84

Table 5-5: 28-day concrete cube strength – ANOVA test results for 19 mm aggregate ..... 85

Table 5-6: 28-day cube strength – multiple comparisons for 19 mm coarse aggregate ..... 86

Table 5-7: Shear force VL at failure - descriptive statistics for the different aggregates ..... 91

Table 5-8: Shear force VL scaled for targeted cube strengths - descriptive statistics for the different aggregates ..... 92

Table 5-9: Shear force VL at failure – ANOVA test results for 13.2 mm aggregate ..... 93

Table 5-10: Shear force VL scaled for targeted cube strengths – ANOVA test results for 13.2 mm aggregate ..... 93

Table 5-11: Shear force VL at failure – multiple comparisons for 13.2 mm coarse aggregate ..... 94

Table 5-12: Shear force VL scaled for targeted cube strengths – multiple comparisons for 13.2 mm coarse aggregate ..... 94

Table 5-13: Shear force VL at failure – ANOVA test results for 19 mm aggregate ..... 96

Table 5-14: Shear force VL scaled for targeted cube strengths – ANOVA test results for 19 mm aggregate ..... 96

Table 5-15: Shear force VL at failure – multiple comparisons for 19 mm coarse aggregate ..... 97

Table 5-16: Shear force VL scaled for targeted cube strengths – multiple comparisons for 19 mm coarse aggregate ..... 97

Table 5-17: Regression analysis – models and variables ..... 103

Table 5-18: Regression analysis – model summary ..... 103

Table 5-19: Regression analysis – ANOVA tests of models ..... 104

Table 5-20: Regression analysis - coefficients ..... 105

Table 5-21: Regression analysis – excluded variables ..... 105

Table 5-22: Shear failure loads and scaled shear failure loads for all beams ..... 108

Table 5-23: Shear failure loads and scaled shear failure loads for beams constructed with 13.2 mm coarse aggregates ..... 110

Table 5-24: Shear failure loads and scaled shear failure loads for beams constructed with 19 mm coarse aggregates ..... 111

Table 5-25: Shear failure loads and scaled shear failure loads for beams constructed with tillite coarse aggregate ..... 113

Table 5-26: Shear failure loads and scaled shear failure loads for beams constructed with quartzite coarse aggregate ..... 114

Table 5-27: Shear failure loads and scaled shear failure loads for beams constructed with dolerite coarse aggregate ..... 116

# LIST OF FIGURES

Figure 1-1: Reinforced concrete beam with longitudinal steel to resist flexure and shear but without transverse shear reinforcement ..... 1

Figure 1-2: Reinforced concrete beam with longitudinal steel to resist flexure and shear AND added transverse shear reinforcement (stirrups) to resist shear ..... 2

Figure 1-3: Transmission of shear stresses across a crack by aggregate interlock ..... 5

Figure 1-4: Graphical presentation of research design ..... 9

Figure 2-1: Proportions of materials used in concrete by volume ..... 11

Figure 2-2: Walters model ..... 19

Figure 2-3: Reinick's model ..... 20

Figure 2-4: Kani's model. The formation of the comb-like structure due to vertical flexural cracks ..... 21

Figure 2-5: Kani's model. Tied arch action after failure of the concrete cantilevers ..... 22

Figure 2-6: Significance of the a/d ratio illustrated for a sample of beams known as the Toronto Series C ..... 22

Figure 2-7: Fenwick's model of shear resistance due to beam action in a cracked beam. $H_t$ & $V_t$ are the aggregate interlock components ..... 23

Figure 2-8: Sketch showing crack pattern on a beam according to Taylor's beam action model. The diagonal failure crack develops from a previous flexural crack. Also illustrated is the dowel splitting crack ..... 24

Figure 2-9: Shear transfer through compression zone shear, aggregate interlock and dowel action ..... 24

Figure 2-10: Equations of the modified compression field theory ..... 26

Figure 2-11: Formation of a critical shear crack A & B. Lamination occurs at C ..... 28

Figure 2-12: Shear components. $V_{cc}$ = shear in compression concrete, $V_{csc}$ = shear in critical shear crack, $V_{DA}$ = dowel action ..... 28

Figure 2-13: Critical shear crack theory – formation of struts and ties in the concrete after flexural cracking occurs. The top chord (shaded light grey) is concrete, the diagonals (shaded light and dark are concrete and the bottom tie is the flexural steel reinforcement ..... 28

Figure 2-14: Critical shear crack theory – solid dark lines are ties and shaded dotted lines are struts ..... 29

Figure 2-15: Critical shear crack theory – cracking of the tension tie B leads to the diagonal crack at B, and, dowel failure leads to the horizontal crack C at the reinforcement level ..... 29

Figure 2-16: The three mechanisms of shear resistance according to critical shear crack theory – (a) cantilever action, (b) interlocking action and (c) doweling action ..... 29

Figure 3-1: Sketches of various push-off test arrangements as depicted by Walraven ..... 49

Figure 3-2: A type of push-off test conducted by Sagaseta & Vollum ..... 50

Figure 3-3: A type of shear panel (membrane) test by Vecchio & Collins. A jack and link assembly is used to apply a shear force on the concrete panel (membrane element) (left). The picture on the right, with the man at the bottom left corner, gives an indication of the size of the shear panel (membrane element) testing rig ..... 51

Figure 3-4: DUT's beam press apparatus ..... 52

Figure 3-5: The point load P is the dependent variable. Also shown are the position of the point load P on the beam, the span of the beam and the support reactions (shear force) in terms of the dependant variable P ..... 57

Figure 3-6: Reusable beam moulds ready for use ..... 60

Figure 3-7: Beam moulds were designed for sturdiness when pouring concrete, easy disassembly and to maintain a constant reinforcement cover ..... 60

Figure 3-8: Y20 longitudinal steel reinforcing bars used for all beams ..... 62

Figure 3-9: Straight Y20 reinforcing steel bars passing through 22 mm diameter holes at the beam ends of the mould, maintain a constant effective depth and bar spacing for all beams ..... 62

Figure 3-10: Sample of the type of cement used ..... 63

Figure 3-11: Drying of fine aggregate (sand) in the midday sun on a concrete surface bed..... 64

Figure 3-12: 19 mm tillite..... 65

Figure 3-13: 13 mm tillite..... 65

Figure 3-14: 19 mm quartzite ..... 65

Figure 3-15: 13 mm quartzite ..... 65

Figure 3-16: 19 mm dolerite ..... 65

Figure 3-17: 13 mm dolerite ..... 65

Figure 3-18: Drying out of a sample of coarse aggregate in the midday sun on a concrete surface bed..... 66

Figure 3-19: All the concrete constituent materials were weighed in bags ..... 69

Figure 3-20: Cement, sand and aggregate ready for mixing..... 69

Figure 3-21: Mixing of the concrete in an electric drum mixer ..... 69

Figure 3-22: Slump tests being performed..... 69

Figure 3-23: Concrete transported from mixer to moulds in a wheelbarrow ..... 70

Figure 3-24: Placing of concrete into moulds..... 70

Figure 3-25: Vibration of concrete in moulds ..... 70

Figure 3-26: Preparation of cubes while concrete was placed in moulds ..... 70

Figure 3-27: Drum washed out before next batch of concrete is mixed..... 71

Figure 3-28: Elevation – dimensions of the reinforced concrete beams ..... 73

Figure 3-29: Section showing dimensions of concrete beams..... 73

Figure 3-30: Showing position of point load P applied to the beam and the reactions (shear force) in terms of P ..... 74

Figure 3-31: The hydraulic press at the University of KwaZulu-Natal (UKZN) heavy structures laboratory..... 75

Figure 3-32: Conversion of the UKZN hydraulic press to a beam press for this study ..... 76

Figure 3-33: Conversion of the hydraulic press to a beam press ..... 77

Figure 4-1: The point load P and maximum shear force VL at failure ..... 78

Figure 4-2 - Shear Force Diagram Showing the Maximum Shear Force in the Beam ..... 78

Figure 5-1: 28-day concrete cube strength – 13.2 mm coarse aggregate comparison for the three aggregate types ..... 85

Figure 5-2: 28-day concrete cube strength – 19 mm coarse aggregate comparison for the three aggregate types ..... 87

Figure 5-3: 28-day concrete cube strength – tillite coarse aggregate comparison for the two aggregate sizes ..... 87

Figure 5-4: 28-day concrete cube strength – quartzite coarse aggregate comparison for the two aggregate sizes ..... 88

Figure 5-5: 28-day concrete cube strength – dolerite coarse aggregate comparison for the two aggregate sizes ..... 88

Figure 5-6: 28-day concrete cube strength – summary of coarse aggregate comparison for aggregate size and aggregate type ..... 89

Figure 5-7: Shear force $V_L$ at failure – 13.2 mm coarse aggregate comparison for the three aggregate types ..... 95

Figure 5-8: Shear force $V_L$ scaled for targeted cube strengths – 13.2 mm coarse aggregate comparison for the three aggregate types ..... 95

Figure 5-9: Shear force $V_L$ at failure – 19 mm coarse aggregate comparison for the three aggregate types ..... 98

Figure 5-10: Shear force $V_L$ scaled for targeted cube strengths – 19 mm coarse aggregate comparison for the three aggregate types ..... 98

Figure 5-11: Shear force $V_L$ at failure – tillite coarse aggregate comparison for the two aggregate sizes ..... 99

Figure 5-12: Shear force $V_L$ scaled for targeted cube strengths – tillite coarse aggregate comparison for the two aggregate sizes ..... 99

Figure 5-13: Shear force $V_L$ at failure – quartzite coarse aggregate comparison for the two aggregate sizes ..... 100

Figure 5-14: Shear force $V_L$ scaled for targeted cube strengths – quartzite coarse aggregate comparison for the two aggregate sizes..... 100

Figure 5-15: Shear force $V_L$ at failure – dolerite coarse aggregate comparison for the two aggregate sizes ..... 101

Figure 5-16: Shear force $V_L$ scaled for targeted cube strengths – dolerite coarse aggregate comparison for the two aggregate sizes..... 101

Figure 5-17: Shear force $V_L$ at failure – mean shear force ± the standard deviation for aggregate size and aggregate type ..... 102

Figure 5-18: Shear force $V_L$ scaled for targeted cube strengths – mean shear force ± the standard deviation for aggregate size and aggregate type..... 102

Figure 5-19: Shear failure load $V_L$ vs concrete cube strength $f_{cu}$ for all beams.... 109

Figure 5-20: Scaled shear failure load $V_{L\text{-scaled}}$ vs scaled concrete cube strength $f_{cu}$ for all beams ..... 109

Figure 5-21: Shear failure load $V_L$ vs concrete cube strength $f_{cu}$ for 13.2 mm coarse aggregate beams..... 110

Figure 5-22: Scaled shear failure load $V_{L\text{-scaled}}$ vs scaled concrete cube strength $f_{cu}$ for 13.2 mm coarse aggregate beams ..... 111

Figure 5-23: Shear failure load $V_L$ vs concrete cube strength $f_{cu}$ for 19 mm coarse aggregate beams..... 112

Figure 5-24: Scaled shear failure load $V_{L\text{-scaled}}$ vs scaled concrete cube strength $f_{cu}$ for 19 mm coarse aggregate beams ..... 112

Figure 5-25: Shear failure load $V_L$ vs concrete cube strength $f_{cu}$ for tillite coarse aggregate beams ..... 113

Figure 5-26: Scaled shear failure load $V_{L\text{-scaled}}$ vs scaled concrete cube strength $f_{cu}$ for tillite coarse aggregate beams..... 114

Figure 5-27: Shear failure load $V_L$ vs concrete cube strength $f_{cu}$ for quartzite coarse aggregate beams..... 115

Figure 5-28: Scaled shear failure load $V_{L\text{-scaled}}$ vs scaled concrete cube strength $f_{cu}$ for quartzite coarse aggregate beams ..... 115

Figure 5-29: Shear failure load $V_L$ vs concrete cube strength $f_{cu}$ for dolerite coarse aggregate beams ..... 116

Figure 5-30: Scaled shear failure load $V_{L\text{-}scaled}$ vs scaled concrete cube strength $f_{cu}$ for dolerite coarse aggregate beams ..... 117

# LIST OF SYMBOLS

| | |
|---|---|
| $b$ | width of cross section |
| $b_w$ | width of web |
| $I$ | moment of inertia |
| $Q$ | first moment of an area about centroidal axis |
| $V$ | shear force |
| $v$ | shear stress |
| $v_c$ | predicted shear stress capacity of a beam |
| $z$ | the flexural leverarm of the cross section |
| $\tau$ | shear stress |

# LIST OF ABBREVIATIONS

| | |
|---|---|
| AASHTO | American Association of State Highway and Transportation Officials |
| ALWC | all lightweight concrete |
| CC | conventional concrete |
| CFT | compression field theory |
| CSCT | critical shear crack theory |
| FC | foam concrete |
| HSSCC | high strength self-compacting concrete |
| HVFAC | high volume fly ash concrete |
| ITZ | interfacial transition zone |
| LRFD | load resistance factor design |
| LWAFC | lightweight aggregate foam concrete |
| LWC | lightweight concrete |
| LWSCC | lightweight self-compacting concrete |
| MCFT | modified compression field theory |
| NSSCC | normal strength self-compacting concrete |
| NWC | normal weight concrete |
| RAC | recycled aggregate concrete |
| RC | reinforced concrete |
| RCA | recycled concrete aggregate |
| SCC | self-compacting concrete |
| SLWC | sand lightweight concrete |
| SMCFT | simplified modified compression filed theory |

# CHAPTER 1:INTRODUCTION

This dissertation is primarily concerned with investigating the influence of coarse aggregate on the shear strength of a reinforced concrete beam without shear reinforcement.

## 1.1 Background and Context to the Study

### 1.1.1 Reinforced Concrete Beam Without Transverse Shear Reinforcement

A reinforced concrete beam without transverse shear reinforcement refers to a reinforced concrete beam that has longitudinal steel to resist flexure and shear but does not have any stirrups (transverse shear reinforcement) to resist shear. An example of such a beam is shown in Figure 1-1 below.

Common structural elements designed as reinforced concrete beams without transverse shear reinforcement are suspended floor slabs, retaining walls, foundation bases, etc.

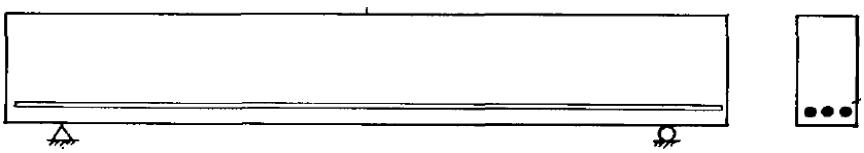

**Figure 1-1: Reinforced concrete beam with longitudinal steel to resist flexure and shear but without transverse shear reinforcement**
Source: Adapted from Mphonde **(1988, p. 399)**

A reinforced concrete beam with transverse shear reinforcement is a reinforced concrete beam that has longitudinal steel to resist flexure and shear and also transverse reinforcing steel (stirrup shear reinforcement) to increase the shear resistance of the beam. An example of such a beam is shown in Figure 1-2 below.

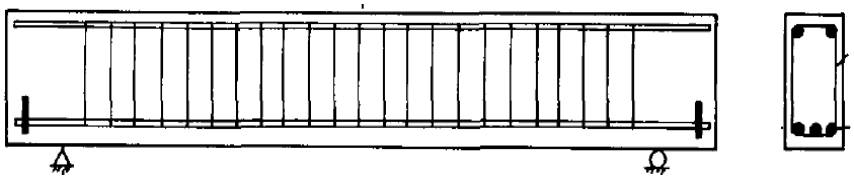

**Figure 1-2: Reinforced concrete beam with longitudinal steel to resist flexure and shear AND added transverse shear reinforcement (stirrups) to resist shear**
Source: Adapted from Mphonde **(1988, p. 399)**

### 1.1.2 Shear Strength of a Reinforced Concrete Beam

Reinforced concrete beams are designed to resist flexural and shear stresses. While there is good correlation between experimental tests and the theoretical predictions for the flexural strength of reinforced concrete beams, the same cannot be said for predicting the shear strength. Reinforced concrete design codes used by engineers to check the adequacy of a beam in shear employ empirical equations for shear strength that are safe and conservative lower bound formulations but do not accurately predict the shear strength of the beam. Accurately predicting the shear strength of a reinforced concrete beam is still open to discussion and is a much-researched topic to this day. Presvyri, et al. (2019, p. 937) corroborate this in their introductory observation:

> The shear capacity of reinforced concrete (RC) members without transverse shear reinforcement remains a challenging research topic over years. In recent years, several new theoretical models … and experimental observations … have been made, which improved our understandings on the shear failure mechanism. These progresses have shown that the aggregate interlock actions across the cracks turns out to be a critical mechanism in the failure process.

Bentz, Vecchio & Collins (2006, p. 614) remarked:

> Even though the behaviour of reinforced concrete in shear has been studied for more than 100 years, the problem of determining the shear strength of reinforced concrete beams remains open to discussion. Thus the shear strength predicted by different current design codes [in different countries] for a particular beam section can vary by factors more than 2 … In shear, there is no agreed basis for a rational theory, and experiments cannot be conducted on reinforced concrete beams subjected to pure shear … .

The reason for the lack of agreement in a rational theory is because the shear failure mechanism of a reinforced concrete beam is a “complex problem involving many variables” (Joint ASCE-ACI Committee 445 on shear and torsion, 1998 reapproved 2009, p. 1376). Collins, Bentz, Sherwood and Xie (2007, p. 75) cite the keynote address by Professor Fritz Leonhardt on “Shear and Torsion” at the 1970 FIP Congress “that one of the prime reasons for the poor quality of design provisions was that shear and torsional strengths were influenced by about 20 variables”.

Designing a reinforced concrete beam to have adequate shear strength is an important design consideration. The shear failure of a reinforced concrete beam is a brittle failure. Unlike a ductile failure which undergoes very large deflections before collapse, thus giving some warning of an impending collapse, a brittle failure usually occurs suddenly, without warning, and results in catastrophic collapse and possible fatalities. It is not surprising then that understanding the variables and mechanisms of shear transfer in a reinforced concrete beam has been and continues to be a widely researched topic since the beginning of the twentieth century.

### 1.1.3 Aggregate Interlock as a Contributory Mechanism of Shear Strength

Amongst the variables found to significantly influence the shear strength of reinforced concrete beams is aggregate interlock. Presvyri et al. (2019, p. 937) observed:

> In recent years, several new theoretical models … and experimental observations … have been made, which improved our understandings on the shear failure mechanism. These progresses have shown that the aggregate interlock action across the cracks turns out to be a critical mechanism in the failure process.

Johannes Moe hypothesised in a discussion of the report on “Shear and diagonal tension" by the ACI-ASCE committee 326 “that the majority of shear is carried by aggregate interlock stresses for members without shear reinforcement” (Collins, Bentz, Sherwood & Xie (2007, p. 77)).

The Joint ASCE-ACI Committee 445 on Shear and Torsion (1998 reapproved 2009, p. 27) describe interface shear transfer (aggregate interlock) as a widely accepted and important shear transfer mechanism.

Earlier investigations and experimental work by Kani (1964), Fenwick (1966), Taylor (1974), Hamadi and Regan (1980), etc. and more recent experimental work and investigations by Ruiz, Muttoni and Sagaseta (2015, pp. 361-363), Sneed and Ramirez (2014, pp. 157-158) and Campana, Ruiz, Anastasi and Muttoni (2013, p. 7 & 11 Table 3) and numerous other researchers all confirm aggregate interlock as one of the actions significantly contributing to shear transfer in beams without shear reinforcement.

It can therefore be concluded that aggregate interlock at the crack interface of a cracked reinforced concrete beam is an important, if not a major, contributor to the shear strength of the beam.

## 1.2 What is Aggregate Interlock?

The tensile strength of concrete is approximately one tenth that of its compressive strength. The low tensile strength results in the development of tensile cracks in a reinforced concrete beam subjected to lateral loads. The cracks occur in regions where the tensile stresses due to bending or shear are greater than the tensile strength of the concrete. To increase the strength of a concrete beam, steel reinforcement is therefore built into the beam, to resist the tensile stresses in the beam when the beams cracks.

For normal strength concrete (NSC) the aggregate strength is much larger than the cement paste. Therefore the tensile crack described above occurs in the cement paste. Since the cement paste in the concrete develops the crack, the crack profile will pass around the coarse aggregate particles in the concrete and not go through the coarse aggregate particle, resulting in a rough irregular crack surface due to the coarse aggregate protrusions.

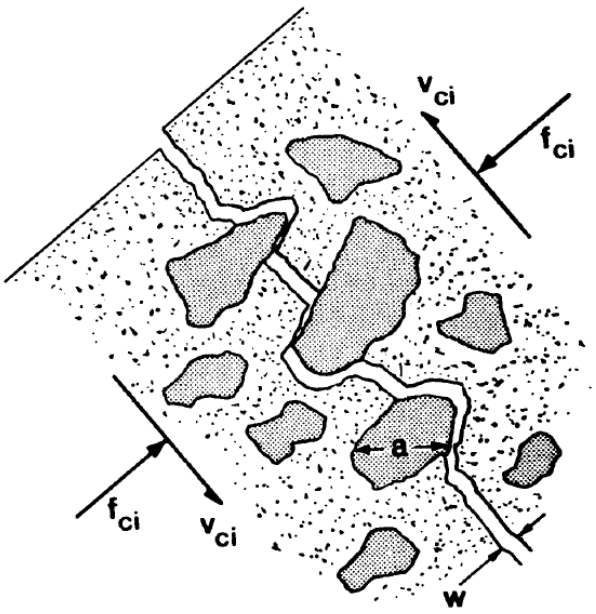


**Figure 1-3: Transmission of shear stresses across a crack by aggregate interlock**
Source: **(Vecchio & Collins, 1986, p. 226 Fig 13)**

The coarse aggregate particles remain embedded in one of the two crack surfaces. Any displacement of the crack surfaces parallel to the crack face brings coarse aggregate particles on the one face into contact with the concrete matrix on the other face. Further displacement of the surface will be resisted by the friction between the aggregate and the matrix. As the initial frictional resistance is overcome and the surfaces begin to slide, dilation of the crack occurs due to the aggregate protrusions at the crack. The dilation will in turn “stretch” the reinforcement, increasing the normal force on the frictional surface, thus increasing the frictional resistance. In this way shear forces can be transmitted between the crack faces. This transmission of shear forces at the crack interface through the frictional resistance between the coarse aggregate particles and the matrix is called aggregate interlock or shear friction (see Figure 1-3 above).

Walraven (1980) developed a theoretical model for aggregate interlock strength at the shear crack interface. The model is based on spherically shaped aggregate particles and a Fuller curve distribution of the coarse aggregate.

Walraven's model for aggregate interlock has been applied in shear strength theories such as the modified compression field theory, the simplified modified compression field theory, and the critical shear crack theory. Its application in these theories can be easily ascertained from the presence of the maximum aggregate size as a shear strength parameter. The compression field theories have found application in the Canadian "Design of Concrete Structures" code and the critical shear crack theory has been applied in the Swiss Design code.

### 1.3 Significance of Aggregate Interlock at the Crack Interface

Aggregate interlock at the crack interface of a cracked reinforced concrete beam is one of the most important mechanisms contributing to the shear strength of the beam.

### 1.4 The Rationale for the Study

The advent of sophisticated computer technology has led to the development of sophisticated computational methods, such as nonlinear finite element analysis, which can be used to design complex and slender structural elements which do not fall within the ambit of conventional design codes, criteria and techniques. However, a pre-requisite for the use of sophisticated computational methods is the development of realistic constitutive laws to predict the strength and deformation behaviour of concrete. One such law is related to the shear strength and deformation of reinforced concrete without shear reinforcement, which will include either the aggregate interlock mechanism or coarse aggregate as a parameter of shear strength, or both. This can be used to advantage in the design of elements where shear is an important factor.

### 1.5 Statement of the Problem

Since aggregate interlock is a function of the maximum aggregate size and is also a major contributory mechanism to the shear strength of reinforced concrete beams without shear reinforcement, it follows that the coarse aggregates in the concrete have an influence on the shear strength. Coarse aggregates differ in crushing strength, structure, geological origin, shape and surface texture. Therefore, in addition to maximum aggregate size, it is

plausible that variations in some of these coarse aggregate properties may also influence the shear strength.

Furthermore, most current shear strength models incorporate Walravens's aggregate interlock model which is based on spherically shaped aggregate particles and a Fuller Curve distribution of the aggregates. The concrete aggregates used in Durban are angular in shape, being derived from crushing of larger rock fragments. Concretes in Durban are manufactured using gap graded aggregates that will not have a Fuller Curve distribution. The three common aggregate types sourced from quarries in Durban are dolerite, natal group quartzite and tillite. These aggregates differ in crushing strength, geological origin and structure and vary in aggregate interlock strength (friction).

Therefore, a plausible question arises. Does the type of coarse aggregate influence the shear strength of reinforced concrete beams without lateral shear reinforcement?

## 1.6 Research Problem and Aims

The aims of this research were:

1. To ascertain, from the literature, the influence of coarse aggregates on the shear strength of reinforced concrete beams without shear reinforcement.
2. To experimentally investigate the influence of coarse aggregate type on the shear strength of reinforced concrete beams without shear reinforcement, for three aggregate types commonly used in Durban.

## 1.7 Scope of the Study

The scope of this research study was limited to the study of shear strength of reinforced concrete beams without transverse shear reinforcement. This study excluded the study of shear strength in reinforced concrete beams with shear reinforcement. Also excluded was shear strength in the context of road pavement design, construction joints in concrete slabs and slab on-grade (surface beds).

## 1.8 Methodology

The methodology employed in this study was as follows:

- A literature study comprising a brief description of concrete, the properties of coarse aggregates, theories on the shear strength of reinforced concrete beams without transverse shear reinforcement and parameters influencing the shear strength, all in the context of the influence of coarse aggregates on the shear strength.
- An experimental investigation of the variation in shear strength of reinforced concrete beams with respect to aggregate type, aggregate size and concrete strength for three types of coarse aggregate commercially used in Durban.
- A statistical analysis of the results obtained from the experimental investigation.

## 1.9 Overview of Chapters

This dissertation comprises six chapters.

| | |
|---|---|
| Chapter 1 | Introduces the research title, provides the background of the study, and highlights the problem statement, objectives and the scope of the study. |
| Chapter 2 | Reviews the literature on some properties of concrete, the properties of coarse aggregates in concrete and the mechanisms and parameters of shear transfer. |
| Chapter 3 | Discusses the experimental program in this study. |
| Chapter 4 | Presents the results of the experimental program. |
| Chapter 5 | Presents a statistical analysis & discussion of the experimental results. |
| Chapter 6 | Presents the conclusion and recommendations. |

Figure 1-4 is a graphical presentation of the research design.

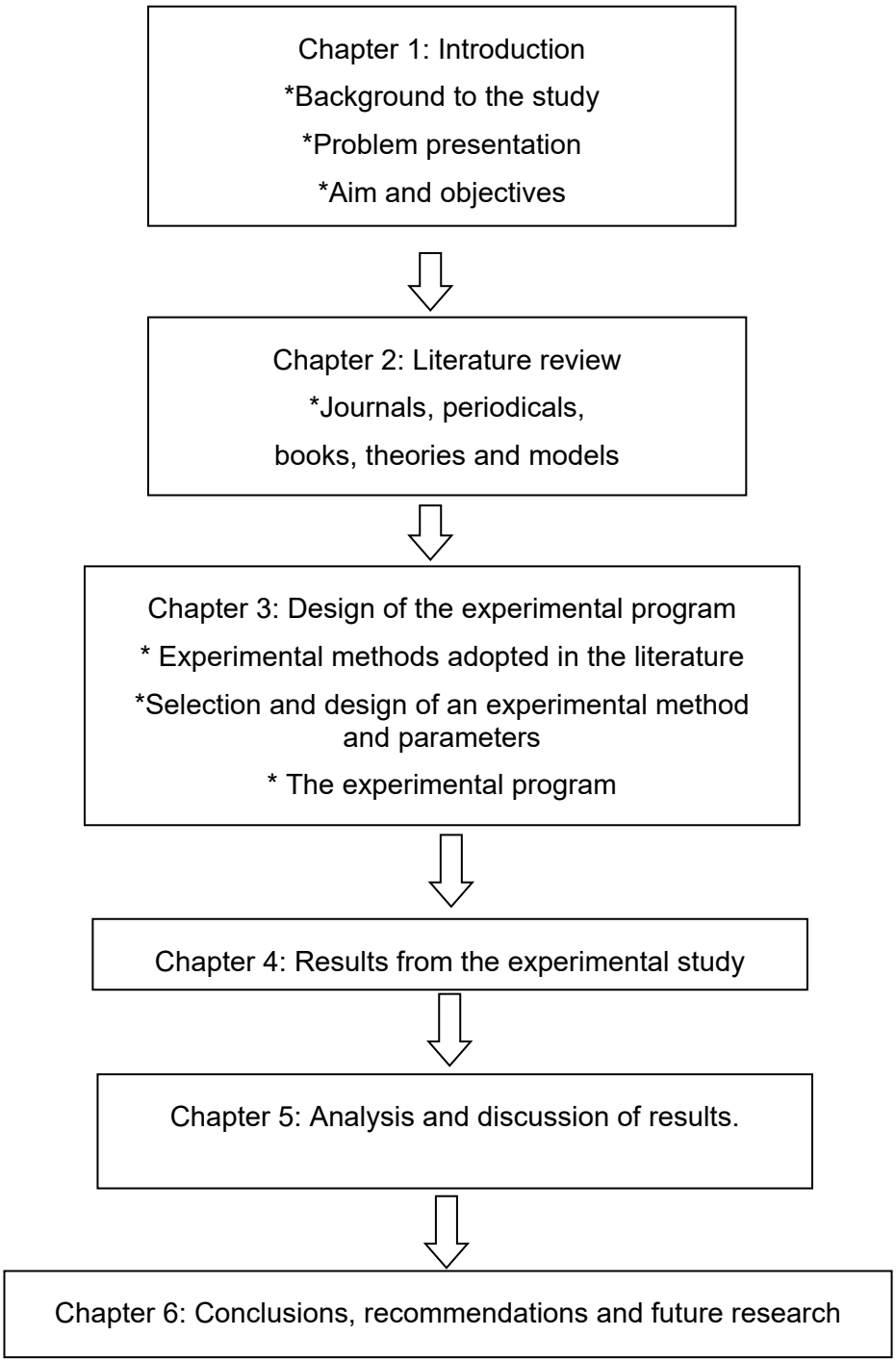


**Figure 1-4: Graphical presentation of research design**

## 1.10 Conclusion

This chapter introduced the relevance of the study, the research problem and aims of the study and presented an overview of the chapters that follow.

# CHAPTER 2:LITERATURE REVIEW

## 2.1 Purpose of the Literature Review

1) To understand the role of coarse aggregate in concrete.
2) To understand the physical properties of coarse aggregate used in concrete.
3) To evaluate aggregate interlock as a mechanism of shear resistance in reinforced concrete beams.
4) To identify and evaluate variables for the experimental program.

## 2.2 Brief Description of Concrete

Today concrete is second only to water as the most widely used engineering material of any type (Alexander & Mindess, 2005, p. preface). Hardened concrete has two components: aggregates and paste. The paste, comprised of portland cement, supplementary cementitious materials and water, binds the aggregates (usually sand and crushed stone or gravel) into a solid rocklike mass as the paste hardens because of the chemical reaction between the cement and water. The aggregates, which comprise approximately 60 % to 75 % of the concrete by volume (70 % to 85 % by mass) (Kosmatka, et al., 2003, p. 1 & 79), are materials composed of rock fragments which are used in their natural state except for operations such as crushing, washing and sizing (Alexander & Mindess, 2005, p. 16). Aggregates reduce the cost of concrete and impart to concrete important engineering properties like strength, stiffness, rigidity, volume stability, thermal compatibility with steel, reduced shrinkage, improved wear resistance, restraint to creep deformations and durability (Alexander & Mindess, 2005, pp. 4-5). See Figure 2-1.

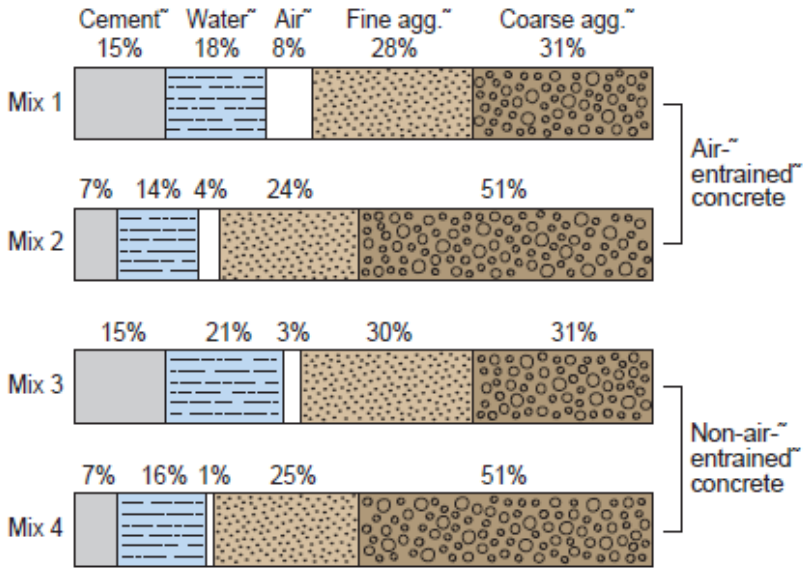


**Figure 2-1: Proportions of materials used in concrete by volume**
Source: **(Kosmatka, et al., 2003, p. 1)**

### 2.2.1 Classification of Concrete Aggregates

Aggregate used in concrete is classified into two groups: fine aggregate (sand) and coarse aggregate (stone). Fine aggregates (sand), which have particle sizes ranging between 0.07 mm and 4.75 mm, fill the voids between the coarse aggregates. Coarse aggregates (stone), which have particle sizes > 4.75 mm, and typically have a maximum size of 19 mm or 25 m, comprise 30 % to 50 % of concrete.

### 2.2.2 Strength Characteristics of Concrete

Concrete “can be conceived as a two-phase material which is composed of a collection of [coarse] aggregate particles with high strength and stiffness (phase I), and a matrix material consisting of hardened cement paste with fine sand with lower strength and stiffness (phase II)” (Walraven & Reinhardt, 1981, p. 5). Except for high strength concrete the strength of an aggregate does not influence the strength of conventional concrete as much as the strength of the paste and the paste-aggregate bond (Kosmatka, et al., 2003, p. 91).

Hardened concrete is an anisotropic brittle material having high compressive strength but low tensile, flexural and shear strength. Its strength is primarily

determined in terms of its compressive strength. As explained by Kosmatka et al., the

> ... compressive strength of concrete is a primary physical property and frequently used in design calculations for bridges, buildings, and other structures … the flexural strength of normal-weight concrete is often approximated as 0.7 to 0.8 times the square root of the compressive strength in megapascals … the direct tensile strength of concrete is about 8% to 12% of the compressive strength and is often estimated as 0.4 to 0.7 times the square root of the compressive strength in megapascals (Kosmatka, et al., 2003, p. 8).

### 2.2.3 Tensile Cracking of Concrete Beams

Any concrete beam loaded transversely will be subjected to compressive, tensile and shear stresses. Newman (2003, pp. 19-21) describes the mechanism of cracking of concrete due to the tensile stresses. The low tensile and shear strengths of concrete, relative to its compressive strength, results in the formation of cracks in regions of tensile stresses, orthogonal to the direction of the tensile stress. These cracks propagate rapidly because “under uniaxial tension, cracking reduces the loaded area of the specimen whereas under uniaxial compression the cracks are aligned in the direction of loading and do not significantly influence the loaded area”. Newman (2003, p. 19) cites McCreath, D.R., Newman, J.B. and Newman, K. (1964) in explaining the reason for crack formation “the probable mechanism of crack propagation and ultimate failure in concrete under a uniaxial stress state is by cracks forming in the cement paste matrix due to the presence of microcracks and flaws and the stress and strain intensification around aggregate particles”. The shape of the crack profile in normal strength concrete (NSC) “tends to follow the aggregate–paste interface” and for HSC “the fracture path passes through the aggregate particles”.

### 2.2.4 Shear Transfer at the Crack Interface

It can be concluded from the previous paragraph that the crack face will not be a smooth surface but will be “rough” due to the aggregate profile at the crack. Because of the roughness at the crack face it is possible to transfer

shear stresses parallel to the crack face through friction at the crack face. **This is called shear friction or aggregate interlock.** The capacity to resist tensile stresses normal to the crack face will be lost at a crack face.

## 2.3 Concrete Aggregates

Aggregates used in concrete are classified into two groups, fine aggregate and coarse aggregate. Fine aggregates (sand), which have particle sizes ranging between 0.07 mm and 4.75 mm, fill the voids between the coarse aggregates (Neville, 1995, p. 108). Coarse aggregates (rock) have particle sizes > 4.75 mm and typically have a maximum size of 19 mm or 25 m. An intermediate-sized aggregate of about 9.5 mm, is sometimes added to improve the aggregate gradation (Kosmatka, et al., 2003, p. 1).

Some properties of the aggregate, such as strength, hardness, colour, mineral and chemical composition will depend on the parent rock from which it was derived. Other properties of the aggregate such as particle shape, size, surface texture and absorption are independent of the parent rock (Neville, 1995, p. 109).

### 2.3.1 Strength of Aggregates

Aggregate tensile strength ranges from 2 MPa to 15 MPa and compressive strengths from 65 MPa to 270 MPa (Kosmatka, et al., 2003, p. 91).

### 2.3.2 Sampling of Aggregates

When tests are performed to determine the properties of aggregates it is important to ensure that the sample of aggregate used in the test is representative of the average properties of the bulk of the material used. This is normally achieved by drawing at least ten portions from different parts of the whole and then reducing the size of the sample through quartering or riffling (Neville, 1995, p. 111).

### 2.3.3 Geometrical Characteristics of Aggregate Particles

The geometrical characteristics of aggregate particles are described in terms of shape and surface texture. “The shape of three dimensional bodies is rather difficult to describe, and it is, therefore, convenient to define certain geometrical characteristics of such bodies”. Therefore Neville (1995, pp. 112-

117) identifies, amongst others, the aggregate characteristics defined in Table 2-1 to describe the shape of aggregate.

**Table 2-1: Particle shape classification (BS 812: Part 1: 1975) with examples**

| Classification | Description | Examples |
|---|---|---|
| Rounded | Fully water-worn or completely shaped by attrition | River or seashore gravel: desert, seashore and windblown sand |
| Irregular | Naturally irregular, or partly shaped by attrition and having rounded edges | Other gravel; land or dug flint |
| Flaky | Material of which the thickness is small relative to the other two dimensions | Laminated rock |
| Angular | Possessing well-defined edges formed at the intersection of roughly planer faces | Crushed rocks of all types; talus; crushed slag |
| Elongated | Material usually angular, in which the length is considerably larger than the other two dimensions. | - |
| Flaky and elongated | Material having the length considerably larger than the width, and the width considerably larger than the thickness | - |

Source: (Neville, 1995, p. 114)

Neville (1995, p. 117), based on data presented by Kaplan, argues that aggregate shape and surface texture appear to considerably influence the strength of concrete, more so for high strength concrete. Rougher surface texture and larger surface area of aggregates possibly result in larger bond forces between aggregates and the cement matrix.

### 2.3.4 Particle Shape

Aggregate particles equidimensional in shape will pack in an isotropic manner while elongated and flaky particles pack in an anisotropic manner. Therefore equidimensional aggregate particles are preferred for aggregate.

Due to the shape of aggregate particles a sample of aggregate cannot be compacted without voids. A sample of aggregate comprises solid particles and voids. Neville (1995, p. 114) cites Shergold's data as proof that "the

percentage volume of voids in an aggregate is dependent on the shape of aggregate particles".

### 2.3.5 Roundness

Roundness measures the relative sharpness or angularity of the edges and corners of a particle. Roundness is controlled largely by the strength and abrasion resistance of the parent rock and by the amount of wear to which the particle has been subjected. In the case of crushed aggregate, the particle shape depends not only on the nature of the parent material but also on the type of crusher and its reduction ratio, i.e. the ratio of the size of material fed into the crusher to the size of the finished product (Neville, 1995, p. 112).

### 2.3.6 Angularity Number

Angularity number can be used to estimate the angularity of a sample of aggregate with particles size confined within a narrow limit (Neville, 1995, p. 113). A compacted sample of spherical particles all of the same size has a solid volume of 67 % and a void volume of 33 %. The angularity number measures the percentage of voids in excess of 33 %. A higher angularity number implies a more angular aggregate.

### 2.3.7 Angularity Factor

The "Angularity factor is defined as the ratio of the solid volume of loose aggregate to the solid volume of glass spheres of specified grading, thus, no packing is involved and the attendant error is avoided" (Neville, 1995, p. 112).

### 2.3.8 Sphericity

Sphericity is defined as the ratio of the surface area of the particle to its volume. "Sphericity is related to the bedding and cleavage of the parent rock, and is also influenced by the type of crushing equipment when the size of particles has been artificially reduced" (Neville, 1995, p. 114).

### 2.3.9 Flakiness and Elongation

A particle is flaky if its thickness (least dimension) is less than 0.6 times the mean size of size fraction to which the particle belongs. An elongated particle

has length (largest dimension) 1.8 times the mean sieve size fraction (Neville, 1995, p. 115).

Flakiness index is defined as the mass of flaky particles as a percentage of the total sample mass. Elongation index is defined as the mass of elongated particles as a percentage of the total sample mass. For the manufacture of concrete it is undesirable that the mass of elongated coarse aggregate particles exceed 15 % of the mass of coarse aggregates and BS 882:1992 limits the flakiness index of coarse aggregate to 50 (Neville, 1995, p. 115).

### 2.3.10 Surface Texture of Aggregate

The surface texture of aggregates may be rough, polished, dull, smooth or rough and depends on the parent rock it originated from and on how forces applied to the particle have smoothed or roughened it. Surface roughness can reliably be estimated using visual methods and other methods of measuring surface roughness are not commonly used (Neville, 1995, p. 116). Neville (1995, p. 116) identifies the aggregate surface textures defined in Table 2-2 below.

**Table 2-2: Surface texture of aggregates (BS 812: Part 1: 1975) with examples**

| Group | Surface Texture | Characteristics | Examples |
|---|---|---|---|
| 1 | Glassy | Conchoidal fracture | Black flint, vitreous slag |
| 2 | Smooth | Water-worn, or smooth due to fracture of laminated or fine-grained rock | Gravels, chert, slate, marble, some rhyolites |
| 3 | Granular | Fracture showing more or less uniform rounded grains | Sandstone, oolite |
| 4 | Rough | Rough fracture of fine or medium-grained rock containing no easily visible crystalline constituents | Basalt, felsite, porphyry, limestone |
| 5 | Crystalline | Containing easily visible crystalline constituents | Granite, gabbro, gneiss |
| 6 | Honeycombed | With visible pores and cavities | Brick, pumice, foamed slag, clinker, expanded clay |

Source: (Neville, 1995, p. 116)

### 2.3.11 Bond of Aggregate

Bond between the aggregate and the cement matrix occurs due to the electrostatic bonding between chemical constituents of the hydrated cement paste. Bonding also occurs due to the interlocking of the aggregate and the hydrated cement paste.

### 2.3.12 Strength of Aggregate

Considering that concrete is a conglomerate of aggregate and hydrated cement paste, that coarse aggregate is the major component of concrete, constituting approximately 30 % to 50 % of the concrete, and that aggregate is a brittle material, the strength of concrete cannot significantly exceed the strength of the coarse aggregate.

In normal strength concrete the required strength of the aggregate must be considerably higher than nominal strength of the concrete. Due to the “wall effect” (Neville, 1995, pp. 609-610), the actual internal stresses at the interface between concrete and aggregate can far exceed the nominal compressive stress applied. Less redistribution of these internal stresses will occur in aggregates of higher modulus of elasticity which can result in cracking of the surrounding cement paste. High internal stresses may also lead to pulverisation of weaker strength aggregates.

### 2.3.13 Coarse Aggregates (Stone) Used in Durban

Two types of coarse aggregates are mainly used for the manufacture of concrete in Durban, namely quartzite and tillite. It is estimated that 60 % of the aggregate is derived from quartzite, a pinkish quartzite from the Table Mountain Group of the Cape Supergroup. The other 40 % is derived from Dwyka Formation tillite (Grieve, 2009, pp. 42 & 45-46). A third aggregate, dolerite, quarried in the Balllito area north of Durban, is also used in some concrete applications.

### 2.3.14 Fine Aggregates (Sand) Used in Durban

Sands used in Durban for the manufacture of concrete are mainly derived from processed crusher sand commonly blended with river sand derived from the Mgeni or Umdloti rivers (Grieve, 2009, p. 53).

## 2.4 Shear Resistance Theories on Reinforced Concrete Beams Without Transverse Shear Reinforcement

Gere and Goodno (2013, p. 458 & 1004) credit the Russian railway engineer D.J Jourawski for the development of the widely used approximate theory for shear stress in beams. In 1856 Jourawski observed that the timber beams in a railway bridge had split horizontally at the centre of the beam, where the bending stress was zero. This led him to develop the widely accepted approximate theory for the shear stress in beams which can be used to predict the shear stress at any level in the cross section using the equation $= \frac{VQ}{Ib}$. This equation is premised on the hypothesis of plane sections remaining plane. However this formula is not applicable to a reinforced concrete beam which is a composite beam of concrete and reinforcing steel and develops tension cracks in the concrete when subjected to bending and shear stresses.

Ritter (1899) proposed that after cracking, a reinforced concrete beam with transverse shear reinforcement can be modelled as a pin jointed truss with a compression top cord, a tension bottom chord, 45º compression diagonals and vertical tension members. Talbot (1909, pp. 44-46), based on 106 beam tests, concluded that the shear stress in a beam at failure is a function of, amongst other factors, the percentage of longitudinal reinforcement, the strength of the concrete (Talbot stated this as amount of cement) and whether the beam is long and slender or short and deep. The actual terminology used by Talbot was amount of reinforcement, amount of cement and effect of ratio of length of span to depth of beam. Unfortunately, Talbot's findings were not taken into consideration in design equations until after the 1955 shear failure of reinforced concrete beams at a warehouse at Wilkins Air Force Depot in the USA. Extensive research into shear conducted after this failure revealed that shear failure of reinforced concrete beams was a more complex phenomenon than previously understood with many variables (Joint ASCE-ACI Committee 445 on shear and torsion, 1998 reapproved 2009, pp. 3-4).

In 1962 Walter proposed a shear model containing a 45º crack with rotation occurring about the tip of the crack and crushing of the concrete above the crack leading to failure of the beam. His model recognised that the hypothesis

of plane sections remaining plane was not valid for shear deflection in a beam and took into account shear deformation of the beam section (Haas, 1996, pp. 4-11) and (Regan, 1993, p. 341).

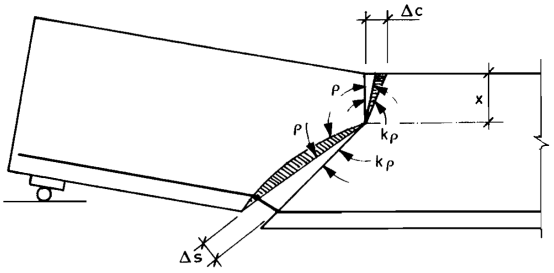


**Figure 2-2: Walters model**
Source: **(Regan, 1993, p. 341)**

The model of Walter was further developed by Reineck in 1991 to include aggregate interlock, which is flexure due to the cantilever tooth and dowel action from the longitudinal reinforcement (Figure 2-3). He compared results from his model to the tests conducted by Leonhardt and found his model correlated well with the experimental results. His model is however too complex for practical application (Haas, 1996, pp. 13-19).

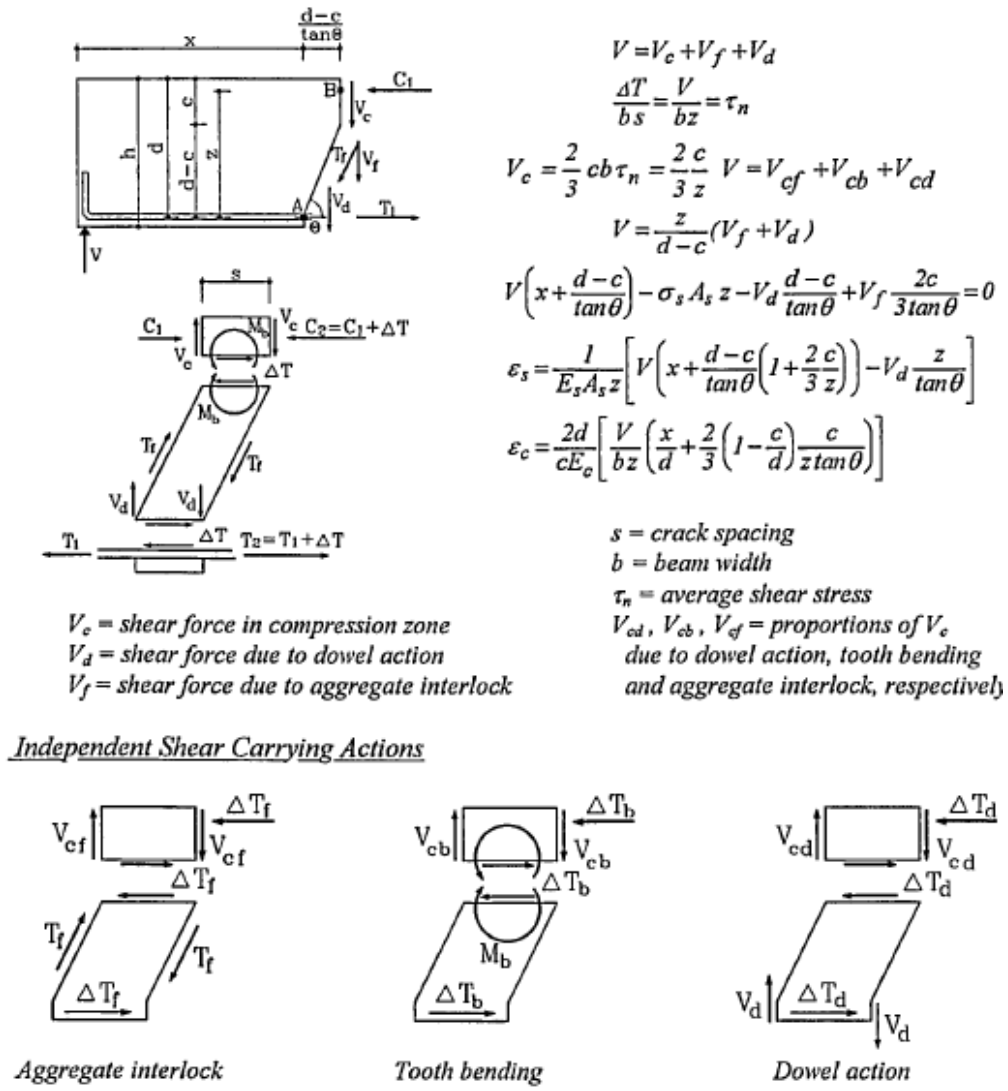


**Figure 2-3: Reinick's model**
Source: **(Haas, 1996, p. 14)**.

Kani (1964, pp. 441 - 463), who preferred to refer to shear failure as diagonal failure, proposed a model that takes into account the bending of concrete cantilevers formed between flexural cracks. Under increasing load vertical flexural cracks develop in the tensile zone below the neutral axis of the beam since concrete has almost zero tensile strength. Above the neutral axis of the beam the concrete is in compression and the concrete remains uncracked since concrete has high compressive strength. The segments between tensile cracks combined with the uncracked upper compression zone resemble a comb-like structure (Figure 2-4), the segments forming the "teeth" of the comb and the compression zone the "backbone". After cracking, the tensile stress below the neutral axis of the beam is solely transmitted by the steel

reinforcement which remains bonded to the concrete segments between cracks. With increasing load the shear strength of the beam is initially derived from these “comb-like” cantilevers cantilevered from the compression “backbone”, and when the concrete cantilevers fail, then the compression “backbone” transforms onto a tied arch (Figure 2-5), which if strong enough, will provide additional shear strength until the tied arch collapses with the increasing load. By sketching the compressive and tensile stress trajectories in the beam, Kani (1964, p. 456) was able to explain why the shear failure crack “starts rising perpendicular to the tension face of the beam, passing the reinforcement in the end section of the beam with a curvature and then straightening out, sometime abruptly, in the direction of the applied load”. Kani derived an analytical equation for the “the critical bending moment $M_{CR} = M_0 \cdot \frac{\Delta x}{s} \cdot \frac{a}{d}$ at which the concrete teeth break”, which is a “linear function of the shear arm ratio $a/d$”. Kani showed that the shear strength of a beam depended on the strength of the concrete cantilevers for ratios of ${}^{a}/_{d} < 2.5$ and on arch action for ${}^{a}/_{d} > 2.5$ (Figure 2-6). Futhermore, Kani (1964, pp. 459 - 461) also derived an equation to determine the transition point $\alpha_{TR} = {}^{a}/_{d} = \frac{M_{FL}}{M_0} \cdot \frac{s}{\Delta x}$ where the “transition from diagonal failure to flexural failure takes place”.

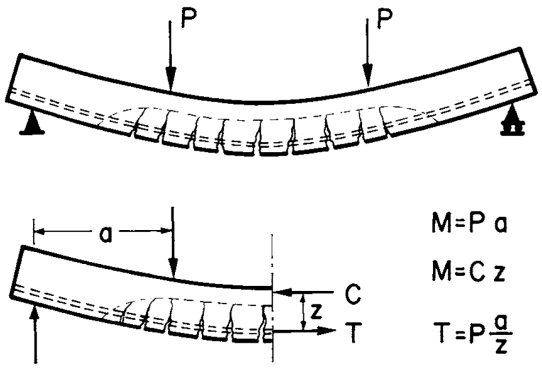


**Figure 2-4: Kani's model. The formation of the comb-like structure due to vertical flexural cracks**
Source: **(Kani, 1964, p. 445 Fig. 3)**

A shortcoming in Kani’s (1964) model is that it completely overlooks frictional contact between the cantilever segments. Indeed looking at Figure 2-4 which shows a gap between the comb-like teeth, it appears as if the teeth are not in

contact. In an actual beam, the actual crack gap is small, less than a millimetre, and the crack surfaces remain in contact (aggregate interlock).

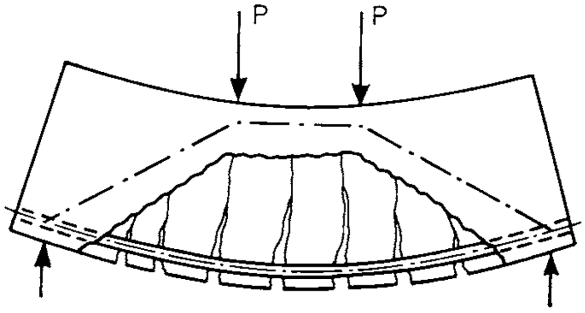


**Figure 2-5: Kani's model. Tied arch action after failure of the concrete cantilevers**
Source: **(Kani, 1964, p. 453 Fig. 11)**

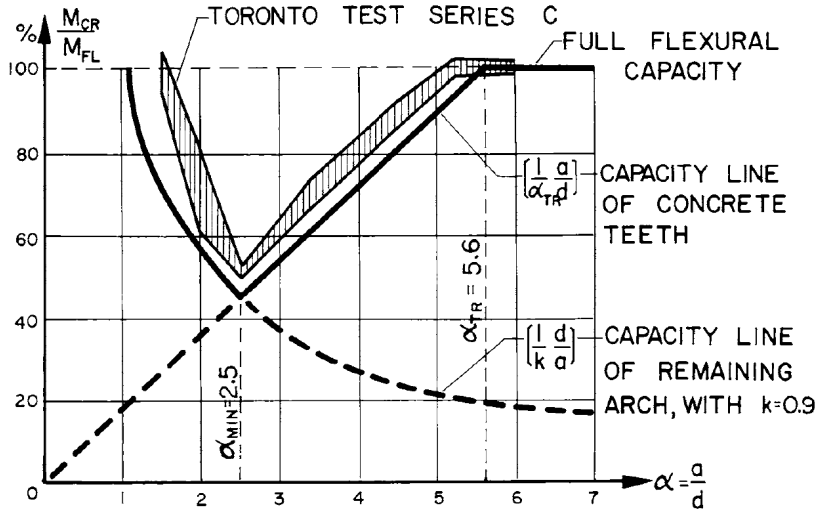


**Figure 2-6: Significance of the a/d ratio illustrated for a sample of beams known as the Toronto Series C**
Source: **(Kani, 1964, p. 461 Fig. 17)**.

Fenwick's (1966) model marked a significant improvement on Kani's (1964) model by taking into consideration contact of the concrete cantilevers, i.e., aggregate interlock. Fenwick (1966) conducted an experimental investigation into the basic mechanism of shear resistance of a reinforced concrete beam and concluded that the shear stress in a reinforced concrete beam without shear reinforcement is resisted initially by beam action and after the beam action fails by arch action. Fenwick (1966, pp. 235-236) concluded that beam action comprised three actions, i.e., dowel action, **aggregate interlock at the**

**crack interface** and flexural resistance of the “Kani” concrete cantilevers (Figure 2-7). The contribution of each action to the total shear resistance, for a typical rectangular beam, was found to be approximately 20 % by flexural resistance of the concrete cantilevers, 60 % or more by aggregate interlock and less than 20 % by dowel action.

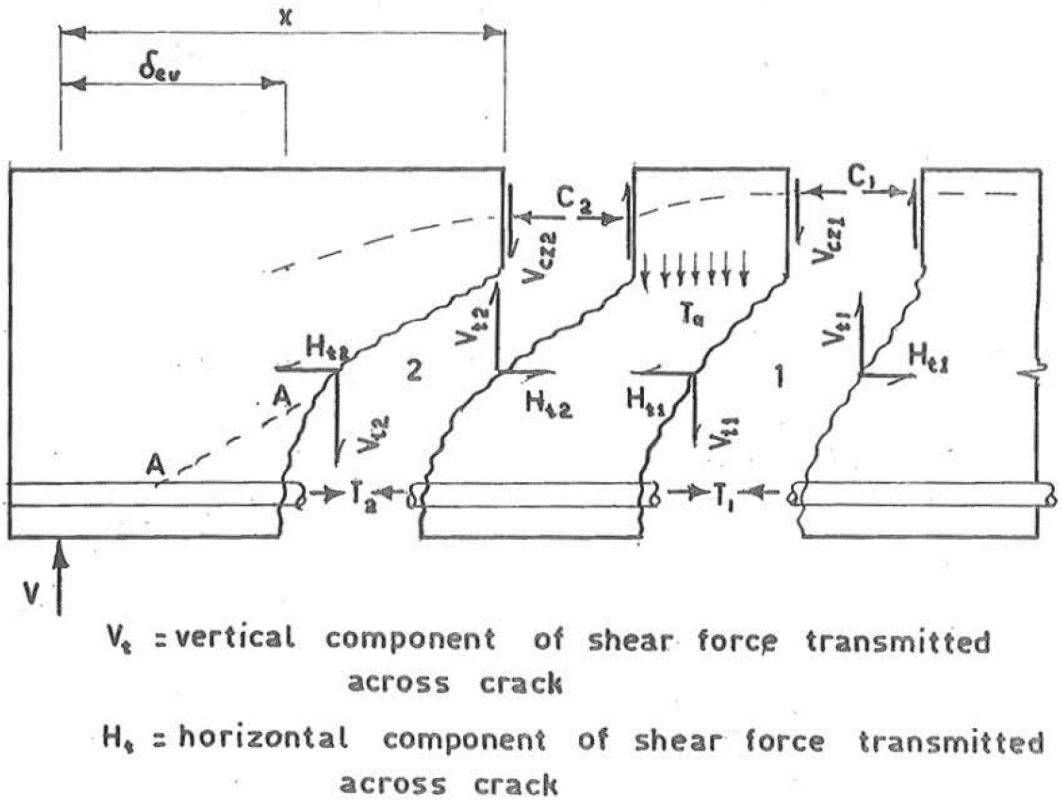


**Figure 2-7: Fenwick’s model of shear resistance due to beam action in a cracked beam. $H_t$ & $V_t$ are the aggregate interlock components**
Source: (Fenwick, 1966, p. 48 Fig 2.6)

In an experimental program using a variety of specially devised tests to determine the proportion of shear force transmitted in beams by aggregate interlock, dowel action and the compression zone, Taylor (1974, pp. 55-59) determined that 33 % to 50 % of the shear force was transmitted through aggregate interlock, 20 % to 40 % through the compression zone and 15 % to 25 % through dowel action (Figure 2-9). Furthermore, Taylor found (p. 49) that the ultimate aggregate interlock strength “depended on concrete strength, aggregate type and displacement ratios” and concluded that “the **aggregate interlock** shears will depend on the surface roughness of the cracks,

aggregate type and the displacements across the cracks". Taylor (p:49) also observed that for high strength concrete specimens "the aggregate did not tear out of the matrix to give a rough crack but tended to split. The crack surface was therefore relatively smooth, giving low interlock strengths". The important shear parameters identified by Taylor (p. 56) were concrete strength, steel percentage, steel strength, the shear span ration $a_v/d$, aggregate type, beam size and stirrups. The sequence of failure (p. 55) in his study was initiated by dowel action failure followed by aggregate interlock failure and compression zone failure (Figure 2-8).

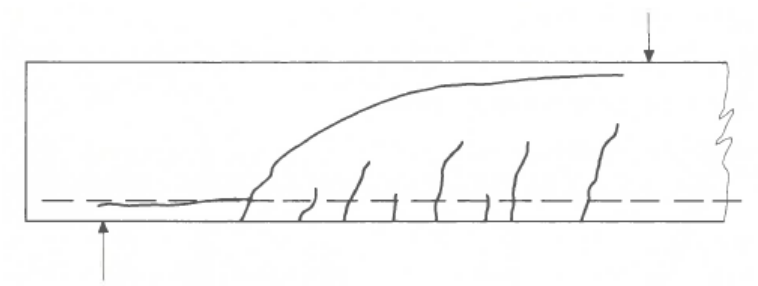

**Figure 2-8: Sketch showing crack pattern on a beam according to Taylor's beam action model. The diagonal failure crack develops from a previous flexural crack. Also illustrated is the dowel splitting crack**
Source: **(Taylor, 1974, p. 44 & Fig1 on p. 60)**.

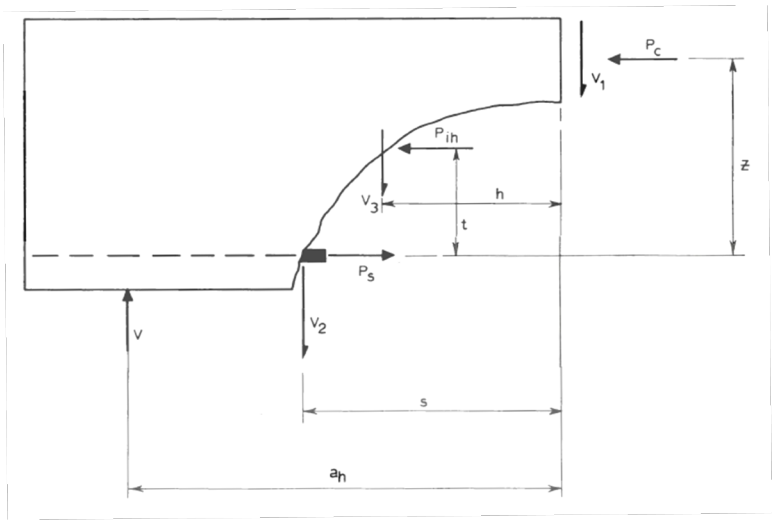


**Figure 2-9: Shear transfer through compression zone shear, aggregate interlock and dowel action**
Source: **(Taylor, 1974, p. 61 Fig. 4 )**.

Hamadi and Regan (1980) conducted push-off tests (p. 68), divided beam tests (pp. 69-70), and beam tests (pp. 70-71), to measure the contribution of

the compression zone above the crack line, **aggregate interlock**, aggregate type (lightweight and normal weight) and dowel action to the shear strength of beams. The authors attribute the up to 50 % reduced shear strength to the lightweight aggregate because such aggregates have much reduced aggregate interlock strength.

Mitchell and Collins (1974) formulated the compression field theory (CFT) to model shear in reinforced concrete beams due to pure torsion. The model uses multiple trusses smeared over the beam, each positioned parallel to a face of the beam and forming a 3-dimensional framework. The model assumes that the principal stresses and principal strains have the same inclination, assumes the concrete has no tensile strength, and does not take aggregate interlock into consideration. Some of the strain assumptions used in this theory are valid for shear from pure torsion but not valid for shear from flexure (Haas, 1996).

An analytical model for shear strength, the modified compression field theory (MCFT) proposed by Vecchio and Collins (1986) builds on the compression field theory (CFT) by assuming uniform compression fields inclined at an angle to the horizontal. The model takes into account “equilibrium, compatibility and stress-strain relationships in terms of average stresses and average strains”. Using Walraven’s model to determine shear transfer through aggregate interlock, a relationship is derived for the maximum shear stress transferred at the crack interface through aggregate interlock, which is a function of the concrete cube strength, the crack width and the aggregate size. Like the CFT, the MCFT also assumes that the principle stress and principle strain are in the same direction and as a result does not treat aggregate interlock as an independent shear transfer mechanism. This model is also too complex for practical design application, requiring an iterative solution to the many equations listed in Figure 2-10: Equations of the modified compression field theory

Source: (Bentz, et al., 2006, p. 615). Iteration is required to determine the angle of the failure plane. The modified compression field theory for shear formed the basis for a more general shear design method in the 1994

Canadian Standard for the design of concrete structures as well as the shear provisions of the 1994 American Association of State Highway and Transportation Officials (AASHTO) LRFD bridge design specifications (Collins, et al., 2007).

The simplified modified compression theory (SMCFT) devised by Bentz, Vecchio and Collins (2006) simplified the MCFT model for practical “back of the envelope” design use.

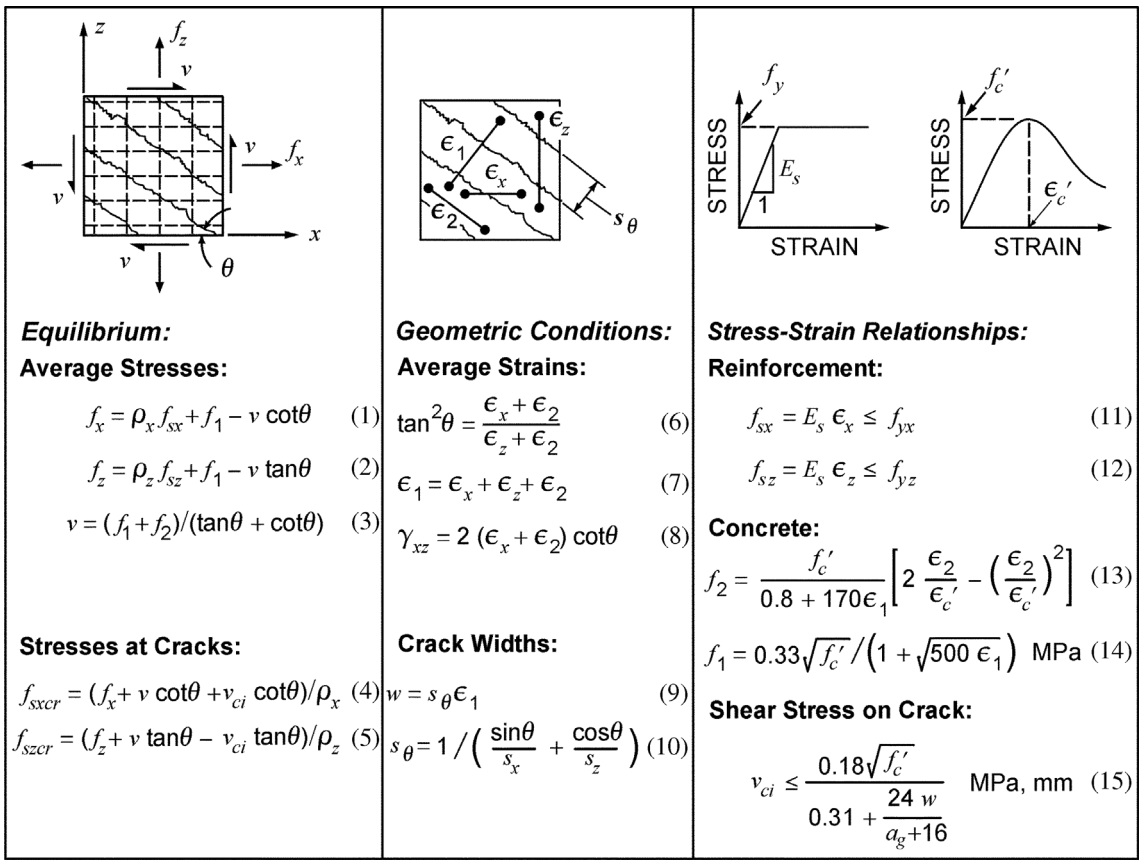


**Figure 2-10: Equations of the modified compression field theory**
Source: **(Bentz, et al., 2006, p. 615)**

An experimental study by Sherwood, Bentz and Collins (2007) found **aggregate interlock** to be the major mechanism of shear transfer in thick slab strips and furthermore that maximum aggregate size plays an important role in strip slab shear capacity.

Muttoni and Schwartz (1991, pp. 704-706) proposed a conceptual model for the transfer of shear in reinforced concrete beams. The model which has become known as the critical shear crack theory (CSCT), states that after

vertical flexural cracks develop in a beam, shear transfer occurs through the formation of inclined concrete struts (compression members) and ties (tension members) transferring load from the compression zone at the top to the longitudinal reinforcement at the bottom (dowel action), as can be seen in Figure 2-13, Figure 2-14 and Figure 2-16. Diagonal cracking is initiated when the tensile force in the concrete tie exceeds its tensile strength. The tie (labelled B in Figure 2-14) develops a crack perpendicular to the tie and the crack (the critical shear crack) propagates from the adjacent vertical flexural crack towards the applied point load (see crack B in Figure 2-11, Figure 2-12 and crack B in Figure 2-15). The tie is thus “lost” as no tensile load can be transferred through a crack. The strut orientates itself with this diagonal crack and shear transfer occurs through **aggregate interlock** at the crack interface. As the load increases, the crack width increases beyond the point where shear transfer through aggregate interlock can occur, which initiates the failure of the beam. The model correlates well with the observed crack pattern in beams failing in shear.

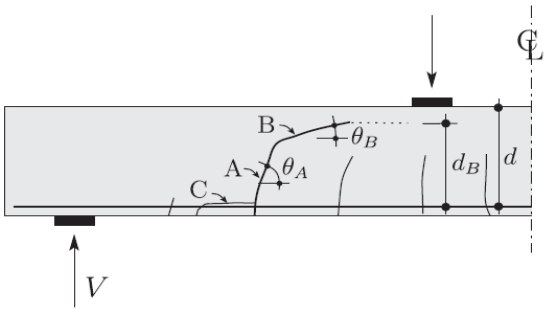


**Figure 2-11: Formation of a critical shear crack A & B. Lamination occurs at C**
Source: **(Ruiz, et al., 2015)**

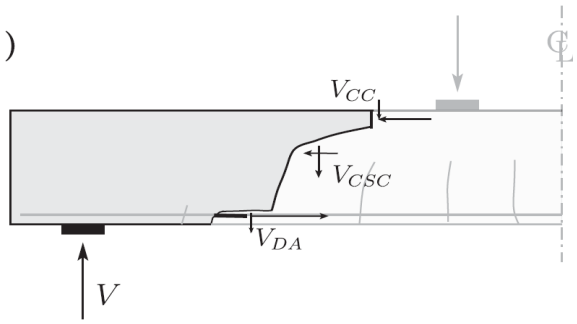


**Figure 2-12: Shear components. $V_{cc}$ = shear in compression concrete, $V_{csc}$ = shear in critical shear crack, $V_{DA}$ = dowel action**
Source: **(Ruiz, et al., 2015)**

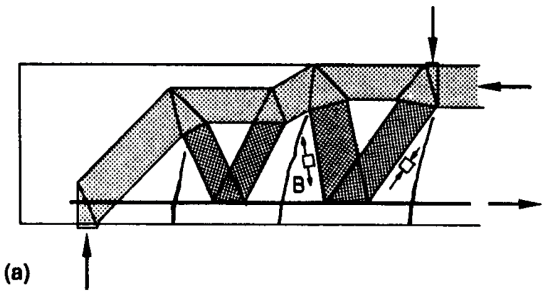


**Figure 2-13: Critical shear crack theory – formation of struts and ties in the concrete after flexural cracking occurs. The top chord (shaded light grey) is concrete, the diagonals (shaded light and dark are concrete and the bottom tie is the flexural steel reinforcement**
Source: **(Muttoni, 1990, p. 100 (Bild 6.4))**.

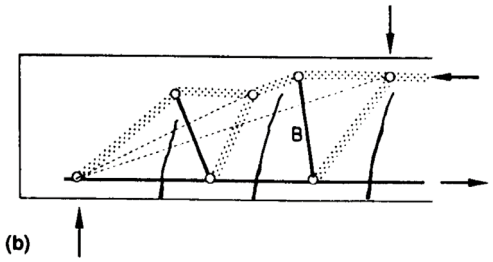


**Figure 2-14: Critical shear crack theory – solid dark lines are ties and shaded dotted lines are struts**
Source: **(Muttoni & Schwartz, 1991, p. 704)**

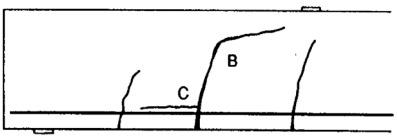


**Figure 2-15: Critical shear crack theory – cracking of the tension tie B leads to the diagonal crack at B, and, dowel failure leads to the horizontal crack C at the reinforcement level**
Source: **(Muttoni & Schwartz, 1991, p. 704)**

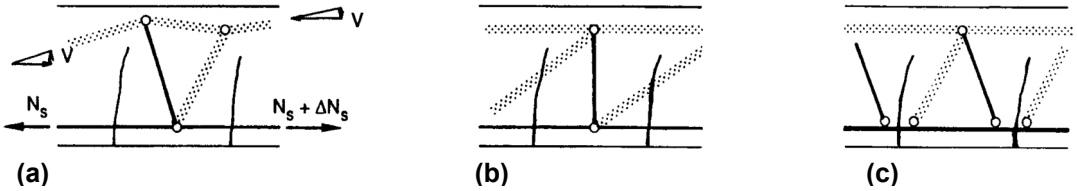


**Figure 2-16: The three mechanisms of shear resistance according to critical shear crack theory – (a) cantilever action, (b) interlocking action and (c) doweling action**
Source: **(Muttoni & Schwartz, 1991, p. 704)**

Muttoni and Ruiz (2008, pp. 163-171) developed an analytical model and proposed an equation for calculating the shear strength of beams without shear reinforcement based on the shear carrying mechanisms after the opening of the critical shear crack. The dependency of the shear strength on the a/d ratio and the Kani's valley phenomenon is explained in terms of the critical shear crack theory. The model assumes the width of the critical shear crack to be equal to the elastic strain at a depth of $0.6\,d$ from the compression face, and also takes into account the roughness of the crack [**aggregate interlock**] and the compressive strength of the concrete". The shear strength $V_R$ is calculated using the three equations below and is a function of the

bending moment in the critical section, the longitudinal steel reinforcement, the effective depth, the beam width, the strength of the concrete, the aggregate size, and the modulus of elasticity of the concrete and steel.

The width of the critical shear crack is assumed to be equal to the elastic strain at a depth 0.6 d from the compression face.

The depth of the compression zone is:

$$c = d\rho\frac{E_s}{E_c}\left(\sqrt{1+\frac{2E_c}{\rho E_s}}-1\right)$$

The strain ε at a depth 0.6 d from the compression face is:

$$\varepsilon = \frac{M}{bd\rho E_s\left(d-{}^{c}/_{3}\right)}\cdot\frac{0.6d-c}{d-c}$$ where $E_c \sim 10\,000\sqrt[3]{f}_c$ in MPa

The proposed analytical equation for the shear strength is:

$$V_r = bd\sqrt[2]{f_c}\cdot\frac{1}{6}\cdot\frac{2}{1+120\frac{\varepsilon d}{16+d_g}}$$ SI units: MPa, mm

By making some simplifying assumptions about the strain, the above equation was reduced to the equation below that has been adopted by the Swiss SIA Code 262 for concrete structures.

$$V_r = bd\sqrt[2]{f_{ck}}\cdot\frac{0.2}{1+0.0022d\frac{m_{Ed}}{m_{Rd}}}$$ SI units: MPa, mm

where:

$b$ = width of member

$d$ = effective depth

$d_g$ = aggregate size

$E_c$ = modulus of elasticity of concrete

$E_s$ = modulus of elasticity of the reinforcing steel

$M$ = bending moment at the critical section. For a point load the critical section is located at a distance ${}^{d}/_{2}$ from the point load.

$f_c$ = compressive strength of concrete

$\varepsilon$ = strain

$\rho$ = longitudinal reinforcement steel ratio $= \frac{A_s}{b \cdot d}$

$m_{Ed}$ = design (factored ) moment divided by width of cross section

$m_{Ed}$ = design (factored ) moment per unit length in critical cross section

$m_{Rd}$ = plastic design (factored ) moment per unit length in critical cross section

$V_R$ = shear strength

$x_{crit}$ = location of critical section.

Campana, Ruiz, Anastasi and Muttoni (2013, pp. 7,11 & Table3) recorded detailed experimental measurments of the cracking patterns and actual shear failure kinematics of four beam specimens. The high precision measurements were recorded by attaching Dermec strain gauges on a 100 mm equilateral triangular grid on one side of the beam. The amount of shear transferred by each of the following shear transfer mechanisms:

- the vertical component of **aggregate interlock** action,
- forces developed in the stirrups,
- the vertical component of concrete residual tensile strength,
- the dowelling action of the flexural bars,
- the vertical component of the inclined compression chord,

was estimated based on the observed measurements and kinematics and the results compared reasonably well with the acting shear force at the time of the measurement. The contribution of each of the above actions to the shear strength of the four sample beams was measured and the aggregate interlock component was found to be the dominant shear transfer mechanism for beams without transverse shear reinforcement. The amount of shear transferred by each mechanism depended on the shape of the cracks that formed and the kinetics (opening or sliding) at failure. The steeper and more

curved the shape of the crack the greater was the contribution of aggregate interlock.

Zhang, Vistin and Oehlers (Zhang, et al., 2015)(2015 p:2) formulated a “mechanics-based segmental approach” model to analyse the shear strength of “a reinforced concrete beam with any type of concrete and reinforcement and which can explain the physical process of shear failure”. The model “incorporates the partial interaction mechanics of tension stiffening and its associated crack widths, crack spacings, and reinforcement-force/crack-width relationships; and the partial interaction mechanics of shear friction to quantify the shear resistance along inclined sliding planes attributable to rigid body displacements”. In this model the shear resistance arising from aggregate interlock incorporates the increase in normal force, and therefore aggregate interlock, due to the elongation of the stirrups at the crack interface.

## 2.5 Influence of Coarse Aggregate Type on Aggregate Interlock

Taylor and Brewer (1963) performed comparative shear tests on beams without shear reinforcement made from three different types of coarse aggregates. The beams were fabricated from two lightweight aggregates, i.e., **sintered pulverised-fuel ash** and **expanded clay** and one normal river gravel aggregate. Beams fabricated from the expanded clay aggregate developed on average only 78 % to 80 % of the shear strength of the gravel aggregate beams while the beams fabricated from sintered pulverised-fuel ash developed on average 83 % to 93 % of the shear strength of the gravel aggregate beams.

Hamadi and Regan (1980) conducted push-off tests (p. 68), divided beam tests (pp. 69-70) and beam tests (pp. 70-71) to measure the contribution of the compression zone above the crack line, aggregate interlock, aggregate type (lightweight and normal weight) and dowel action to the shear strength of beams. Three aggregate types were tested, a **normal weight gravel** and two lightweight aggregates, namely, **slate (solite)** and **clay (leca)**. Their findings indicate that the shear strength was significantly reduced (by up to 50 %) for the lightweight aggregates and they attributed this reduction to the assumption that lightweight aggregates have much reduced aggregate interlock strength.

Brink, Horak and Visser (2003, p. 1 & 8) conducted four tests on South African granite and dolomite aggregates (p. 1) in order to obtain an improved aggregate interlock equation that could be implemented in a local software program for mechanistic concrete pavement design. One of the conclusions of their study was that South African aggregates have a greater aggregate interlock potential (p. 7). Although this study was in the context of concrete pavement design and not the transfer of shear in reinforced concrete beams, its relevance to this study is the mention in the conclusions that "it is clear that the **South African aggregates** have a greater aggregate interlock potential" to what is still a shear/aggregate interlock phenomenon.

Arezoumandi, Drury, Volz and Khayat (2015a, pp. 559-562 & 566) conducted an experimental investigation to determine if replacing coarse aggregate in a conventional concrete (CC) with **recycled aggregate concrete** (RAC) would affect the shear strength of concrete beams. This was achieved by replacing either 50 % or 100 % of the coarse aggregate in a conventional concrete (CC) with recycled aggregate concrete (RAC) derived from grinding of the same conventional concrete parent material to a nominal aggregate size of 25 mm. While there was no statistical difference between the shear capacity of the 50 % RAC and CC it was found that the 100 % RAC had a statistically lower shear capacity compared to CC beams tested. The lower shear capacity was ascribed to the " microcrack formation in the interfacial transition zone (ITZ)" between virgin aggregate and residual mortar in RAC and also ITZ between residual mortar and fresh mortar compared with only ITZ (between virgin aggregate and fresh mortar) in the CC beams".

Another investigation by Knaack and Kurama (2015, p. 1 & 11) found that replacement of coarse aggregate **with recycled aggregate**, ranging from 0 % to 100 % replacement, has a small effect on the shear strength and flexural strength of beams. However, the study found "there is a considerable reduction in the initial stiffness and an increase in the ultimate flexural deflections as the amount of RCA is increased"

From an aggregate interlock point of view the frictional properties between aggregate and concrete matrix would have remained almost unchanged and therefore the similarity in shear strengths between CC and RACs.

An experimental study by Roskos, White and Berry (2015, pp. 1, 5 & 9) to evaluate the performance of beams manufactured with “self-cementitious fly ashes as the sole binders and **pulverised reused glass** as the [fine and coarse] aggregate [3.2 mm to 9.5 mm]” concluded that with respect to the shear strength of the beams the “fly ash/glass beams did not perform as well as the conventional concrete beams”. The reduced shear strength was attributed in part to “the smaller aggregates used in the fly ash/glass beams and subsequent reduction in aggregate interlock” and to the “reduced tensile capacity of the fly ash/glass concretes”.

In an experimental study on the influence of aggregates and concrete strength on the shear strength of self-compacting concrete (SCC) beams, Hassan, Ismail and Mayo (2015, pp. 1, 7 & 10) investigated the following parameters: coarse/fine aggregate ratio (0.7 – 1.2), coarse aggregate size (10 mm and 20 mm), **aggregate type/density (slag, expanded slate and crushed stone)** and compressive strength (26 MPa to 72 MPa). They reported that “increasing the coarse/fine aggregate ratio … improved the postdiagonal cracking resistance of all normal strength self-compacting concrete (NSSCC)” but the increase was much less for high strength self-compacting concrete beams (HSSCC) where much more fracture of the aggregate occurred. The increase was also less for lightweight self-compacting concrete (LWSCC) and differed for the two different types of lightweight aggregates (slag and expanded slate). The decrease was attributed to fracture of the lightweight aggregates.

## 2.6 Influence of Fine Aggregate on Aggregate Interlock

An experimental investigation in Brazil by Savaris and Pinto (2017, pp. 30, 32 & 39) “demonstrated a lower shear resistance of self-compacting concrete beams”. Concrete “beams cast with conventional concrete mixes showed higher shear strengths than the ones for self-consolidating concrete mixes with same size and volume fraction of coarse aggregate”. The self-

compacting concrete was made by replacing a percentage of the coarse aggregate with dry fine aggregate limestone filler and a polycarboxylate-based superplasticizer. The authors attribute this **reduction in shear resistance to the higher content of fine aggregate** (includes the fine limestone filler) in self-compacting concrete. They assert that the higher content of "fine materials" and … reduced aggregate size" reduces aggregate interlock.

## 2.7 Influence of Aggregate Size on Aggregate Interlock

Bentz (2005, pp. 234, 237 & 240) analysed some of the experimental data on shear strength ranging from Leonardt's investigation in 1962 to Ghannoum's investigation in 1998, that would have included size effects, to derive a purely empirical equation for the shear stress in a member at failure. Notably, the equation includes aggregate size as a variable where the failure stress increases with increasing aggregate size. One of the conclusions in this study was that "**aggregate size is important in equations that determine the shear strength of beams without stirrups**".

An experimental program to determine among other parameters "the role played by the maximum coarse aggregate size in transferring shear stress across cracks", by Sherwood, Bentz and Collins (2007, p. 187 & 189) found that the **shear stress at failure increased with increasing coarse aggregate size** (9.5 mm, 19 mm) but that "beyond an aggregate size of 25 mm the increase appears unreliable." One of their concluding remarks is that "Experimental and analytical studies reported in this paper show that decreasing maximum aggregate size can significantly decrease the shear capacity of thick slabs." (p. 189).

One of the conclusions of an experimental study by Yang, Sim, Choi and Lee (Yang, et al., 2011, p. 509) was that while "maximum aggregate size had little influence on the normalized inclined cracking shear strength … **ultimate shear strength increased with the aggregate size**". The investigation compared the effect of aggregate size on the shear behaviour of all lightweight concrete (ALWC), sand lightweight concrete (SLWC) and normal weight concrete (NWC) continuous slender beams (pp. 501-503). Since aggregate interlock only occurs after cracking, it may be reasonable to infer that the

increased ultimate strength was due to increased aggregate interlock due to the increase in aggregate size.

## 2.8 Influence of the Type of Concrete on Aggregate Interlock

Sagaseta and Vollum (2011, pp. 119-137) conducted push-off tests and parallel beam tests on **high strength concrete** specimens made from crushed limestone coarse aggregate and conventional concrete made from rounded gravel coarse aggregate. Unlike the high strength concrete where aggregate fracture was observed at the crack interface, most of the gravel aggregate in the conventional strength concrete remained intact and the crack interface passed around the aggregate. However, despite aggregate fracture occurring in the high strength concrete they concluded that " significant shear stresses were transferred through the cracks in the limestone specimens (p. 135) even though the aggregate fractured. This unexpected shear transfer capacity is believed to be due to the so-called 'macro-level roughness' (p. 136) observed in the tests". They also found "that the shear strength of beams with stirrups was unaffected by aggregate fracture".

Emiko et al. (2011, p. 393 & 399), used pre-cracked push-off specimens with shear reinforcement to study shear transfer in **lightweight concrete** (LWC) and **foam concrete** (FC). They observed that the shear transfer behaviour of foam concrete (FC) and lightweight aggregate foam concrete (LWAFC) differed significantly from that of normal weight concrete (NWC) and lightweight concrete (LWC). They also concluded "that in general, shear transfer strength is 20% lower for LWC compared with NWC for the same amount of reinforcement and the same concrete strength".

Yang and Ashour (2015, pp. 485-491) assessed the frictional modification factor λ found in the ACI 318-11 code equations for calculating the shear capacity of deep and slender beams without shear reinforcement. A database comprising shear tests on 1716 normal weight concrete (NWC) beams, 73 all light weight concrete beams (ALWC) and 54 sand light weight concrete (SLWC) beams, all without shear reinforcement, was analysed, and a new equation for calculating frictional modification factor λ proposed. Whereas the code recommends λ = 0.75 for ALWC, λ = 0.85 for SLWC and λ = 1.0 for

NWC, the new proposed equation is a function of concrete strength, aggregate size and the ratio of the longitudinal reinforcing steel. The authors attribute the reduced shear capacity in **lightweight concrete** beams to the reduced aggregate lock capacity due to fracture of the lightweight aggregates used in the lightweight concrete.

Arezoumandi, Volz Ortega and Myers (2015b, pp. 1, 6, 8 & 10) conducted tests on beams to compare the shear behaviour of **high volume fly ash concrete** (HVFAC) beams with conventional concrete (CC) beams. In the high volume fly ash concrete 70 % of the portland cement content had been replaced with fly ash. "Overall, results of the statistical data analysis showed that the normalised shear capacity of the HVFAC is statistically higher [by a small amount] than the CC for the beams tested" and this is attributed to HVFAC concrete having "higher fracture energies than a conventional Portland cement matrix" The "crack morphology, crack progression and load deflection response … was virtually identical" for both types of concrete. They also found, from a separate investigation, that "the total cementatious content had little effect on the shear behaviour of HVFAC beams".

It may therefore be assumed that the addition of fly ash binder to portland cement in concrete has very little, if any, effect on the aggregate interlock response at the crack interface.

## 2.9 Influence of Beam Longitudinal Steel Reinforcement on Aggregate Interlock

One of the conclusions of the comparative experimental study by Taylor and Brewer (1963, p. 87 & 92) to investigate " the effect of the type of aggregate on the diagonal cracking of reinforced concrete beams" was that the shear strength of beams fabricated "with **cold-worked deformed bars** was … approximately 10% lower than for corresponding beams reinforced with **plain mild-steel** [longitudinal] bars."

Rodrigues (2012, pp. 751 & 759-760) investigated how yielding of the beam longitudinal reinforcing steel influences shear transfer through aggregate interlock at the crack interface. Analysis showed "that the amount shear transferred across a crack decreases with increasing rotation, for all the

beams failing in shear". For the beam specimens that failed in shear without **yielding of the longitudinal steel reinforcement**, it was calculated that aggregate interlock could account for close to 50 % of the shear transfer. However, in beam specimens that failed in shear after yielding of the longitudinal steel reinforcement, aggregate interlock could account for only about 5% of the total shear transfer. Thus "yielding of the flexural reinforcement significantly affects the amount of shear that can be sustained by aggregate interlock action".

Yielding of the longitudinal flexural reinforcement is often encountered in the practical design situation of a continuous beam where a fraction of the hogging bending moment at a support is redistributed to a sagging span moment. In such a situation, maximum shear occurs together with yielding of the reinforcement and the decrease of aggregate interlock and shear strength due to yielding of the longitudinal reinforcement should be a matter of concern.

Singh and Chintakindi (2013, p. 257) conducted an appraisal of dowel action as a mechanism of shear transfer in beams by conducting experimental tests on beams with a shear span of either 3 or 4.5. The authors describe **dowel action** as "the capacity of reinforcing bars to transfer forces perperdicular to their axis" through bending, shear and kinking. Amongst the conclusions they made were that:

- **dowel action** was not a significant shear carrying mechanism,
- the shear carrying capacity of beams is insignificantly influenced by **bar diameter**, and
- shear capacity increased with increasing amounts of longitudinal steel. This was attributed to smaller crack widths occurring with increasing **steel ratios** which resulted in " an increase in the sliding resistance along the crack surfaces", i.e., aggregate interlock.

## 2.10 Size Effect on the Shear Capacity of Concrete

The size effect on the shear capacity of a structural element like a reinforced concrete beam represents the reduction in shear capacity predicted by a plastic limit analysis of the beam, where the cause of this reduction is due to

the increase in fracture energy with increasing depth of the beam (Bažant & Planas, 1998, p. 8) and (Bažant, 2005, p. 130).

Bažant (2005, p. 130) lists a string of experimental shear failure investigations dating back from Leonardt and Walter in 1962 through to Walraven and Lehwalter in 1994 where size effect has been documented. The cause of the size effect phenomenon is explained using fracture mechanics methods.

Bentz (2005, p. 232), describes size effect as “the reduction in shear stress at shear failure as member depth of beams and slabs not containing stirrups increases”. Bentz (2005, p. 232) analysed 24 different size effect series of shear experiments with the purpose of formulating a purely empirical equation for the size effect on shear strength. Amongst the conclusions of the study was that “the size effect is real and shows decreasing shear stress at shear failure for larger beams that do not contain stirrups” and “the aggregate size is important in equations that determine the shear strength of beams without stirrups” Bentz (2005, p. 240).

In an experimental program to investigate “the size effect in shear and the role played by the maximum coarse aggregate size in transferring shear stress across cracks”, Sherwood, Bentz and Collins (2007, pp. 184-185 & 189) observed that “the large specimens failed at approximately half of the shear stresses of the smaller specimens”. They attributed this reduction in shear stress at failure to “reduced aggregate interlock capacity in large members” as a result of the increase in crack width at mid-depth with increasing beam depth. Furthermore they conclude “that it is reduced aggregate interlock capacity in large members that causes the size effect in shear.”

In another experimental investigation “to test the hypothesis that effective depth influences the shear strength of reinforced concrete (RC) beams.” Sneed and Ramirez (2014, pp. 157-158) attributed “the observed size effect” in the “observed reduction in shear strength with increasing effective depth” to the “lack of geometric scale in the cracking behaviou”. This “lack of geometric scale” in the cracking behaviour was because the concrete cover remained constant for all the eight beams tested while the effective depth was scaled. Flexural crack spacing is a function of the concrete cover to the centroid of the

longitudinal steel reinforcing and is not a function of the effective depth. However, in the investigation, the concrete cover remained constant for all eight beams tested while the effective depth was scaled. The investigators observed that the flexural crack spacing remained the same for all eight beams while the effective depth was scaled. Since “in beams arch action occurs outside the outermost cracks” and the crack patterns were not scaling in proportion to the change in effective depth, it follows that the tied arch shear resisting mechanism in beams will also not scale in proportion to the change in effective depth. This is the reason cited for the “observed size effect in shear”.

Ruiz, Muttoni and Sagaseta (2015, pp. 363-371) performed various numerical integrations of the stresses developed along the full length of the critical shear crack and developed equations for ‘the contribution of the various shear transfer actions to the shear strength” of a rectangular beam without shear reinforcement”. These equations were then analysed to determine how the various shear transfer actions “are influenced by the size and level of deformation of the member”. The shear transfer actions analysed were:

- cantilever action
- aggregate interlock
- dowelling action
- residual tensile strength of concrete
- arching action

The authors argue that “size effect exhibits a significant influence on the shear strength of members without transverse reinforcement” and “the critical shear crack theory (CSCT) accounts directly for size and strain effects”.

### 2.11 Models (Theoretical Framework) of Aggregate Interlock

Walraven (1980) developed a mathematical model for aggregate interlock strength at the shear crack interface and also conducted experimental investigations to verify the model. By idealising aggregate particles as spheres, the model predicts the frictional resistance (aggregate interlock) at the crack interface as a function of the crack width, maximum aggregate size and concrete strength. He also showed that aggregate interlock contributed

to shear strength for crack widths up to 0.9 mm. The model affords researchers with a means to quantify into their models the shear resistance due to aggregate interlock.

Walraven's model is based on the following assumptions:

- The aggregate particles are spherically shaped.
- The aggregate particles are randomly orientated in the concrete so that no preferred directions exist.
- The overall crack plane is a flat plane.
- The stress-strain relation of the matrix material is rigid-plastic.
- The aggregate particle distribution is according to the Fuller curve.
- Aggregate interlock strength is generated by the frictional resistance between the spherical aggregate particles and the concrete matrix.

Walraven's model has been applied to various shear strength models to calculate the aggregate interlock strength at the shear crack. Shear strength formulations based on compression field theories use Walraven's model to calculate the aggregate interlock strength component of shear strength at the crack interface. The simplified modified compression field theory by Bentz, Vecchio and Collins (2006) and the modified compression field theory by Vecchio and Collins (1986) use the Walraven model to calculate the aggregate interlock strength component of shear strength at the crack interface. The simplified modified compression field theory has found application in the Canadian code A23.3 (2004) - Design of Concrete Structures.

## 2.12 Incorporation of Aggregate Properties into Codes of Practice Clauses on Shear Strength of Beams Without Shear Reinforcement

### 2.12.1 South African Code SANS10100-1 (2000)

The maximum shear resistance of a cross section of a beam without lateral shear reinforcement is given in terms of the maximum average shear stress:

$$v_c = \frac{0.75}{\gamma_m} \cdot \left(\frac{f_{cu}}{25}\right)^{\frac{1}{3}} \cdot \left(\frac{100 \cdot A_s}{b_v \cdot d}\right)^{\frac{1}{3}} \cdot \left(\frac{400}{d}\right)^{\frac{1}{4}}$$

where:

$\gamma_m = 1.4$ is the partial safety factor for materials (limit state design)

$f_{cu}$ = characteristic cube strength of concrete $\leq 40$ MPa

$$\left(\frac{100 \cdot A_s}{b_v \cdot d}\right)^{\frac{1}{3}} \leq 3$$

$A_s$ = area of properly achored tension reinforcement at the cross section

$b_v$ = average width of section (below flange)

$d$ = effective depth

The limitation of $f_{cu} \leq 40$ MPa is an acknowledgement of reduced shear strength for high strength concretes. This reduction in shear strength is confirmed in the literature review and is attributable to an increase in aggregate fracture at the shear crack interface for high strength concrete.

### 2.12.2 American Code ACI 318-19 (2019)

The maximum shear resistance, in US customary units, of a cross section of a beam without lateral shear reinforcement is specified in terms of the maximum shear force (lb), which is:

$$V_c = \left[8 \cdot \lambda_s \lambda \cdot (\rho_w)^{1/3} \cdot \sqrt{f_c'} + \frac{N_u}{6 \cdot A_g}\right] \cdot b_w \cdot d \quad (in\ lb) \quad \leq 5 \cdot \lambda \cdot \sqrt{f_c'} \cdot b_w \cdot d$$

where:

$\frac{N_u}{6 \cdot A_g}$ is a term for axial or prestressing loads

$$\lambda_s = \sqrt{\frac{2}{1 + \frac{d}{10}}}$$

$\leq 1$ is a size effect modification factor (from fracture mechanics)

$\lambda$ is a modification factor for lightweight concrete, varying between 0.75 to 1.0, depending on the composition of the aggregates.

$\rho_w = \frac{A_s}{b_w \cdot d}$ where $A_s$ is the area of anchored tensile reinforcement at the cross section

$f_c' \leq 100\ psi$ *is* the specified compressed strength

$b_w =$ web width

$d =$ effective depth

The inclusion in the code of the modification factor λ based on the aggregate composition is a clear demonstration that the code does recognise that the shear strength of a beam is influenced by the type of aggregates used. Furthermore, the limitation of $f_{cu} \leq 100$ psi is an acknowledgement that aggregate fracture occurs in high strength concretes, thereby reducing the contribution of the aggregate interlock to the shear strength.

### 2.12.3 Eurocode EN 1992-1-1: (2004) (E)

The maximum shear resistance at a cross section of a beam without lateral shear reinforcement is specified in terms of the maximum shear force:

$$V_{Rd,c} = \left[C_{Rd,c} \cdot \eta_1 \cdot k \cdot \sqrt[3]{100 \cdot \rho_l \cdot f_{ck}} + k_1 \cdot \sigma_{cp}\right] \cdot b_w \cdot d \quad (in\ N)$$
$$\geq \left(v_{min} + k_1 \cdot \sigma_{cp}\right) \cdot b_w \cdot d$$

Where $C_{Rd,c} = \dfrac{0.18}{\gamma_c}$ for normal concrete and $C_{Rd,c}$

$= \dfrac{0.15}{\gamma_c}$ for lightweight concrete

$\eta_1$ is only applicable to light weigh aggregate concrete (LWAC) and

$\eta_1 = 0.40 + 0.6 \cdot \dfrac{\rho}{2200}$ where ρ is the density of the light weight aggregate concrete

$$k = 1 + \sqrt{\frac{200}{d}} \leq 2.0 \quad (d \text{ in mm})$$

$\rho_l = \dfrac{A_{sl}}{b_w} \leq 0.02$ and

$A_{sl} =$ area of anchored tensile reinforcement at the cross section (mm)

$k_1 \cdot \sigma_{cp}$ is a term for axial or prestressing loads

$b_w$ is the smallest width of the cross section in the tensile area (mm)

$d =$ effective depth of the cross section (mm)

$f_{ck}$ = Characteristic compressive cylinder strength of concrete at 28 days (MPa)

$v_{min} = 0.035 \cdot k^{\frac{3}{2}} \cdot f_{ck}^{\frac{1}{2}}$ for normal concrete and

$v_{min} = 0.030 \cdot k^{\frac{3}{2}} \cdot f_{ck}^{\frac{1}{2}}\ for\ LWAC$

$\gamma_c = p$artial factor for concrete (in limit state design)

It can be observed from the above formulation that the coarse aggregate can indeed influence the shear strength of the beam. The inclusion of the $\eta_1$ factor for lightweight aggregates (which includes both fine and coarse aggregates) and the specification of a different $C_{Rd,c}$ values for normal concrete and lightweight concrete demonstrates that the code does recognise that the shear strength of a beam is influenced by the type of aggregate.

### 2.12.4 Canadian Code CSA A23.3 (2004)

The calculation of maximum shear resistance of a cross section of a beam without lateral shear reinforcement is based on the simplified modified compression field theory. A simplified method for calculating $\beta$ is given (shown below) and a more general (and complex) method is also described in the code. The maximum shear resistance, in terms of shear force $V_c$, is given by the equation:

$$V_c = \phi_c \cdot \lambda \cdot \beta \cdot \sqrt{f_c'} \cdot b_w \cdot d_v$$

where:

$\phi_c = 0.65$ a material factor for concrete (in limit state design)

$\lambda\ is$ a factor accounting for low density concrete. Varies between $1.0 - 0.75$

$\beta = \dfrac{230}{\left(1000 + \dfrac{35 \cdot s_z}{15 + a_g}\right)}$ accounts for the shear resistance of cracked concrete

$s_z$ is a crack spacing parameter, and

$a_g$ = the specified nominal maximum size of coarse aggregate

$f_c' = s$pecified compressive strength of concrete and $\sqrt{f_c'} \leq 8$ MPa

$b_w$ = minimum effective web width

$d_v$ = effective shear depth, takrn as the greater of 0.9 $d$ or 0.72 $h$

That the aggregates influence the shear strength of the beam can be ascertained from the inclusion of the $\beta$ factor which accounts for cracked concete. It may be inferred that this factor therefore accounts for the aggregate interlock mechanism. Furthermore, the inclusion of the aggregate size variable $a_g$ in the $\beta$ term reinforces the roles of the coarse aggregate. The $\lambda$ for low density concrete is also an indicator of the influence of the type of aggregate on the shear strength. Capping the value $\sqrt{f_c'}$recognises the decrease in shear strength due to extensive aggregate fracture occurring at the crack interface in high strength concrete.

### 2.12.5 fib Model Code for Concrete Structures 2010 (2013)

The purpose of the fib Model Code is to be a source of information and contribute to the development of new structural concrete codes. The maximum shear resistance at a cross section, without prestressing, in terms of shear force $V_{Rd,c}$, is given by the equation:

$$V_{Rd,c} = k_v \cdot \frac{\sqrt{f_{ck}}}{\gamma_c} \cdot z \cdot b_w \quad (f_{ck}\ in\ MPa)$$

where,

$$k_v = \frac{0.4}{1 + 1500 \cdot \varepsilon_x} \cdot \frac{1300}{1000 + k_{dg} \cdot z}$$

$$\varepsilon_x = \frac{1}{2 \cdot E_s \cdot A_s} \cdot \left(\frac{M_{Ed}}{z} + V_{Ed}\right) \leq 0.003 \text{ and substitute } \varepsilon_x = 0\ if\ \varepsilon_x \text{ is negative}$$

$$k_{dg} = \frac{32}{16 + d_g} \geq 0.75 \qquad \text{and } k_{dg} = 1.0 \text{ for } k_{dg} \geq 16 \text{ mm}$$

$d_g$ = maximum size of aggregate particles,

but $d_g = 0\ for$ lightweight concrete or if $f_{ck} > 70$ MPa

$f_{ck}$ = characteristic value of compressive strength of concrete and $\sqrt{f_{ck}}$ $\leq 8$ MPa

$\gamma_c = s$afety factor for concrete

$z = e$ffective shear depth, assumed to be $0.9\,d$ ($d =$ effective depth in flexure)

$b_w =$ width of web

The influence of aggregates on the shear strength can be gleamed from the inclusion of the maximum aggregate size variable $d_g$ in the above formula, the limitation of $d_g = 0$ for lightweight concrete and when $f_{ck} > 70MPa$. Furthermore, capping the value of $\sqrt{f_{ck}} \leq 8\,MPa$ takes cognisance of the decrease in shear strength due to extensive aggregate fracture occurring at the crack interface in high strength concrete.

### 2.12.6 Swiss Codes SIA 262 (2003), SIA 262 (2013 - corrigenda 2017)

The code is written in the Swedish language. Muttoni and Ruiz (2007) have compared the Swiss code SIA262 (2003) shear strength predications for three beams with predictions based on the crictical shear crack theory which has been implemented in this code. The code equation for the shear strength of RC beams without lateral shear reinforcement is cited as:

$$\frac{V_{Rd}}{b \cdot d \cdot \sqrt{f_{ck}}} = \frac{0.3/\gamma_c}{1 + \frac{50}{16 + d_g} \cdot \frac{f_{yk}}{\gamma_s \cdot E_s} \cdot d \cdot \frac{m_{Ed}}{m_{Rd}}} \quad \text{[SI units: MPa, mm]}$$

where $d_g =$ aggregate size

In the SIA (2013 - corrigenda 2017) version of the code the shear resistance is given as:

$$V_{Rd} = k_d \cdot \tau_{cd} \cdot d_v$$

where,

$$k_d = \frac{1}{1 + \varepsilon_v . d \cdot k_g}$$

$$k_g = \frac{48}{16 + D_{max}}$$

$D_{max} =$ maximum grain in concrete. $D_{max} = 0$ for lightweight concrete.

$\tau_{cd} = \frac{0.3 \cdot \eta_t \cdot \sqrt{f_{ck}}}{\gamma_c}$ is the shear stress limit

$d =$ static height

$d_v = e$ffective static height

$\eta_t = 1\ is$ a load duration factor

Both editions of the code are based on an implementation of the critical shear crack theory in which aggregate interlock plays a prominent role in resisting shear. As can be seen from the above equations the shear resistance of a beam without lateral shear reinforcement is a function of the maximum aggregate size amongst many other variables and the shear resistance is reduced for lightweight aggregates.

## 2.13 Discussion and Conclusion

From the preceding literature review in this chapter it can be concluded that the shear strength of a concrete beam without shear reinforcement is influenced by the coarse aggregates in the beam. The coarse aggregate type influences the shear strength, coarse aggregate fracture may reduce the shear strength, and the maximum size of the aggregate influences the shear strength. No investigation of the influence of local aggregates (Durban) on the shear strength of beams without lateral shear reinforcement was found in the literature.

# CHAPTER 3:EXPERIMENTAL PROGRAM

## 3.1 Introduction

Experimental tests were conducted to investigate the influence of coarse aggregate type on the shear strength of reinforced concrete beams without shear reinforcement, for the following three coarse aggregates types commonly used in Durban:

1) Dolerite
2) Natal group quartzite, and
3) Tillite

These coarse aggregates differ from each other in crushing strength, crushed shape, surface texture, geological origin and structure and a variation in the aggregate interlock component of the shear strength may thus be anticipated. By controlling the parameters known to influence shear strength, which were determined from the literature study, it may then be inferred that any statistically significant variation in shear strength, if any, may be due to the variation in aggregate type.

The experimental program was designed to investigate the variation in shear strength with respect to:

1) Aggregate type,
2) Aggregate size, and
3) Concrete strength.

## 3.2 Methods of Experimentally Determining the Shear Strength of Reinforced Concrete Beams

A search of the literature (refer to the literature review) revealed three different methods are used to investigate the shear strength of reinforced concrete beams without transverse shear reinforcement. These are:

- Push-off test
- Shear panel test
- Beam press test

### 3.2.1 Push-off Test

Push-off tests are a type of test used to measure the shear resistance of reinforced concrete. Push-off tests directly measure the force required to overcome aggregate interlock (friction) at the crack interface for a **constan**t crack width. Typical push-off test arrangements are shown in Figure 3-1 below.

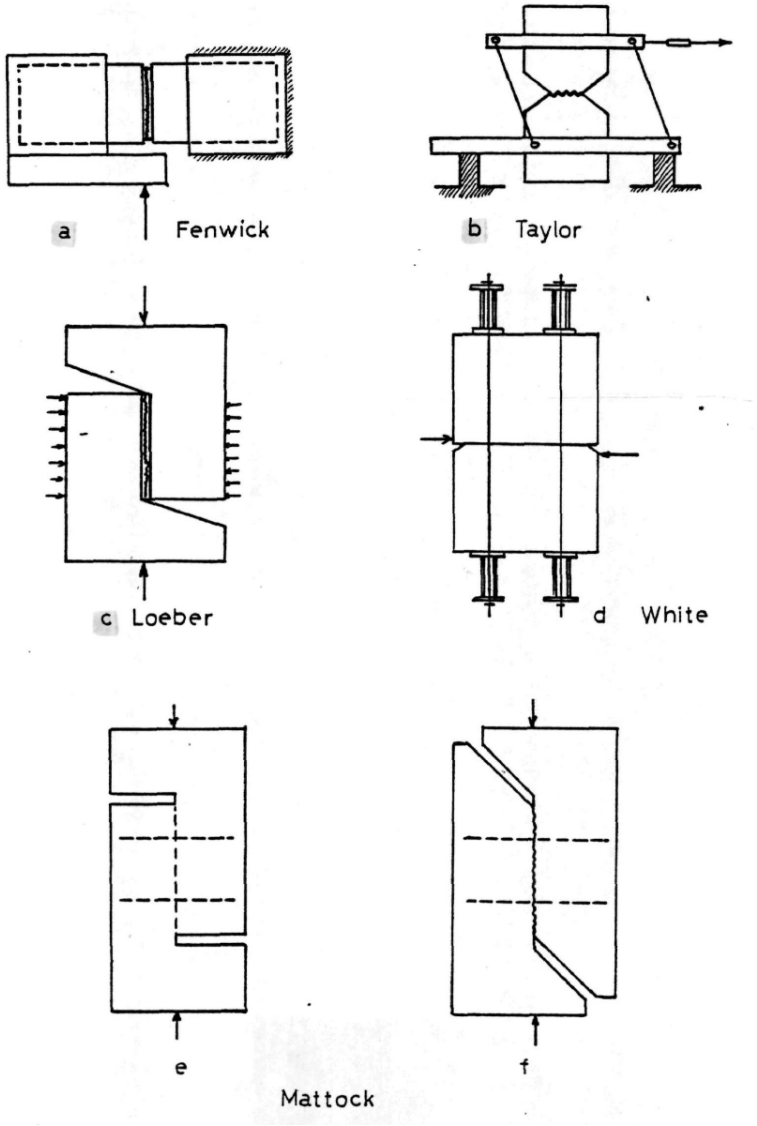


**Figure 3-1: Sketches of various push-off test arrangements as depicted by Walraven**
Source: Walraven, Vos & Reinhardt **(1979, p. 4)**

A concrete block is cast with a preformed groove on the surface of the block, diving the block into two symmetrical sections. A typical push-off test specimen (concrete block) is shown in Figure 3-2. An oversize rod is placed over the grove on the surface of the block and a force, perpendicular to the

block, is applied on the surface length of the rod so as to split the block along the length of the groove but without allowing the two pieces to separate and ensuring the two crack surfaces remain fully in contact. A clamping force, perpendicular to the crack line (groove), is then applied oppositely to each half, thus holding the two cracked halves together. Thereafter, a transverse force P (shear force), as shown in Figure 3-2, parallel to the crack line is applied to the cracked pair and the transverse force and opening of the crack is measured. The transverse shear force is the aggregate interlock force (shear force) and the opening of the crack parallel to the normal force is the crack width. The transverse force P (shear force) is gradually increased until the two pieces slip at the crack interface and the maximum shear force P for the given clamping force is recorded.

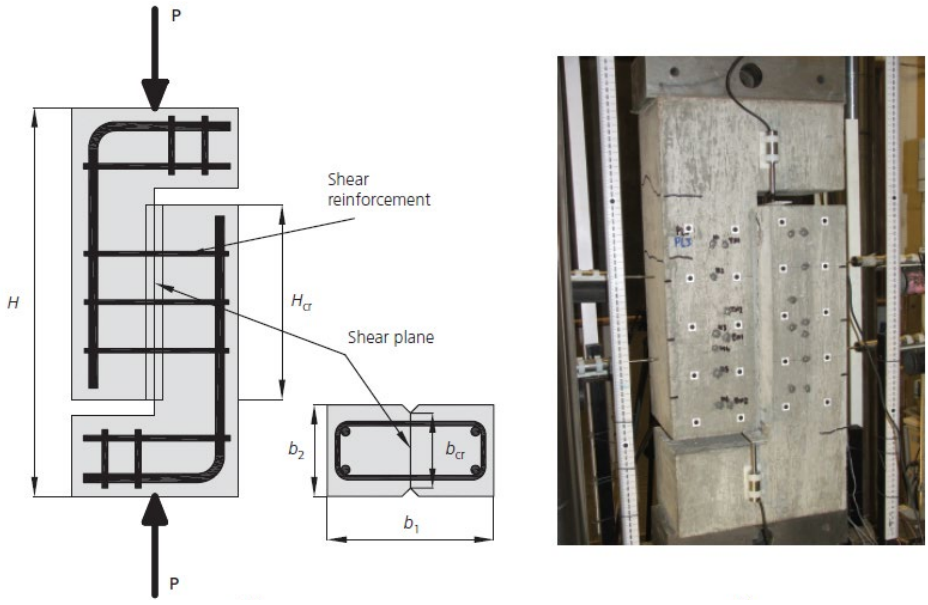


**Figure 3-2: A type of push-off test conducted by Sagaseta & Vollum**
Source: Sagaseta & Vollum (2011, p. 120)

### 3.2.2 Shear Panel (Membrane Element) Test

Another type of shear test is the shear panel test where a square reinforced concrete panel specimen is subjected to direct shear or torsional stresses along the perimeter of the panel. The shear panel test arrangement shown in Figure 3-3 was used by Vecchio and Collins (1986, p. 223) to validate their modified compression field theory.

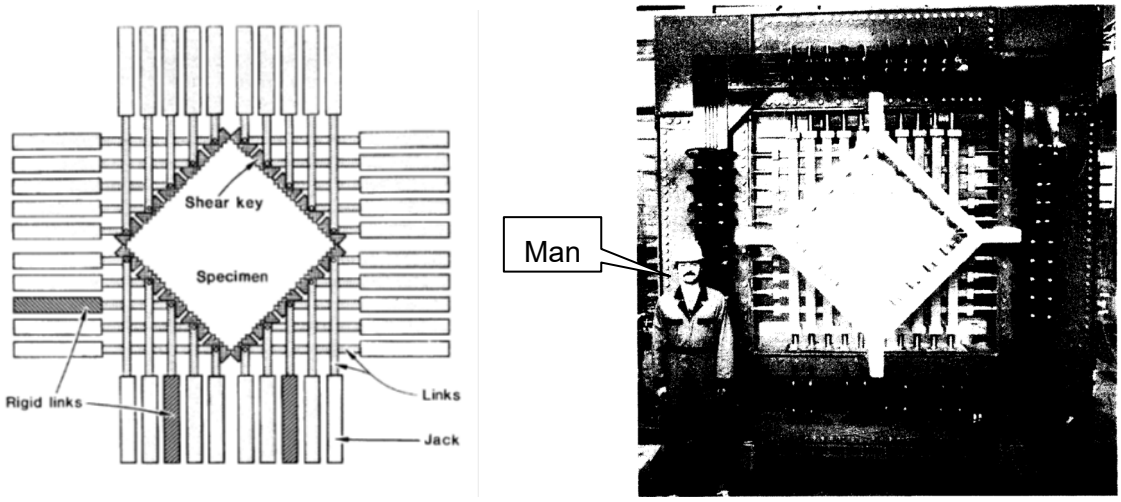


**Figure 3-3: A type of shear panel (membrane) test by Vecchio & Collins. A jack and link assembly is used to apply a shear force on the concrete panel (membrane element) (left). The picture on the right, with the man at the bottom left corner, gives an indication of the size of the shear panel (membrane element) testing rig**
Source: Vecchio & Collins (1986, p. 223)

A very large specialised purpose-made rig is required and therefore these tests are not common in the literature.

### 3.2.3 Beam Press Test

A beam press test is the most common type of shear test used to measure the **actual** shear resistance of a reinforced concrete beam.

A lateral shear load is applied to a reinforced concrete beam using a beam press. The lateral shear load is gradually increased until failure of the beam occurs (usually in shear). Beam press tests provide a direct measure of the shear strength of the beam for a given loading arrangement. If strain gauges are attached to the beam the crack width and deformation of the beam can be measured. The beam press test apparatus available at DUT is shown in Figure 3-4 below.


**Figure 3-4: DUT's beam press apparatus**

## 3.3 Selection of an Experimental Test Method

In Table 3-1 below, the types of shear tests conducted in some of the studies referenced in the literature review, are tabulated.

**Table 3-1: Types of shear tests conducted in some of the experimental programs referenced in the literature review**

| Reference Study | Coarse Aggregate (mm) | Considers Aggregate Interlock Action | Type of Shear Test | | | No. of specimens |
|---|---|---|---|---|---|---|
| | | | Push-off test | Beam press test | Shear panel test | |
| (Taylor & Brewer, 1963) | ¾ in. river gravel, ⅜ in. expanded clay & ⅜ in. sintered pulverised-fuel ash | | | ✓ | | 36 beam tests |
| Fenwick (1966) | alluvial gravels (greywacke) | ✓ | ✓ | ✓ | | 35 push-off tests & 1 beam test |
| Taylor (1974) | unspecified | ✓ | ✓ | ✓ | | 9 beam tests, 2 direct aggregate. interlock tests on beams & unspecified no. |

| | | | | | | |
|---|---|---|---|---|---|---|
| | | | | | | of push-off tests |
| Paulay & Loeber (1974) | 9.5 mm or 19 mm round or 19 mm crushed alluvial gravel | ✓ | ✓ | | | 44 |
| Hamadi & Regan (1980) | 5 mm to 20 mm gravel or exp. clay or exp. slate | ✓ | ✓ | ✓ | | 14 beam & 11 push-off tests |
| Vecchio & Collins (1986) | | | | | ✓ | 30 |
| (Muttoni & Schwartz, 1991) | | ✓ | | | | 0 |
| Sherwood, Bentz & Collins (2007) | 9.5 mm, 19 mm, 38 mm or 51 mm crushed limestone | ✓ | | ✓ (large beam & 1/5 scaled model) | | 10 large scale & 10 1/5 scaled model |
| Emiko, et al. (2011) | Unspecified size leca (exp. clay) | ✓ | ✓ | | | 14 series of 3 specimens |
| Yang, et al. (2011) | 8 mm, 13 mm or 19 mm andersite or exp. clay | ✓ | | ✓ | | 12 |
| Sagaseta & Vollum (2011) | 10 mm max. crushed limestone or marine dredged gravel | ✓ | ✓ | | | 6 |
| Rodrigues (2012, pp. 753-756) | 16 mm max. gravel | ✓ | ✓ (on cores from beams) | ✓ | | 11 beam & 9 push-off tests |
| Knaack & Kurama (2015) | 19 mm max. crushed limestone or 19mm max recycled aggregate from a demolition recycling plant | × | | ✓ | | 12 normal concrete beams & 12 recycled concrete beams |
| Arezoumandi, et al. (2015a) | 25 mm max. crushed limestone or 25mm recycled aggregate | × | | ✓ | | 18 |

| | | | | | | |
|---|---|---|---|---|---|---|
| Arezoumandi, et al. (2015b) | 19 mm crushed limestone | × | | ✓ | | 32 |
| Hassan, Ismail & Mayo (2015) | 10 mm and 20 mm unspecified crushed stone, 12.5 mm LW expanded slate or 10 mm LW slag | × | | ✓ | | 16 |
| Roskos, White & Berry (2015) | 3.2 mm to 9.5 mm pulverised glass | briefly on page 5 | | ✓ | | 8 shear specimens |
| Savaris & Pinto (2017) | 9.5 mm or 19 mm. crushed granite | ✓ | | ✓ | | 18 |

### 3.3.1 Suitability Assessment of a Beam Press Test for this Study

It can be observed from Table 3-1 above that the beam press test is the most commonly used test for investigating shear strength mechanisms and/or parameters.

For a determinate beam, depending on the support conditions, the shear resistance of the beam is a function of the applied load, the position of the applied load and the support reactions. Therefore, if the supports of a beam tested in a beam press match those of a simply supported beam then the shear resistance will be a direct function of the applied point load P and the position of the point load on the beam. Both of these variables are easily measurable in a beam press test, rendering the beam press test a suitable test for determining the shear resistance of a beam.

A small-scale beam press was available at DUT, but the maximum possible simply supported beam span was too small for the purposes of this study. A much larger press was available at the University of KwaZulu-Natal (UKZN) and with simple adaptation the press was used for this study.

### 3.3.2 Suitability Assessment of a Push-off Test for this Study

Push-off tests are common tests, especially for investigating aggregate interlock properties, but require special purpose-made loading equipment, moulds and high precision instrumentation that was not accessible/available for this study. Furthermore, in push-off tests, it is not realistically possible to

achieve a varying crack width in the specimen during a push-off test and the test is therefore done for a constant crack width whereas the diagonal shear crack in a beam is always of varying crack width. A further consideration is that push-off tests only measure the aggregate interlock (shear friction) component of shear resistance and do not take into consideration bending stresses present in a beam. Therefore, the shear resistance of the push-off specimen would not be the same as the shear resistance of a beam. Therefore, push-off tests were deemed unsuitable for this investigation.

### 3.3.3 Suitability Assessment of a Shear Panel (Membrane Element) Test for this Study

A shear panel test measures the shear resistance of a concrete panel (membrane) in pure shear or torsion. Since a beam resists both shear and bending stresses at the same time the shear resistance obtained from a shear panel test would not be the same as the shear resistance of a beam.

Furthermore, no shear panel test rig, which is a large sophisticated purpose-made rig, was accessible/available for this study.

### 3.3.4 Adoption of a Test Method for this Study

Based on the above assessment of the different test methods, **the beam-press test method** of determining the shear resistance of a reinforced concrete beam **was adopted** for the experimental component of this study.

## 3.4 The Shear Strength Parameters Varied in this Experimental Investigation (the Independent Variables)

For the purpose of this experimental program, the influence of the following concrete parameters on the shear strength of reinforced concrete beams without transverse shear reinforcement were independently investigated.

### 3.4.1 Concrete Strength

Concrete beams specimens having the same type of aggregate and aggregate size were manufactured in the following strength gradations:

- 30 MPa
- 40 MPa
- 50 MPa

The chosen strength denominations are commonly specified in “normal strength concrete” structural applications in South Africa. 30MPa is commonly specified for reinforced concrete slabs which are usually designed as beam strips. Concrete strength beyond 50 MPa would be classified as high strength concrete and requires the addition of silica fume.

### 3.4.2 Coarse Aggregate Size

Concrete beam specimens made from the same type of coarse aggregate and “same” concrete strength were manufactured in the following aggregate size gradations:

- 13.2 mm maximum size continuously graded aggregate
- 19 mm maximum size continuously graded aggregate

Larger coarse aggregate size denominations place limitations on the reinforcing steel spacing and are therefore not commonly specified in South Africa.

### 3.4.3 Coarse Aggregate Type

Concrete beam specimens made from the “same” concrete strength and same size of aggregate were manufactured from the following three types of coarse aggregate:

- quartzite from NPC Coedermore quarry, south of Durban
- tillite from Lafarge Ridgeview quarry in Cato Manor
- dolerite from Ballito Crushers quarry

These are the coarse aggregate types available in Durban.

## 3.5 The Shear Strength Parameter Measured in this Experimental Investigation (the Dependent Variable)

The dependent variable for this investigation was the maximum point load **P** that resulted in the failure of the beam, as annotated in Figure 3-5 below.

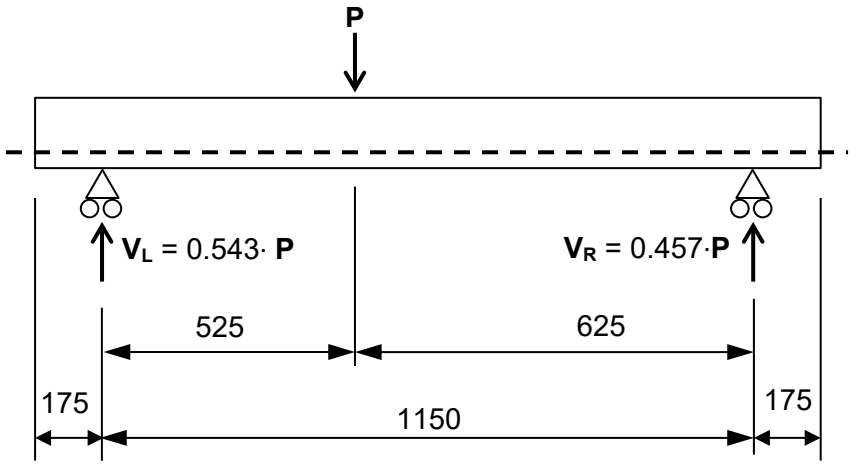


**Figure 3-5: The point load** P **is the dependent variable. Also shown are the position of the point load** P **on the beam, the span of the beam and the support reactions (shear force) in terms of the dependant variable P**

From the statics and geometry of the simply supported beam, loading and supports, the maximum shear force in the beam is easily calculated to equal $\mathbf{V_L}$ = 0.543· **P**.

## 3.6 The Shear Parameters Controlled in this Experimental Investigation (Variables Kept Constant)

In order to compare the influence of the three selected variables on the shear strength of a reinforced concrete beam without shear reinforcement, the following parameters, which from the literature review have been determined to influence the shear strength of the beam, were kept the same (constant) for all beams:

- Fine aggregate – the same type of fine aggregate and the grading were used to manufacture all beam specimens.
- Cement – the same type of cement binder was used to manufacture all beam specimens.
- Reinforcing steel – the same type, grade, diameter, spacing, cover and percentage ratio of reinforcing steel was used to manufacture all beam specimens.
- Spacing and cover of reinforcing steel (dowel action and bond strength) – the same spacing and cover of reinforcing steel bars was maintained for all beam specimens.

- Beam width and depth – the total height, effective depth and width of all the beam specimens were the same.
- Beam span (a/d) ratio – the spans of all the beam specimens, and therefore the beam span ratio a/d were the same for all beam specimens. The beam span ratio (a/d) for this experimental program was specifically chosen within the “Kani valley” to ensure shear failure of the beam occurs and not flexural failure.
- No admixtures were added to the mix designs.

## 3.7 Description of the Experimental Program to Study the Influence of Coarse Aggregate Type and Size on the Shear Strength

Shear tests, using a beam press, were carried out on a total of 18 reinforced concrete beams without lateral shear reinforcement, varying the concrete strength, aggregate size and aggregate type as described in sections 3.4.1, 3.4.2 and 3.4.3 respectively. The three types of coarse aggregate chosen are commonly used to manufacture concrete in Durban.

### 3.7.1 Trial Beam

Prior to the casting of the 18 beams, a single trial beam was cast and tested to failure. The purpose of the trial beam was to validate the process, iron out any unforeseen or “teething” problems and to refine the experimental program where necessary. Some of the problems identified during the trial beam process were:

- The top edges of the mould bowed out about to 5 mm after the concrete was poured. This was rectified by adding a bracket to hold the top edges of the mould in place while the concrete was poured (see Figure 3-6).
- The fine and coarse aggregates, which were supplied bagged, were found to have had varying water content from bag to bag and this deleteriously impacted on the mix design and slump. Thereafter all the fine and coarse aggregates were completely dried out in the midday sun on a concrete surface bed, re-bagged and stored indoors for later use.

- The capacity of the electric drum concrete mixer initially chosen was a fraction too small after the inevitable wastage and loss that occurred when concrete was poured into the beam & cube moulds. This was rectified by using the slightly larger capacity electric drum concrete mixer available at DUT.
- During handling of the trial concrete beam for transport to UKZN, the labourers instinctively turned the beam over and wanted to use the protruding reinforcing bars as “handles” for lifting the beam. This resulted in a dowel crack forming at one end of the trial beam. The labourers were advised against this practice and transport of the beams was thereafter carefully supervised.

### 3.7.2 Concrete Moulds

Nine beam moulds were constructed from 21 mm thick resin coated Marineplex plywood shutterboard. Resin coated plywood shutterboard was selected because it is reusable, non-absorbent and produces a smooth off shutter concrete finish which makes cracks appearing during loading of the beams more visible.

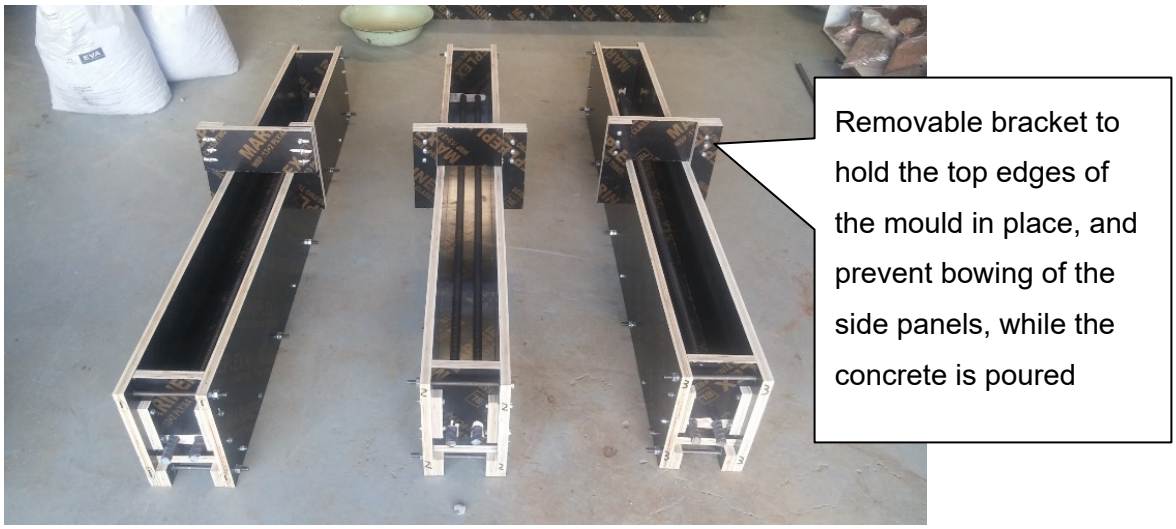


**Figure 3-6: Reusable beam moulds ready for use**

The design of the mould, using removable bolts to hold together the sideboards and floorboard, facilitated easy stripping of the mould to remove the concrete beam, and reassembly of the mould to cast the next beam.

**Figure 3-7: Beam moulds were designed for sturdiness when pouring concrete, easy disassembly and to maintain a constant reinforcement cover**

### 3.7.3 Concrete Cubes

Concrete cubes for testing cube strength were cast and cured in accordance with SANS 5861-3 (2006), as applied to laboratory specimens. Three cubes per beam were cast using standard 150 mm x 150 mm x 150 mm steel cube moulds and cured in a temperature-controlled bath. Testing of the concrete

cubes was carried out in accordance with SANS 5863 (2006). All cubes were cast, cured and tested at Geosure Laboratories, an ISO 17025 SANAS accredited laboratory.

### 3.7.4 Reinforcing Steel

All 18 beams were reinforced with two Y20 longitudinal reinforcing bars (refer to Figure 3-6, Figure 3-7 and Figure 3-8).

The characteristic yield strength of the reinforcing bars was $f_y$ = 455 MPa. No transverse shear reinforcement (stirrups) was provided. Since the shear strength of the beam is a function of the effective depth, which was a constant in this investigation, it was imperative to ensure the effective depth remained the same for all 18 beams. This was achieved by utilising straight, shape code 20, reinforcing steel bars that were longer than the beam and therefore protruded out of the finished beam at the ends. The ribbed diameter of the bars was 22 mm. Two 22 mm diameter holes were drilled through each end panel shutter board of the mould. The straight reinforcing steel bars were pushed thorough these holes which also held them firmly in place at the correct cover distance (see Figure 3-9). No cover blocks were required since the Y20 bars were straight and rigid enough to span the 1500 mm length of the mould with negligible sagging. Furthermore this also ensured that the horizontal spacing, horizontal position and vertical position of the two Y20 bars were identical for all 18 beams. Straight bars were preferred over bars with hooked ends since the latter would have required cover blocks and could have moved out of position while the concrete was being cast or vibrated.


**Figure 3-8: Y20 longitudinal steel reinforcing bars used for all beams**

The overall length of the beam and the position of the supports were calculated so the straight bars had adequate anchorage length.

Some of the steel reinforcing bars were completely free of rust while other bars had minimal spots/areas of rust, which would have been passivated by the alkalinity of the concrete.

**Figure 3-9: Straight Y20 reinforcing steel bars passing through 22 mm diameter holes at the beam ends of the mould, maintain a constant effective depth and bar spacing for all beams**

### 3.7.5 Concrete Materials

#### 3.7.5.1 Cement

The cement used was 50 kg bagged NPC Original Black CEM II/B-S 42.5 N as shown in Figure 3-10 below.


**Figure 3-10: Sample of the type of cement used**

#### 3.7.5.2 Fine Aggregate

The fine aggregate (sand) used was sourced from Genie Sand in Umgeni Park, Durban. The sand was a river sand from Illovu, commonly referred to as “umgeni sand” within the building industry in Durban. To maintain a uniform constant fine aggregate profile for all the beams, a large single load of fine aggregate quarried at the same time, was ordered, stockpiled and used for all 18 beams. During the initial test run it was found that the water content varied considerably between bags of sand – some bags were almost drenched in water, some were partially wet and others relatively dry – this was deleterious

to the mix design and slump. Thereafter all aggregates were fully dried out in the sun on a concrete surface bed as shown in Figure 3-11 below.

**Figure 3-11: Drying of fine aggregate (sand) in the midday sun on a concrete surface bed**

#### 3.7.5.3 Coarse Aggregate

The three types of crushed continuously graded coarse aggregates tested were:

- Tillite (Figure 3-12 and Figure 3-13)
- Quartzite (Figure 3-14 and Figure 3-15)
- Dolerite (Figure 3-16 and Figure 3-17)

The coarse aggregates were procured from commercial quarries in Durban, supplied and stored in bags. During the initial test run it was found that the water content varied between bags – some bags contained dry coarse aggregate while in other bags the coarse aggregate was wetted to varying degrees – this was deleterious to the mix design and slump. Thereafter all coarse aggregates were dried in the sun on a concrete surface bed as shown in Figure 3-18 below.

**Figure 3-12: 19 mm tillite**

**Figure 3-13: 13 mm tillite**

**Figure 3-14: 19 mm quartzite**

**Figure 3-15: 13 mm quartzite**

**Figure 3-16: 19 mm dolerite**

**Figure 3-17: 13 mm dolerite**

**Figure 3-18: Drying out of a sample of coarse aggregate in the midday sun on a concrete surface bed**

#### 3.7.5.4 Water

Potable municipal tap water was used to manufacture all concrete.

#### 3.7.5.5 Cement Extenders

While no extenders were added to the concrete, the type of cement of used, CEM II/B-S 42.5N, was a slag blend. Slag cements are commonly used in Durban because of their beneficial effect on the durability of concrete.

#### 3.7.5.6 Admixtures

No admixtures were added to the concrete.

### 3.7.6 Mixing, Casting and Curing of the Concrete

To maintain a uniform concrete quality the following procedure was adhered to for the fabrication of all the concrete beams:

#### 3.7.6.1 Mix Designs

All concrete mix designs were prepared by Geosure (Pty) Ltd in Durban, and were based on the C&CI method described in Fultons Concrete Technology (Addis & Goodman, 2009, pp. 219-227).

### 3.7.6.2 Concrete Slump

Concrete mix designs were proportioned to have a slump of 90 mm to improve workability and prevent segregation of the coarse aggregate. A slump test was done for every batch of concrete, i.e. each beam, prior to casting of the beam. The slumps tests for the 30 MPa and 40 MPa concrete varied between 70 mm and 110 mm. Slump tests for the 50 MPa concrete were very low, and varied between 10 mm and 60 mm, making workability of the 50 MPa concrete difficult. However once the 50 MPa concrete was scooped into the moulds and poker vibrated, workability was markedly improved. Despite the low slump, when the 50 MPa beams were tested to failure, no honeycombing or air voids were observed in any of the beams nor was there any evidence of segregation of the aggregate in the cross sections where failure had occurred. The lowest slumps were for the tillite aggregates and can be attributed to the higher crusher dust content in tillite aggregates as compared to the quartzite of dolerite aggregates.`

### 3.7.6.3 Mixing of the Concrete

- An electric powered rotating drum model CMJ19E Turner Morris concrete mixer was used to mix the concrete. The mixer had a capacity to mix approximately 85 litres of concrete at a time.
- Prior to mixing of a batch of concrete the drum was inspected to ensure it was clean, free of foreign objects and dry. After mixing and placement of a batch of concrete the mixer drum was thoroughly washed clean and allowed to dry.
- The correct mass of cement, coarse aggregate and fine aggregate were weighed separately into plastic bags to an accuracy of 0.01 kg using an electronic digital scale with a capacity of 150 kg. Similarly, the correct mass of water was weighed into a bucket specially reserved for this purpose.
- First, the dry coarse and fine aggregates were placed into the drum and mixed together until they appeared to be uniformly distributed. During mixing a cover was held over the drum opening to prevent loss

(spillage) of materials. Thereafter the dry cement powder was gradually added in small increments into the drum and mixed with the dry aggregates until the aggregate and cement mixture appeared to be homogeneous and uniform. While the cement powder was being mixed, a cover was held over the drum opening to prevent cement loss.

- Thereafter the weighed out water was gradually added to the drum, in small increments, while the drum was rotating. Precaution was taken to prevent spillage of the water since water loss would negatively impact on the mix design.
- At intermittent intervals, the mixer drum was stopped, inspected and any dry material stuck to the drum walls or behind the drum paddles were pried loose, using a trowel or tamping rod, to ensure complete and uniform mixing of the aggregates, cement and water.
- After all the mixture had been fully and uniformly wetted and the concrete had achieved a uniform, homogeneous consistency, a slump test was performed.
- Thereafter the concrete was poured into a clean dry wheel barrow and taken for casting into the mould.
- Immediately after the concrete was placed, the mixer drum was thoroughly washed clean and the drum opening turned downwards and allowed to dry.

Figure 3-19 to Figure 3-27 illustrate the above steps.

**Figure 3-19: All the concrete constituent materials were weighed in bags**

**Figure 3-20: Cement, sand and aggregate ready for mixing**

**Figure 3-21: Mixing of the concrete in an electric drum mixer**

**Figure 3-22: Slump tests being performed**

**Figure 3-23: Concrete transported from mixer to moulds in a wheelbarrow**

**Figure 3-24: Placing of concrete into moulds**

**Figure 3-25: Vibration of concrete in moulds**

**Figure 3-26: Preparation of cubes while concrete was placed in moulds**

**Figure 3-27: Drum washed out before next batch of concrete is mixed**

### 3.7.6.4 Casting of Concrete

- The resin coated Marineplex laminated plywood moulds were washed and cleaned after any previous use, re-assembled, and coated with a concrete releasing oil prior to pouring of concrete into the moulds.
- The concrete was scooped from the wheel barrow and placed into the mould, described in Section 3.7.2, for casting beams 1500 mm long x 200 mm wide x 200 mm high in dimension.
- Immediately after the concrete was cast into the beams moulds, the concrete was vibrated using a petrol powered 26 mm poker vibrator until the entrapped air surfaced.
- Excess concrete was removed and the concrete surface lightly floated to ensure that the height of all the beams remained a constant 200 mm.
- Concrete in the control cubes were similarly poured and vibrated.

### 3.7.6.5 Curing of Concrete

All the beams were cast, cured and stored indoors in the Geosure laboratory building.

Since the Marinplex resin coated shutterboard is non-absorbent, no plastic wrapping or curing agent was used to cure the beam. For the first seven days while the beam remained in the mould, a daily light sprinkling of water was applied to the top of the beam, which was the only exposed concrete surface.

The moulds were stripped after 7 days and the beams carefully moved, while maintaining their as-cast upright orientation, to an area in the building reserved to store the beams for 28 days, after which they were taken for testing.

Concrete cubes were stripped from the moulds 24 hours after being cast and the set of three cubes were placed in a temperature-controlled bath to cure for the 28 days, until they were tested.

### 3.7.7 Dimensional Details of Concrete Beam Specimens

All concrete beams were 1500 mm long x 200 mm wide x 200 mm high reinforced with 2Y20 high tensile straight longitudinal steel reinforcing bars, as illustrated in

Figure 3-28 and Figure 3-29 below. The dimension, diameter, cross sectional area, position and cover of the pair of longitudinal steel reinforcement bars for all 18 beams were the same.

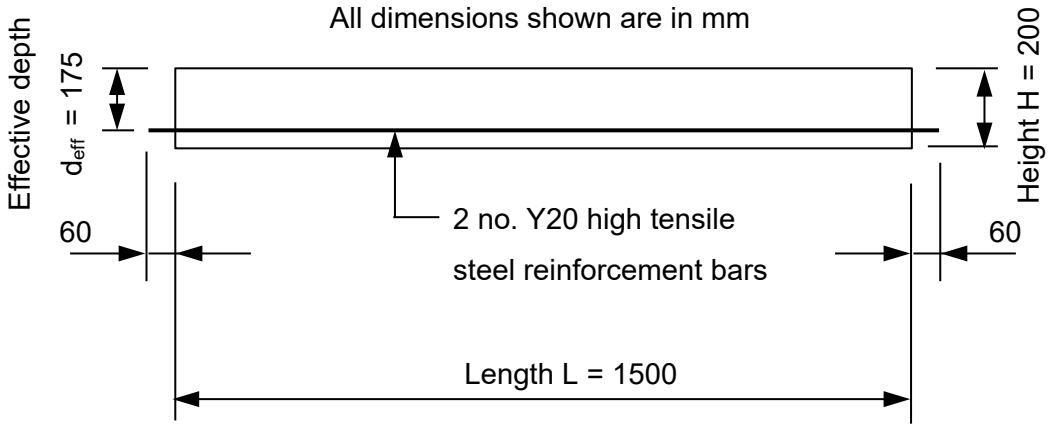


**Figure 3-28: Elevation – dimensions of the reinforced concrete beams**

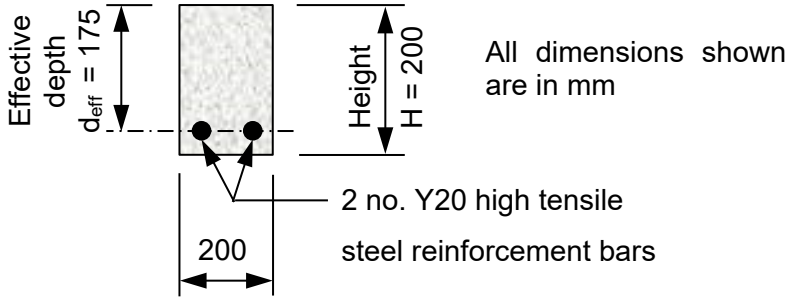


**Figure 3-29: Section showing dimensions of concrete beams**

### 3.7.8 Loading Arrangement

A single point load **P** was applied to the beam, as shown in Figure 3-30 below. The point load was positioned 100 mm closer to one support compared to the other support. The larger reaction (shear force) occurs on the smaller shear

span and therefore shear failure will occur on the shorter span, facilitating observation of the shear failure.

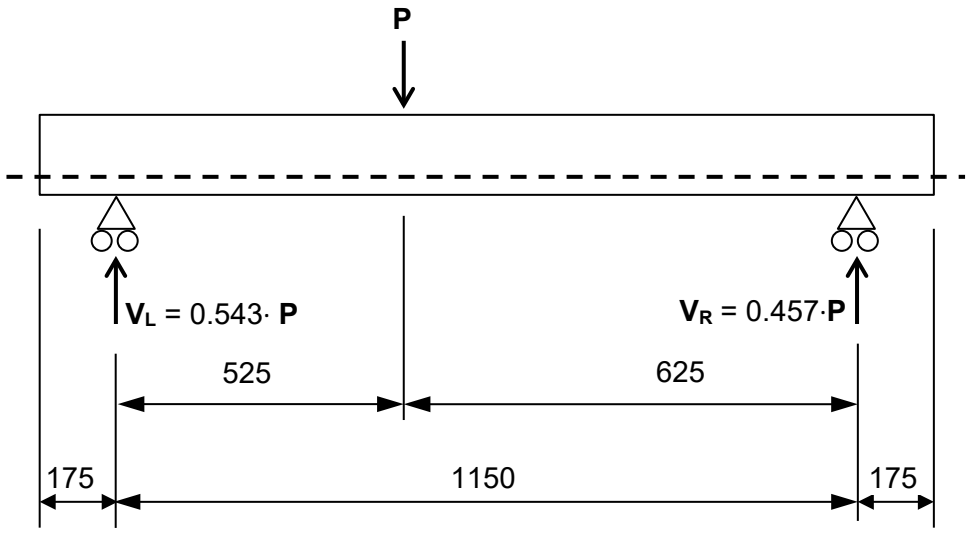


**Figure 3-30: Showing position of point load P applied to the beam and the reactions (shear force) in terms of P**

### 3.7.9 Testing Equipment, Setup and Testing Procedure

The hydraulic press at the University of KwaZulu-Natal (UKZN) heavy structures laboratory (Figure 3-31below) was used to determine the shear strength of the beams. The hydraulic press comprises a thick square presser plate at the top and a hydraulic ram at the bottom that pushes upwards. The presser plate is attached to a two column frame above ground level and can be lowered to any desired height. The hydraulic ram is located below the steel floor plates at ground level and pushes upwards onto the underside of a specially shaped floor trolley, which is rolled into position over the ram and under the presser plate.


**Figure 3-31: The hydraulic press at the University of KwaZulu-Natal (UKZN) heavy structures laboratory**

The hydraulic press was “converted” so as to be used as a beam press as shown in Figure 3-32 and Figure 3-33 below. A 305 mm x 165 mm x 31 UB x 1750 mm long steel beam was fabricated and positioned on the trolley. Two solid steel half round supports were placed into position on the steel beam. Half rounds were chosen since they allow unrestrained rotation of the beam at the supports. A concrete beam, that was to be tested, was placed into position over the supports as shown. A solid steel bar 20 mm x 20 mm x

200 mm long was then positioned on the concrete beam where the point load **P** was to be applied. Thereafter the presser plate was lowered into position just over the solid steel bar and the hydraulic ram was switched on. The load **P** that the hydraulic ram applied was gradually increased until the concrete beam failed in shear.

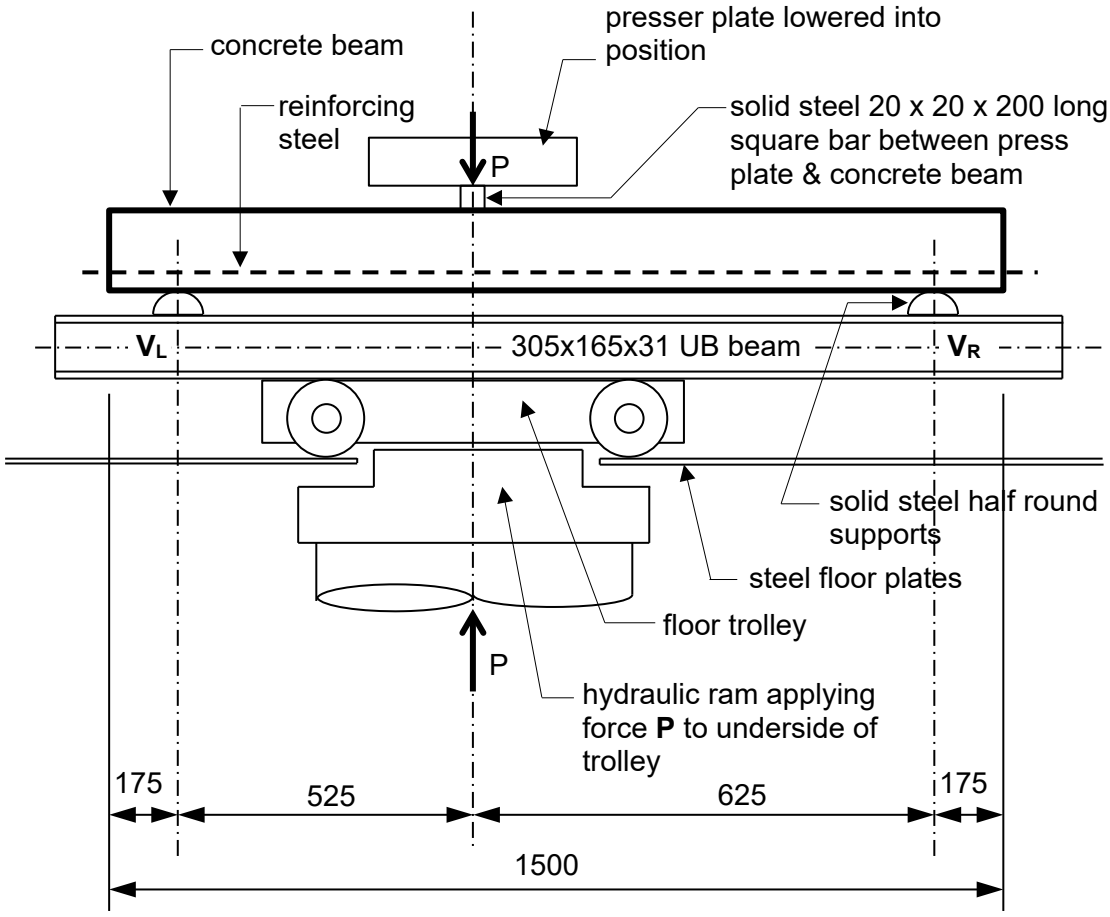


**Figure 3-32: Conversion of the UKZN hydraulic press to a beam press for this study**

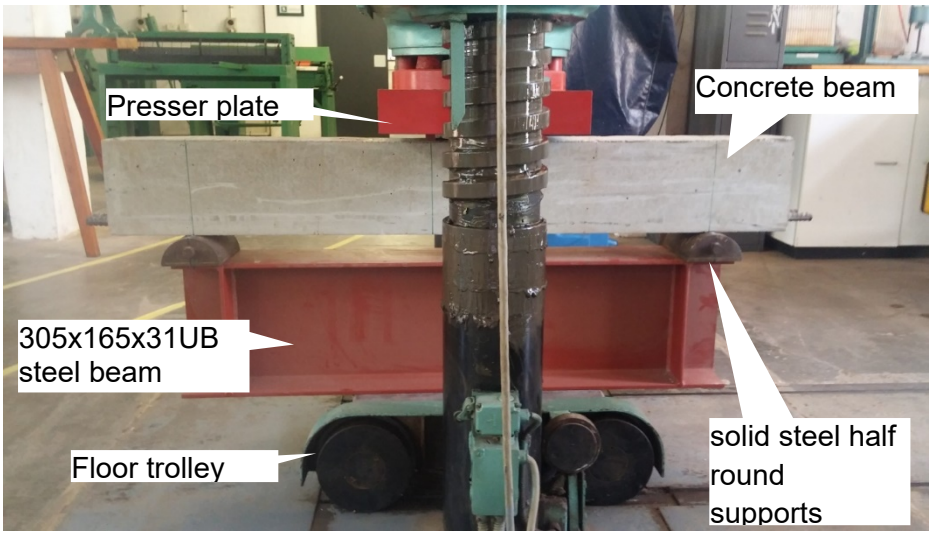


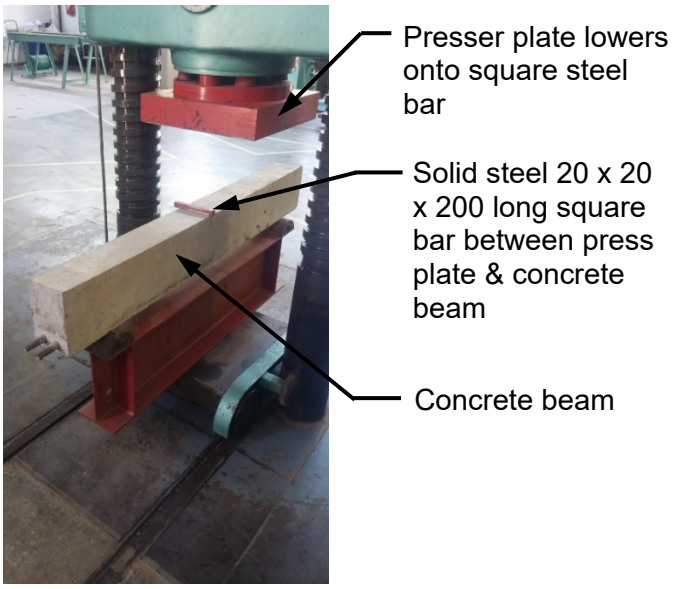


**Figure 3-33: Conversion of the hydraulic press to a beam press**

# CHAPTER 4:EXPERIMENTAL RESULTS

Figure 4-1 shows the single point load **P** that was applied to each beam. $\mathbf{V_L} = 0.543 \cdot \mathbf{P}$ is the larger support reaction and is the maximum shear force applied to the beam. The shear force in the beam between $\mathbf{V_L}$ and the point load **P** will be constant and equals $\mathbf{V_L}$ and shown in Figure 4-2 below.

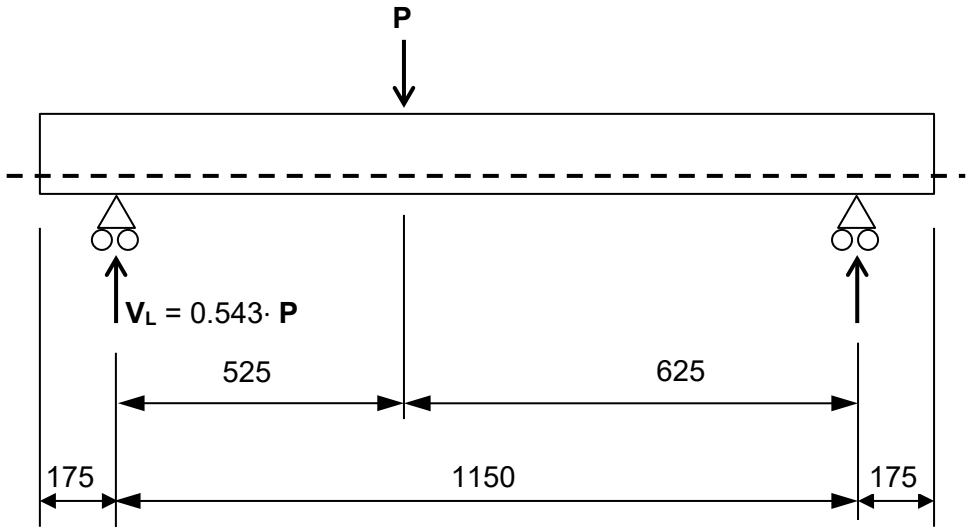


**Figure 4-1: The point load P and maximum shear force VL at failure**

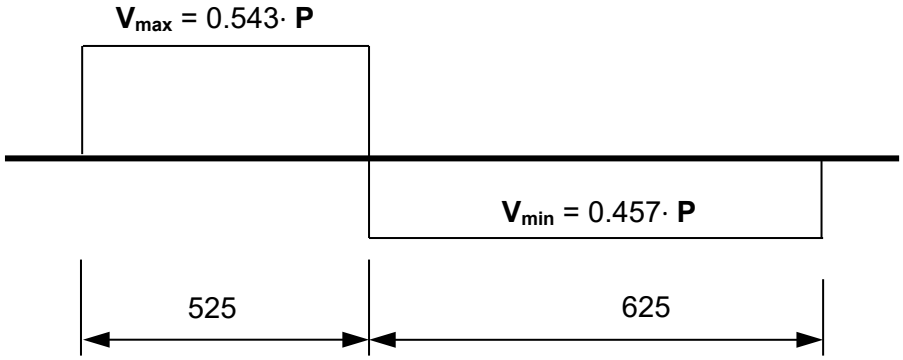


**Figure 4-2 - Shear Force Diagram Showing the Maximum Shear Force in the Beam**

The results from the experimental program are listed in Table 4-1 below. The point load **P** (kN) at failure, listed in column (e) is the failure load measured in the beam press. The maximum shear force in the beam at failure, $\mathbf{V_L} = 0.543 \cdot \mathbf{P}$ is calculated and listed in column (f).

**Table 4-1: Tabulated results of point load P at failure and shear force $V_L$ at failure**

| (a) | (b) | (c) | | (d) | | (e) | (f) |
|---|---|---|---|---|---|---|---|
| Beam no. | Coarse aggregate type | Coarse aggregate size (mm) | | 28-day concrete cube strength (MPa) | | Point load **P** at failure (kN) | Shear force at failure $\mathbf{V_L}$ (kN) |
| 1 | tillite | 13.2 | | 30.8 | | 82.0 | 44.5 |
| 2 | quartzite | 13.2 | | 32.1 | | 83.2 | 45.2 |
| 3 | dolerite | 13.2 | | 30.2 | | 87.5 | 47.5 |
| | | | | | | | |
| 4 | tillite | 19 | | 32.3 | | 68.5 | 37.2 |
| 5 | quartzite | 19 | | 34.9 | | 76.5 | 41.5 |
| 6 | dolerite | 19 | | 34.5 | | ±92.8 | 50.4 |
| | | | | | | | |
| 7 | tillite | 13.2 | | 39.4 | | 73.6 | 40.0 |
| 8 | quartzite | 13.2 | | 42.6 | | 86.6 | 47.0 |
| 9 | dolerite | 13.2 | | 43.1 | | 97.7 | 53.1 |
| | | | | | | | |
| 10 | tillite | 19 | | 41.2 | | 90.1 | 48.9 |
| 11 | quartzite | 19 | | 42.2 | | 81.9 | 44.5 |
| 12 | dolerite | 19 | | 39.0 | | 91.0 | 49.4 |
| | | | | | | | |
| 13 | tillite | 13.2 | | 52.8 | | 81.7 | 44.4 |
| 14 | quartzite | 13.2 | | 47.6 | | 89.0 | 48.3 |
| 15 | dolerite | 13.2 | | 51.7 | | 99.2 | 53.9 |
| | | | | | | | |
| 16 | tillite | 19 | | 39.4 | | 81.4 | 44.2 |
| 17 | quartzite | 19 | | 48.9 | | 86.3 | 46.9 |
| 18 | dolerite | 19 | | 48.1 | | 83.5 | 45.3 |

# CHAPTER 5:STATISTICAL ANALYSIS, INTERPRETATION AND DISCUSSION OF THE RESULTS

## 5.1 Introduction

This chapter presents the results and discuss the findings obtained from the study. The data collected was analysed with SPSS version 25.0. The results will present the descriptive statistics in the form of graphs, cross tabulations and other figures for the quantitative data that was collected. Inferential techniques include the use of correlations and ANOVA test values; which are interpreted using p-values.

## 5.2 The Sample

The sample was constituted as follows:

- The experiment was conducted with three different types of coarse aggregates – tillite quartzite and dolerite.
- Each of these three coarse aggregates was available in two nominal sizes – 13.2 mm and 19 mm.
- Three different targeted strengths of concrete 30 MPa, 40 MPa and 50 MPa were used. The targeted strength is the planned strength of concrete cubes before construction. The 28-day concrete cube strength is the actual strength achieved of the concrete cubes prepared, cured and tested in accordance with SANS 5863 (2006), the South African national standard for measuring the cube strength of concrete. It should however be noted that concrete cubes are “perfectly pampered pieces of concrete that do not reflect poor transporting, compaction, curing, etc.” (Raath, 2013, p. 14)

The aim of the experimental work was to determine if the type of coarse aggregate used in reinforced concrete influenced the shear strength of a reinforced concrete beam without transverse shear reinforcement. The shear strength was calculated by measuring the shear failure load **P** applied to the

beam, as shown in Figure 3-30, and calculating the reactions (shear force $\mathbf{V_L}$) from the static equilibrium of the simply supported beam.

Prior to looking at these relationships, descriptive statistics are derived from the data.

## 5.3 Data Analysis

This data is summarised using the characteristics of the samples by type and size. In addition, inferential statistics were used to look at mean differences between types and sizes.

Prior to commencement of the analysis, a normality test was conducted on the measured variables. The results are presented below.

## 5.4 Normality Test Results

**Table 5-1: One-sample Kolmogorov-Smirnov test**

| | | 28-day concrete cube strength (MPa) | Shear force $V_L$ at failure (kN) | Shear force $V_L$ scaled to targeted cube strengths (kN) |
|---|---|---|---|---|
| N | | 18 | 18 | 18 |
| Normal Parameters[a,b] | Mean | 40.6000 | 46.2333 | 45.7722 |
| | Std. Deviation | 7.19412 | 4.24014 | 4.50056 |
| Most Extreme Differences | Absolute | .119 | .149 | .117 |
| | Positive | .119 | .087 | .063 |
| | Negative | -.113 | -.149 | -.117 |
| Test Statistic | | .119 | .149 | .117 |
| Asymp. Sig. (2-tailed) | | .200[c,d] | .200[c,d] | .200[c,d] |

a. Test distribution is Normal.

b. Calculated from data.

c. Lilliefors Significance Correction.

d. This is a lower bound of the true significance.

As can be seen in Table 5-1, the p-value [Asymp. Sig. (2-tailed)] for cube strength and shear force is greater than the level of significance of 0.05. This

implies that the data are normally distributed. This allows for the use of parametric tests where applicable.

The traditional approach to reporting a result requires a statement of statistical significance. A **p-value** is generated from a **test statistic.** A significant result is indicated with "p < 0.05".

## 5.5 28-Day Concrete Cube Strength (MPa)

Table 5-2 below indicates various descriptive statistics for the different types of aggregate by size.

**Table 5-2: 28-day concrete cube strengths – descriptive statistics for the different aggregates**

| Coarse aggregate type | | | | Coarse aggregate size (mm) = 13.2 mm | | Coarse aggregate size (mm) = 19.0 mm | |
|---|---|---|---|---|---|---|---|
| | | | | Statistic | Std. Error | Statistic | Std. Error |
| 28 day concrete cube strength (MPa) | tillite | Mean | | 41.00 | 6.40 | 37.63 | 2.72 |
| | | 95% Confidence Interval for Mean | Lower Bound | 13.46 | | 25.94 | |
| | | | Upper Bound | 68.54 | | 49.32 | |
| | | 5% Trimmed Mean | | | | | |
| | | Median | | 39.40 | | 39.40 | |
| | | Variance | | 122.92 | | 22.14 | |
| | | Std. Deviation | | 11.09 | | 4.71 | |
| | | Minimum | | 30.80 | | 32.30 | |
| | | Maximum | | 52.80 | | 41.20 | |
| | | Range | | 22.00 | | 8.90 | |
| | | Interquartile Range | | | | | |
| | | Skewness | | 0.64 | 1.22 | -1.45 | 1.22 |
| | | Kurtosis | | | | | |
| | quartzite | Mean | | 40.77 | 4.57 | 42.00 | 4.04 |
| | | 95% Confidence Interval for Mean | Lower Bound | 21.11 | | 24.61 | |
| | | | Upper Bound | 60.42 | | 59.39 | |
| | | 5% Trimmed Mean | | | | | |
| | | Median | | 42.60 | | 42.20 | |
| | | Variance | | 62.58 | | 49.03 | |
| | | Std. Deviation | | 7.91 | | 7.00 | |
| | | Minimum | | 32.10 | | 34.90 | |
| | | Maximum | | 47.60 | | 48.90 | |
| | | Range | | 15.50 | | 14.00 | |
| | | Interquartile Range | | | | | |
| | | Skewness | | -0.99 | 1.22 | -0.13 | 1.22 |
| | | Kurtosis | | | | | |
| | dolerite | Mean | | 41.67 | 6.25 | 40.53 | 4.00 |
| | | 95% Confidence Interval for Mean | Lower Bound | 14.78 | | 23.32 | |
| | | | Upper Bound | 68.55 | | 57.74 | |
| | | 5% Trimmed Mean | | | | | |

| Coarse aggregate type | | | Coarse aggregate size (mm) = 13.2 mm | | Coarse aggregate size (mm) = 19.0 mm | |
|---|---|---|---|---|---|---|
| | | | Statistic | Std. Error | Statistic | Std. Error |
| | | Median | 43.10 | | 39.00 | |
| | | Variance | 117.10 | | 48.00 | |
| | | Std. Deviation | 10.82 | | 6.93 | |
| | | Minimum | 30.20 | | 34.50 | |
| | | Maximum | 51.70 | | 48.10 | |
| | | Range | 21.50 | | 13.60 | |
| | | Interquartile Range | | | | |
| | | Skewness | -0.59 | 1.22 | 0.95 | 1.22 |
| | | Kurtosis | | | | |

The following patterns are observed:

- The mean values for tillite and dolerite at 13.2 mm are greater than those for 19.0 mm
- Quartzite has a higher mean at 19.0 mm than at 13.0 mm

The differences between the types and sizes are tested below.Figure 5-1Figure 5-1 in section 5.5.1 below shows the 13.2 mm coarse aggregate comparison for the three aggregate types while Figure 5-2 in section 5.5.2 below shows the 19 mm coarse aggregate comparison for the three aggregate types. It is noted that the central values are similar.

Table 5-3 and Table 5-4 and Figure 5-1 below indicate the results of the means comparisons by type.

### 5.5.1 Coarse Aggregate Size (mm) = 13.2 mm

**Table 5-3: 28-day concrete cube strength – ANOVA test results for 13.2 mm aggregate**

| ANOVA[a] | | | | | |
|---|---|---|---|---|---|
| 28-day concrete cube strength (MPa) | | | | | |
| | Sum of Squares | df | Mean Square | F | Sig. |
| Between Groups | 1.309 | 2 | .654 | .006 | .994 |
| Within Groups | 605.213 | 6 | 100.869 | | |
| Total | 606.522 | 8 | | | |

a. Coarse aggregate size (mm) = 13.2 mm

The Anova p-value (p = 0.994) in Table 5-3 indicates that, overall, there is no significant difference between the mean values.

Further multiple comparisons (Table 5-4 and Figure 5-1) also indicate that there is no significant difference in the 28-day cube strength between the aggregate types at 13.2 mm, as all of the p-values are greater than the level of significance.

**Table 5-4: 28-day cube strength – multiple comparisons for 13.2 mm coarse aggregate**

| **Multiple Comparisons[a]** | | | | | | |
|---|---|---|---|---|---|---|
| Dependent Variable: 28-day concrete cube strength (MPa) | | | | | | |
| Tukey HSD | | | | | | |
| (I) Coarse aggregate type | (J) Coarse aggregate type | Mean Difference (I-J) | Std. Error | Sig. | 95% Confidence Interval | |
| | | | | | Lower Bound | Upper Bound |
| tillite | quartzite | .23333 | 8.20036 | 1.000 | -24.9276 | 25.3943 |
| | dolerite | -.66667 | 8.20036 | .996 | -25.8276 | 24.4943 |
| quartzite | tillite | -.23333 | 8.20036 | 1.000 | -25.3943 | 24.9276 |
| | dolerite | -.90000 | 8.20036 | .993 | -26.0610 | 24.2610 |
| dolerite | tillite | .66667 | 8.20036 | .996 | -24.4943 | 25.8276 |
| | quartzite | .90000 | 8.20036 | .993 | -24.2610 | 26.0610 |

a. Coarse aggregate size (mm) = 13.2 mm

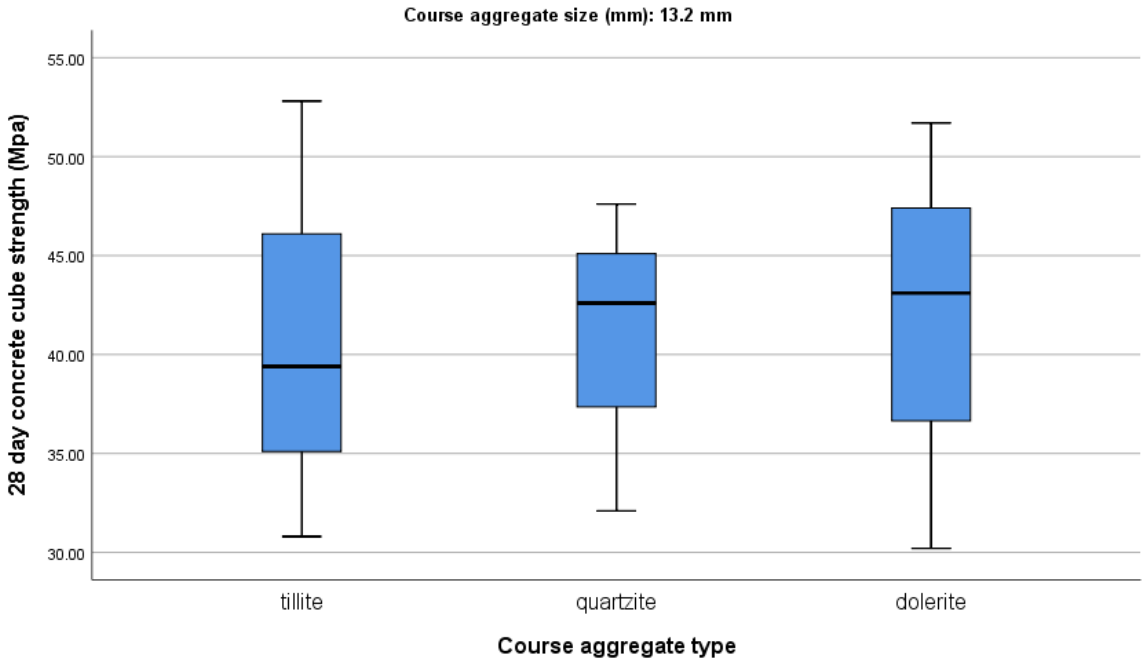


**Figure 5-1: 28-day concrete cube strength – 13.2 mm coarse aggregate comparison for the three aggregate types**

### 5.5.2 Coarse Aggregate Size (mm) = 19.0 mm

**Table 5-5: 28-day concrete cube strength – ANOVA test results for 19 mm aggregate**

| ANOVA[a] | | | | | |
|---|---|---|---|---|---|
| 28-day concrete cube strength (MPa) | | | | | |
| | Sum of Squares | df | Mean Square | F | Sig. |
| Between Groups | 29.629 | 2 | 14.814 | .373 | .704 |
| Within Groups | 238.353 | 6 | 39.726 | | |
| Total | 267.982 | 8 | | | |

a. Coarse aggregate size (mm) = 19.0 mm

The Anova p-value (p = 0.704) in Table 5-5 indicates that, overall, there is no significant difference between the mean values.

Further multiple comparisons (Table 5-6 and Figure 5-2) also indicate that there is no significant difference in the 28-day cube strength between the coarse aggregate types at 19.0 mm, as all of the p-values are greater than the level of significance.

**Table 5-6: 28-day cube strength – multiple comparisons for 19 mm coarse aggregate**

| Multiple Comparisons[a] | | | | | | |
|---|---|---|---|---|---|---|
| Dependent Variable: 28-day concrete cube strength (MPa) | | | | | | |
| Tukey HSD | | | | | | |
| (I) Coarse aggregate type | (J) Coarse aggregate type | Mean Difference (I-J) | Std. Error | Sig. | 95% Confidence Interval | |
| | | | | | Lower Bound | Upper Bound |
| tillite | quartzite | -4.36667 | 5.14623 | .689 | -20.1567 | 11.4234 |
| | dolerite | -2.90000 | 5.14623 | .844 | -18.6901 | 12.8901 |
| quartzite | tillite | 4.36667 | 5.14623 | .689 | -11.4234 | 20.1567 |
| | dolerite | 1.46667 | 5.14623 | .957 | -14.3234 | 17.2567 |
| dolerite | tillite | 2.90000 | 5.14623 | .844 | -12.8901 | 18.6901 |
| | quartzite | -1.46667 | 5.14623 | .957 | -17.2567 | 14.3234 |

a. Coarse aggregate size (mm) = 19.0 mm

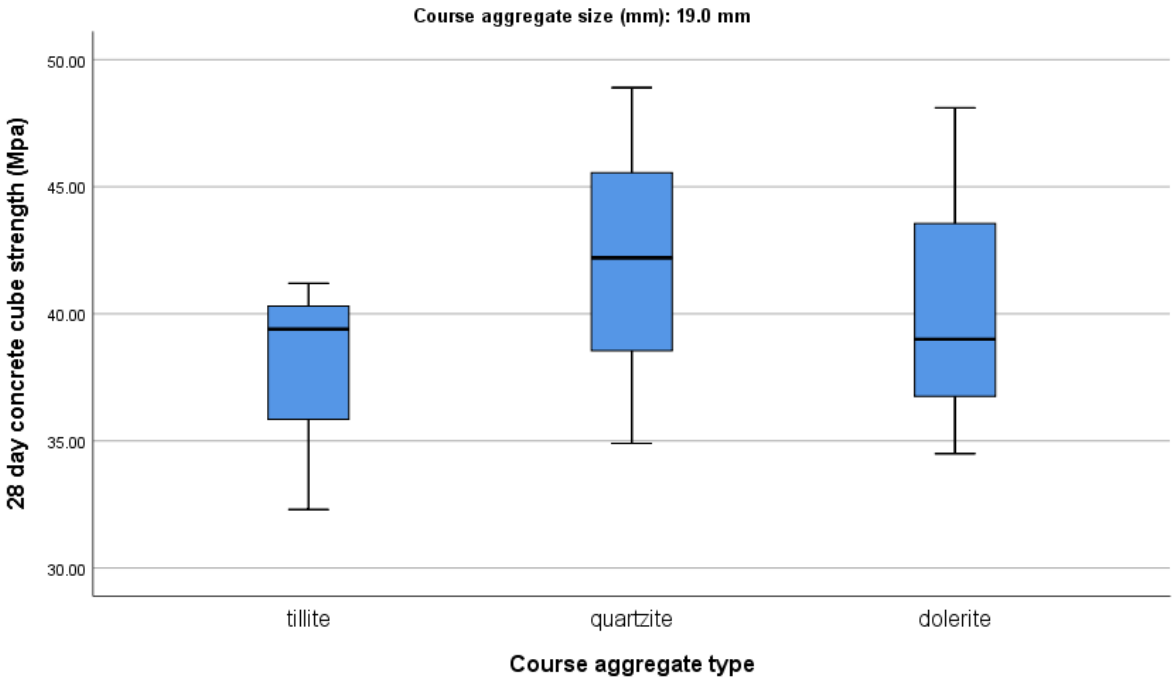


**Figure 5-2: 28-day concrete cube strength – 19 mm coarse aggregate comparison for the three aggregate types**

### 5.5.3 Coarse Aggregate Type – Tillite

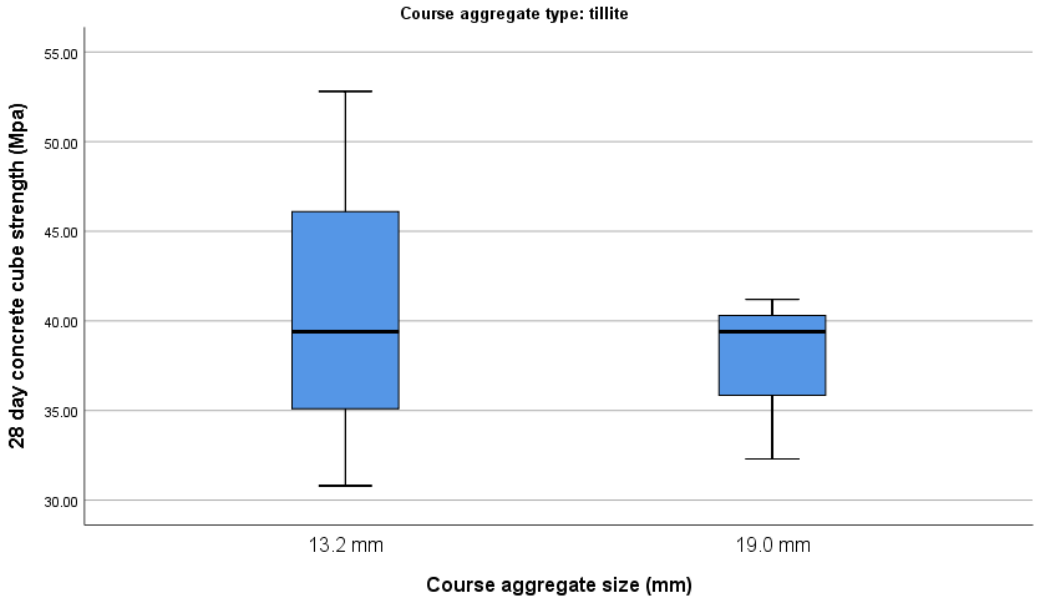


**Figure 5-3: 28-day concrete cube strength – tillite coarse aggregate comparison for the two aggregate sizes**

### 5.5.4 Coarse Aggregate Type – Quartzite

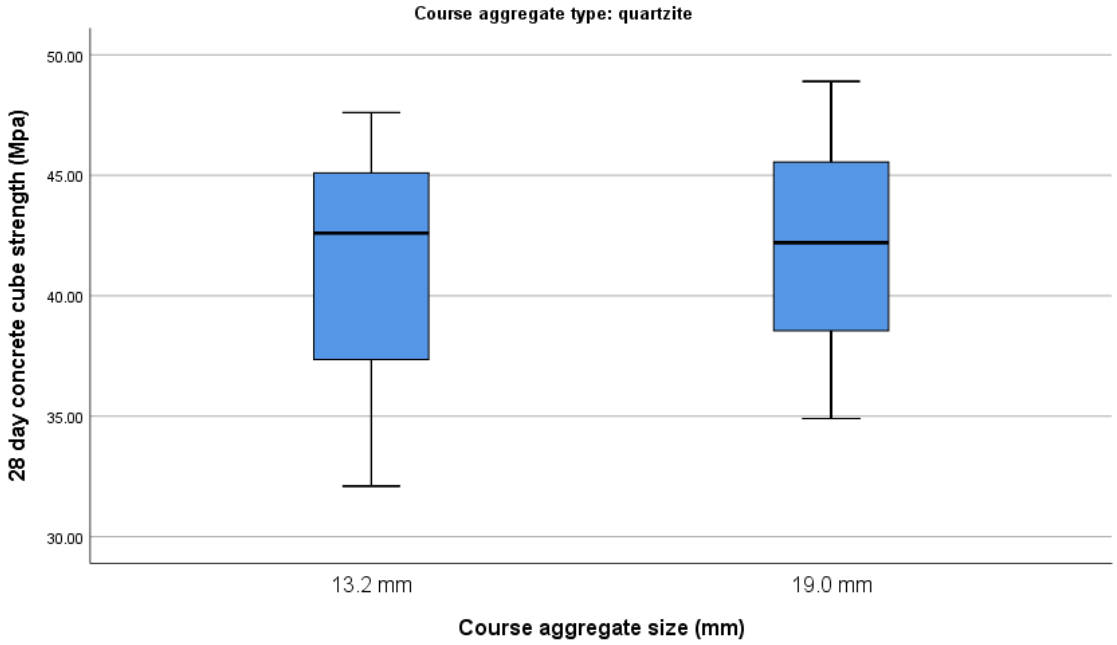


**Figure 5-4: 28-day concrete cube strength – quartzite coarse aggregate comparison for the two aggregate sizes**

### 5.5.5 Coarse Aggregate Type – Dolerite

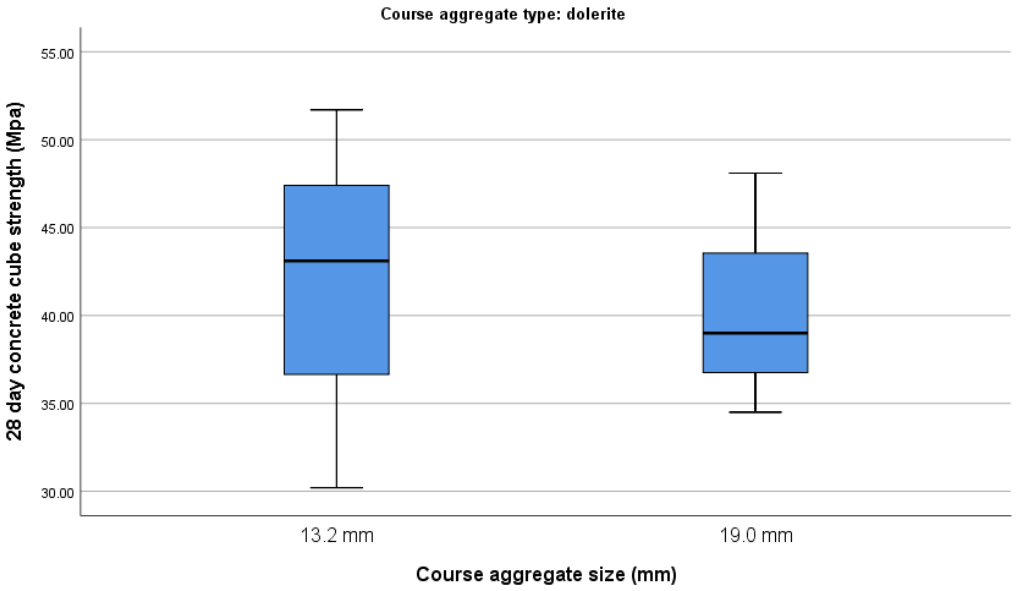


**Figure 5-5: 28-day concrete cube strength – dolerite coarse aggregate comparison for the two aggregate sizes**

### 5.5.6 Summary

Figure 5-6 below summarises the 28-day concrete cube strengths measured in the experiment.

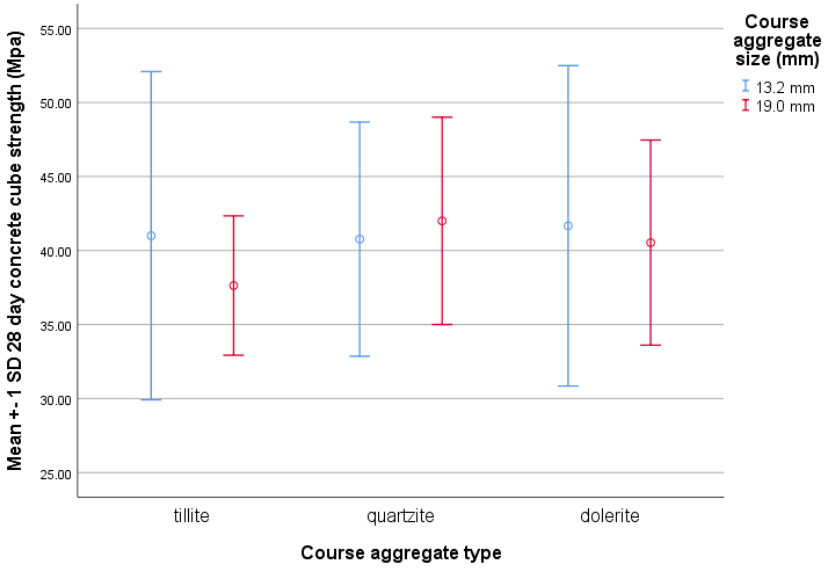


**Figure 5-6: 28-day concrete cube strength – summary of coarse aggregate comparison for aggregate size and aggregate type**

## 5.6 Shear Force $V_L$ at Failure and at Scaled Shear Force (kN)

In order to compare $V_L$ as a function of aggregate size and coarse aggregate type, ideally, the 28-day concrete cube strength should be exactly the same for a set of beam specimens being compared. Practically this is not achievable since the concrete for different beam specimens has different mix designs and is mixed and cast in different batches on different days. The mix design is designed for a targeted 28-day concrete strength and the resulting 28-day concrete cube strengths will fall within a margin of error from the targeted cube strength.

Therefore, the shear force at failure is analysed in two ways:

1. In the first analysis, the shear force $\mathbf{V_L}$ at failure is investigated as a function of coarse aggregate size and coarse aggregate type respectively. The value of the shear force $V_L$ used in this analysis is $\boldsymbol{V_L = 0.543 \cdot P}$ which is the shear force at failure as illustrated in Figure 3-30. This shear force $V_L$ is also a function of the 28-day cube strength $f_{cu}$ (e.g. 30.8 MPa for the 13.2 mm tillite), which is determined in

accordance with SANS5863 (2006) from the sample of concrete cubes for the respective beam specimen.

2. In the second analysis the shear force $V_{L\text{-}scaled}$ at failure is investigated as a function of coarse aggregate size and coarse aggregate type respectively. The value of the shear force $V_{L\text{-}scaled}$ used in this analysis is derived by scaling the 28-day cube strength $f_{cu}$ for the respective beam specimens to a targeted cube strength $f_{cu\text{-}scaled}$ of either 30 MPa, 40 MPa or 50 MPa and then scaling the shear force $V_L$ at failure using the relationship, $V_{L-scaled} = \frac{V_L}{\sqrt{f_{cu}}} \cdot \frac{\sqrt{f_{cu-scaled.}}}{1}$, since the shear force at failure $V_{failure} \propto \sqrt{f_{cu}}$. From a survey of the literature it can be seen that the relationship between $V_L$ and $f_{cu}$ is usually described in the form $V_{failure} \propto \langle f_{cu.} \rangle^{a}$ where $0.33 \leq a \leq 0.5$. $V_{failure} \propto \sqrt{f_{cu.}}$ has been chosen for this analysis since this is the form used in the critical shear crack theory (Ruiz, et al., 2015), the compression field theories (Bentz, et al., 2006) and in some of the methods described by the Joint ASCE –ACI Committee 445 (Joint ASCE-ACI Committee 445 on shear and torsion, 1998 reapproved 2009).

### 5.6.1 Descriptive Statistics

**Table 5-7: Shear force $V_L$ at failure - descriptive statistics for the different aggregates**

| Course aggregate size (mm) | Descriptives | | Tillite | | Quartzite | | Dolerite | |
|---|---|---|---|---|---|---|---|---|
| | | | Statistic | Std. error | Statistic | Std. error | Statistic | Std. error |
| 13.2 mm | Mean | | 42.9667 | 1.48361 | 46.8333 | 0.89876 | 51.5000 | 2.01329 |
| | 95% Confidence Interval for Mean | Lower Bound | 36.5832 | | 42.9663 | | 42.8375 | |
| | | Upper Bound | 49.3501 | | 50.7004 | | 60.1625 | |
| | 5% Trimmed Mean | | | | | | | |
| | Median | | 44.4000 | | 47.0000 | | 53.1000 | |
| | Variance | | 6.603 | | 2.423 | | 12.160 | |
| | Std. Deviation | | 2.56970 | | 1.55671 | | 3.48712 | |
| | Minimum | | 40.00 | | 45.20 | | 47.50 | |
| | Maximum | | 44.50 | | 48.30 | | 53.90 | |
| | Range | | 4.50 | | 3.10 | | 6.40 | |
| | Interquartile Range | | | | | | | |
| | Skewness | | -1.729 | 1.225 | -0.476 | 1.225 | -1.630 | 1.225 |
| 19.0 mm | Mean | | 43.4333 | 3.39918 | 44.3000 | 1.56205 | 48.3667 | 1.56027 |
| | 95% Confidence Interval for Mean | Lower Bound | 28.8078 | | 37.5790 | | 41.6534 | |
| | | Upper Bound | 58.0588 | | 51.0210 | | 55.0800 | |
| | 5% Trimmed Mean | | | | | | | |
| | Median | | 44.2000 | | 44.5000 | | 49.4000 | |
| | Variance | | 34.663 | | 7.320 | | 7.303 | |
| | Std. Deviation | | 5.88756 | | 2.70555 | | 2.70247 | |
| | Minimum | | 37.20 | | 41.50 | | 45.30 | |
| | Maximum | | 48.90 | | 46.90 | | 50.40 | |
| | Range | | 11.70 | | 5.40 | | 5.10 | |
| | Interquartile Range | | | | | | | |
| | Skewness | | -0.576 | 1.225 | -0.331 | 1.225 | -1.469 | 1.225 |

**Table 5-8: Shear force $V_L$ scaled for targeted cube strengths - descriptive statistics for the different aggregates**

| Coarse aggregate size (mm) | Descriptives | | tillite | | quartzite | | dolerite | |
|---|---|---|---|---|---|---|---|---|
| | | | Statistic | Std. Error | Statistic | Std. Error | Statistic | Std. Error |
| 13.2 mm | Mean | | 42.4667 | 1.10202 | 46.2667 | 1.70717 | 50.5000 | 1.64418 |
| | 95% Confidence Interval for Mean | Lower Bound | 37.7251 | | 38.9213 | | 43.4257 | |
| | | Upper Bound | 47.2083 | | 53.6120 | | 57.5743 | |
| | 5% Trimmed Mean | | | | | | | |
| | Median | | 43.2000 | | 45.6000 | | 51.1000 | |
| | Variance | | 3.643 | | 8.743 | | 8.110 | |
| | Std. Deviation | | 1.90875 | | 2.95691 | | 2.84781 | |
| | Minimum | | 40.30 | | 43.70 | | 47.40 | |
| | Maximum | | 43.90 | | 49.50 | | 53.00 | |
| | Range | | 3.60 | | 5.80 | | 5.60 | |
| | Interquartile Range | | | | | | | |
| | Skewness | | -1.474 | 1.225 | 0.963 | 1.225 | -0.906 | 1.225 |
| 19.0 mm | Mean | | 44.6000 | 4.42418 | 43.0667 | 2.57186 | 47.7333 | 1.15662 |
| | 95% Confidence Interval for Mean | Lower Bound | 25.5643 | | 32.0009 | | 42.7568 | |
| | | Upper Bound | 63.6357 | | 54.1325 | | 52.7099 | |
| | 5% Trimmed Mean | | | | | | | |
| | Median | | 48.2000 | | 43.3000 | | 47.0000 | |
| | Variance | | 58.720 | | 19.843 | | 4.013 | |
| | Std. Deviation | | 7.66290 | | 4.45459 | | 2.00333 | |
| | Minimum | | 35.80 | | 38.50 | | 46.20 | |
| | Maximum | | 49.80 | | 47.40 | | 50.00 | |
| | Range | | 14.00 | | 8.90 | | 3.80 | |
| | Interquartile Range | | | | | | | |
| | Skewness | | -1.647 | 1.225 | -0.235 | 1.225 | 1.427 | 1.225 |

The results in Table 5-7 and Table 5-8 indicate that the mean values for quartzite and dolerite for 13.2 mm are greater than that for 19.0 mm. The trend is reversed for tillite.

### 5.6.2 Coarse Aggregate Size (mm) = 13.2 mm

The results of the Anova tests are shown in Table 5-9 and Table 5-10.

**Table 5-9: Shear force $V_L$ at failure – ANOVA test results for 13.2 mm aggregate**

| **ANOVA Tests of Between-Subjects Effects[a]** | | | | | |
|---|---|---|---|---|---|
| Dependent Variable: Shear force VL at failure (kN) | | | | | |
| Source | Type III Sum of Squares | df | Mean Square | F | Sig. |
| Corrected Model | 109.547[b] | 2 | 54.773 | 7.756 | 0.022 |
| Intercept | 19965.690 | 1 | 19965.690 | 2827.112 | 0.000 |
| Coarse Aggregate Type A | 109.547 | 2 | 54.773 | 7.756 | 0.022 |
| Error | 42.373 | 6 | 7.062 | | |
| Total | 20117.610 | 9 | | | |
| Corrected Total | 151.920 | 8 | | | |
| a. Coarse aggregate size (mm) = 13.2 mm<br>b. R Squared = .721 (Adjusted R Squared = .628) | | | | | |

**Table 5-10: Shear force $V_L$ scaled for targeted cube strengths – ANOVA test results for 13.2 mm aggregate**

| **ANOVA Tests of Between-Subjects Effects[a]** | | | | | |
|---|---|---|---|---|---|
| Dependent Variable: Shear force scaled | | | | | |
| Source | Type III Sum of Squares | df | Mean Square | F | Sig. |
| Corrected Model | 96.896[b] | 2 | 48.448 | 7.091 | 0.026 |
| Intercept | 19385.921 | 1 | 19385.921 | 2837.425 | 0.000 |
| Coarse Aggregate Type A | 96.896 | 2 | 48.448 | 7.091 | 0.026 |
| Error | 40.993 | 6 | 6.832 | | |
| Total | 19523.810 | 9 | | | |
| Corrected Total | 137.889 | 8 | | | |
| a. Coarse aggregate size (mm) = 13.2 mm<br>b. R Squared = .703 (Adjusted R Squared = .604) | | | | | |

The p-values p = 0.022 in Table 5-9 and p = 0.026 in Table 5-10 indicate that there is a significant difference in the mean values between the aggregate types at 13.2 mm. The multiple comparisons in Table 5-11 and Table 5-12

indicate that this difference is mainly due to the difference observed between tillite and dolerite. This can also be seen in Figure 5-7 and Figure 5-8 below.

**Table 5-11: Shear force $V_L$ at failure – multiple comparisons for 13.2 mm coarse aggregate**

| **Multiple Comparisons[a]** | | | | | | |
|---|---|---|---|---|---|---|
| Dependent Variable: Shear force VL at failure (kN) | | | | | | |
| Tukey HSD | | | | | | |
| (I) Coarse aggregate type | (J) Coarse aggregate type | Mean Difference (I-J) | Std. Error | Sig. | 95% Confidence Interval | |
| | | | | | Lower Bound | Upper Bound |
| tillite | quartzite | -3.8667 | 2.16983 | 0.253 | -10.5243 | 2.7910 |
| | dolerite | -8.5333* | 2.16983 | 0.018 | -15.1910 | -1.8757 |
| quartzite | tillite | 3.8667 | 2.16983 | 0.253 | -2.7910 | 10.5243 |
| | dolerite | -4.6667 | 2.16983 | 0.159 | -11.3243 | 1.9910 |
| dolerite | tillite | 8.5333* | 2.16983 | 0.018 | 1.8757 | 15.1910 |
| | quartzite | 4.6667 | 2.16983 | 0.159 | -1.9910 | 11.3243 |
| Based on observed means. The error term is Mean Square(Error) = 7.062. | | | | | | |
| *. The mean difference is significant at the 0.05 level. | | | | | | |
| a. Coarse aggregate size (mm) = 13.2 mm | | | | | | |

**Table 5-12: Shear force $V_L$ scaled for targeted cube strengths – multiple comparisons for 13.2 mm coarse aggregate**

| **Multiple Comparisons[a]** | | | | | | |
|---|---|---|---|---|---|---|
| Dependent Variable: Shear force scaled | | | | | | |
| Tukey HSD | | | | | | |
| Coarse aggregate type (I) | Coarse aggregate type (J) | Mean Difference (I-J) | Std. Error | Sig. | 95% Confidence Interval | |
| | | | | | Lower Bound | Upper Bound |
| tillite | quartzite | -3.8000 | 2.13420 | 0.254 | -10.3483 | 2.7483 |
| | dolerite | -8.0333* | 2.13420 | 0.022 | -14.5816 | -1.4850 |
| quartzite | tillite | 3.8000 | 2.13420 | 0.254 | -2.7483 | 10.3483 |
| | dolerite | -4.2333 | 2.13420 | 0.197 | -10.7816 | 2.3150 |
| dolerite | tillite | 8.0333* | 2.13420 | 0.022 | 1.4850 | 14.5816 |
| | quartzite | 4.2333 | 2.13420 | 0.197 | -2.3150 | 10.7816 |
| Based on observed means. The error term is Mean Square (Error) = 6.832. | | | | | | |
| *. The mean difference is significant at the 0.05 level. | | | | | | |
| a. Coarse aggregate size (mm) = 13.2 mm | | | | | | |

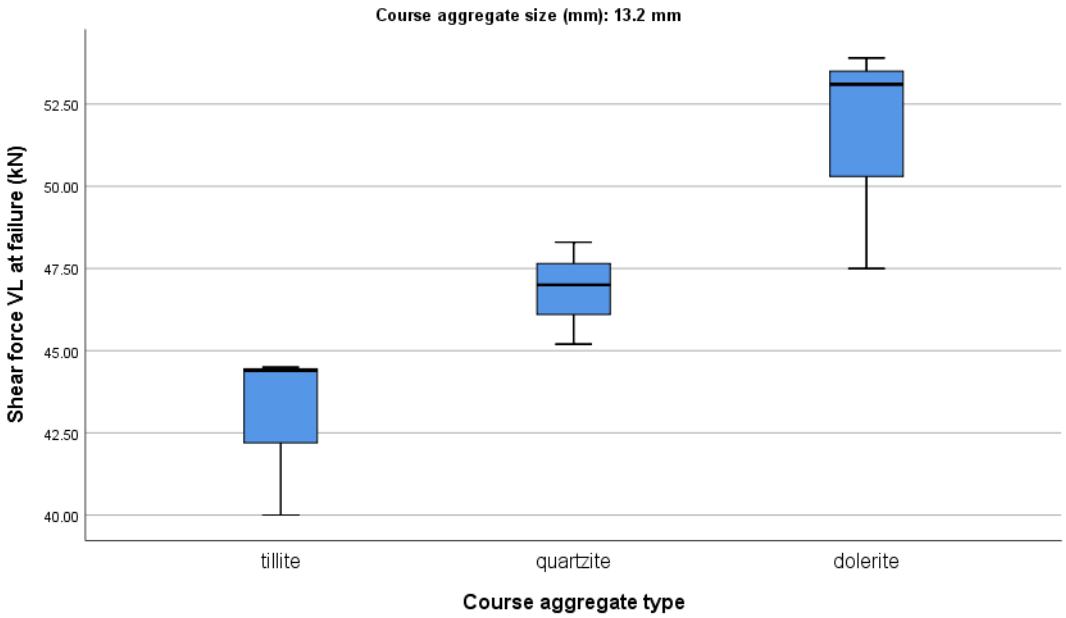


**Figure 5-7: Shear force $V_L$ at failure – 13.2 mm coarse aggregate comparison for the three aggregate types**

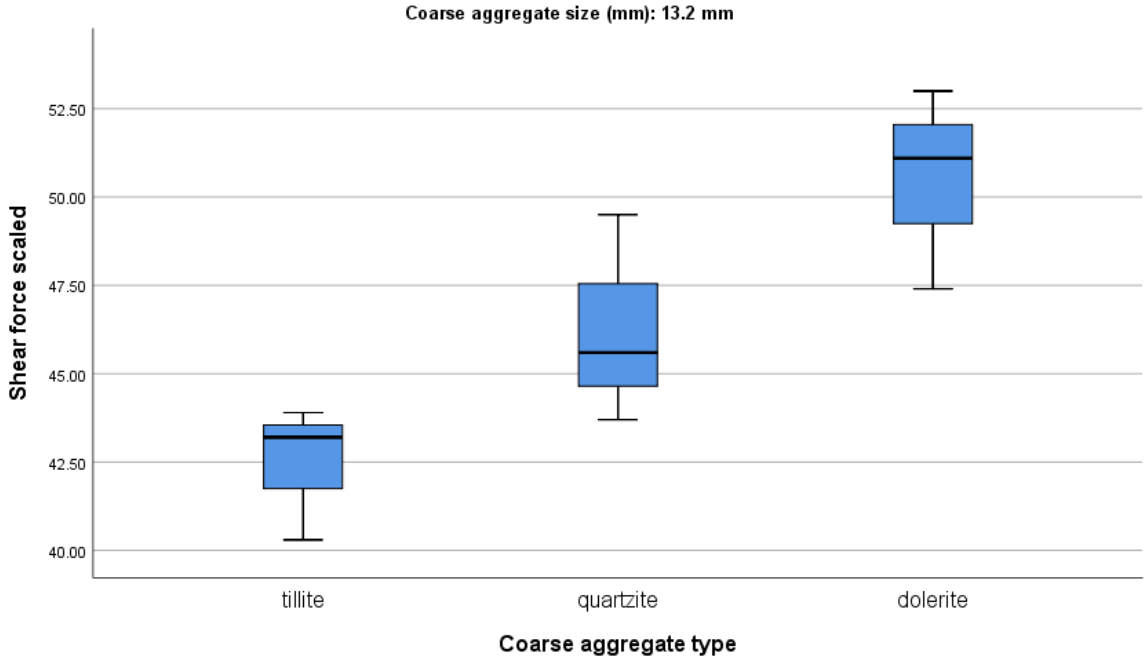


**Figure 5-8: Shear force $V_L$ scaled for targeted cube strengths – 13.2 mm coarse aggregate comparison for the three aggregate types**

### 5.6.3 Coarse Aggregate Size (mm) = 19.0 mm

The between group comparisons for aggregate types at 19.0 mm is shown in Table 5-13 and Table 5-14 below.

**Table 5-13: Shear force $V_L$ at failure – ANOVA test results for 19 mm aggregate**

| **ANOVA Tests of Between-Subjects Effects[a]** | | | | | |
|---|---|---|---|---|---|
| Dependent Variable: | | | | | |
| Source | Type III Sum of Squares | df | Mean Square | F | Sig. |
| Corrected Model | 41.627[b] | 2 | 20.813 | 1.267 | 0.348 |
| Intercept | 18523.210 | 1 | 18523.210 | 1127.478 | 0.000 |
| Coarse Aggregate Type A | 41.627 | 2 | 20.813 | 1.267 | 0.348 |
| Error | 98.573 | 6 | 16.429 | | |
| Total | 18663.410 | 9 | | | |
| Corrected Total | 140.200 | 8 | | | |
| a. Coarse aggregate size (mm) = 19.0 mm<br>b. R Squared = .297 (Adjusted R Squared = .063) | | | | | |

**Table 5-14: Shear force $V_L$ scaled for targeted cube strengths – ANOVA test results for 19 mm aggregate**

| **ANOVA Tests of Between-Subjects Effects[a]** | | | | | |
|---|---|---|---|---|---|
| Dependent Variable: Shear force scaled | | | | | |
| Source | Type III Sum of Squares | df | Mean Square | F | Sig. |
| Corrected Model | 33.947[b] | 2 | 16.973 | 0.617 | 0.571 |
| Intercept | 18333.160 | 1 | 18333.160 | 666.041 | 0.000 |
| Coarse Aggregate Type A | 33.947 | 2 | 16.973 | 0.617 | 0.571 |
| Error | 165.153 | 6 | 27.526 | | |
| Total | 18532.260 | 9 | | | |
| Corrected Total | 199.100 | 8 | | | |
| a. Coarse aggregate size (mm) = 19.0 mm<br>b. R Squared = .171 (Adjusted R Squared = -.106) | | | | | |

The p-values, p = 0.348 in Table 5-13 and p = 0.571 in Table 5-14, indicate that there is no statistically significant difference in the mean values between the 19 mm coarse aggregate types.

The multiple comparisons in Table 5-15 and Table 5-16 below also indicate that there is no statistically significant difference observed between the 19 mm coarse aggregate types. This can also be seen in Figure 5-9 and Figure 5-10 below as well.

**Table 5-15: Shear force $V_L$ at failure – multiple comparisons for 19 mm coarse aggregate**

| **Multiple Comparisons[a]** | | | | | | |
|---|---|---|---|---|---|---|
| Dependent Variable: Shear force VL at failure (kN) | | | | | | |
| Tukey HSD | | | | | | |
| (I) Coarse aggregate type | (J) Coarse aggregate type | Mean Difference (I-J) | Std. Error | Sig. | 95% Confidence | |
| | | | | | Lower Bound | Upper Bound |
| tillite | quartzite | -0.8667 | 3.30947 | 0.963 | -11.0210 | 9.2877 |
| | dolerite | -4.933333 | 3.30947 | 0.359 | -15.0877 | 5.2210 |
| quartzite | tillite | 0.8667 | 3.30947 | 0.963 | -9.2877 | 11.0210 |
| | dolerite | -4.0667 | 3.30947 | 0.481 | -14.2210 | 6.0877 |
| dolerite | tillite | 4.9333333 | 3.30947 | 0.359 | -5.2210 | 15.0877 |
| | quartzite | 4.0667 | 3.30947 | 0.481 | -6.0877 | 14.2210 |
| Based on observed means. The error term is Mean Square(Error) = 16.429. | | | | | | |
| a. Coarse aggregate size (mm) = 19.0 mm | | | | | | |

**Table 5-16: Shear force $V_L$ scaled for targeted cube strengths – multiple comparisons for 19 mm coarse aggregate**

| **Multiple Comparisons[a]** | | | | | | |
|---|---|---|---|---|---|---|
| Dependent Variable: Shear force scaled (kN) | | | | | | |
| Tukey HSD | | | | | | |
| Coarse aggregate type (I) | Coarse aggregate type (J) | Mean Difference (I-J) | Std. Error | Sig. | 95% Confidence Interval | |
| | | | | | Lower Bound | Upper Bound |
| tillite | quartzite | 1.5333 | 4.28373 | 0.933 | -11.6103 | 14.6770 |
| | dolerite | -3.1333 | 4.28373 | 0.755 | -16.2770 | 10.0103 |
| quartzite | tillite | -1.5333 | 4.28373 | 0.933 | -14.6770 | 11.6103 |
| | dolerite | -4.6667 | 4.28373 | 0.554 | -17.8103 | 8.4770 |
| dolerite | tillite | 3.1333 | 4.28373 | 0.755 | -10.0103 | 16.2770 |
| | quartzite | 4.6667 | 4.28373 | 0.554 | -8.4770 | 17.8103 |
| Based on observed means. The error term is Mean Square(Error) = 27.526. | | | | | | |
| a. Coarse aggregate size (mm) = 19.0 mm | | | | | | |

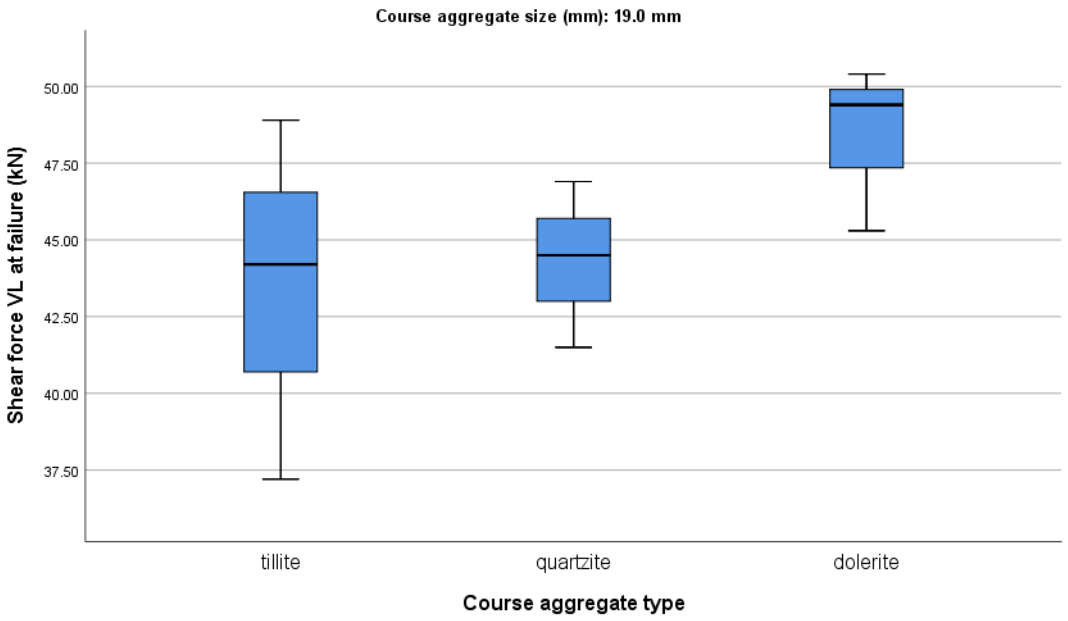


**Figure 5-9: Shear force $V_L$ at failure – 19 mm coarse aggregate comparison for the three aggregate types**

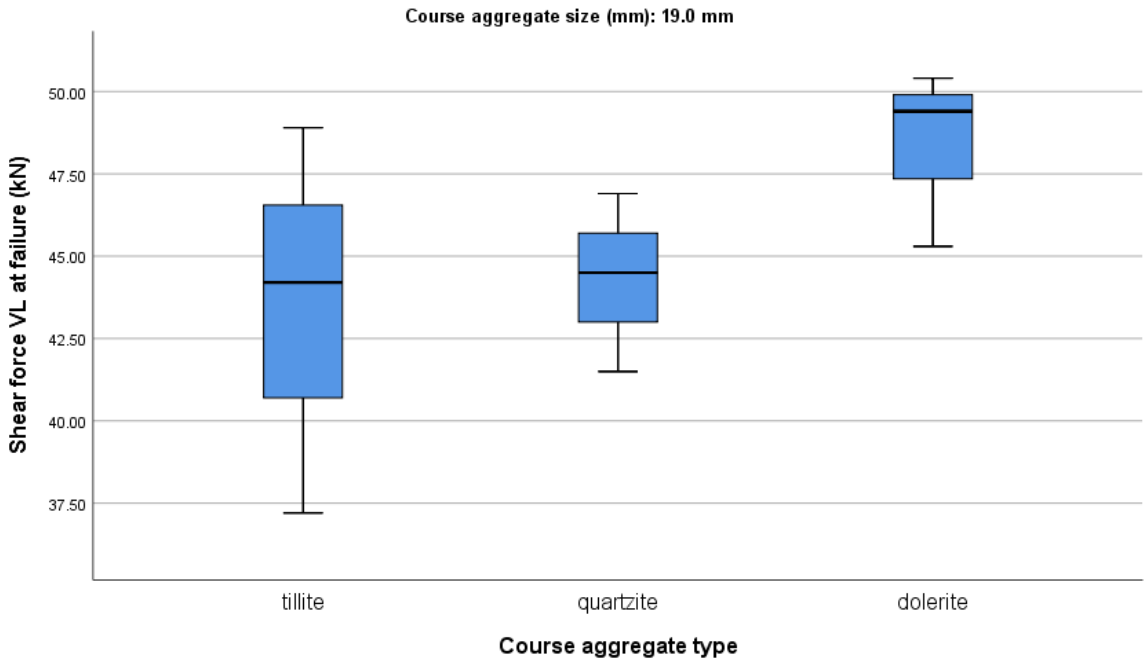


**Figure 5-10: Shear force $V_L$ scaled for targeted cube strengths – 19 mm coarse aggregate comparison for the three aggregate types**

### 5.6.4 Coarse Aggregate Type – Tillite

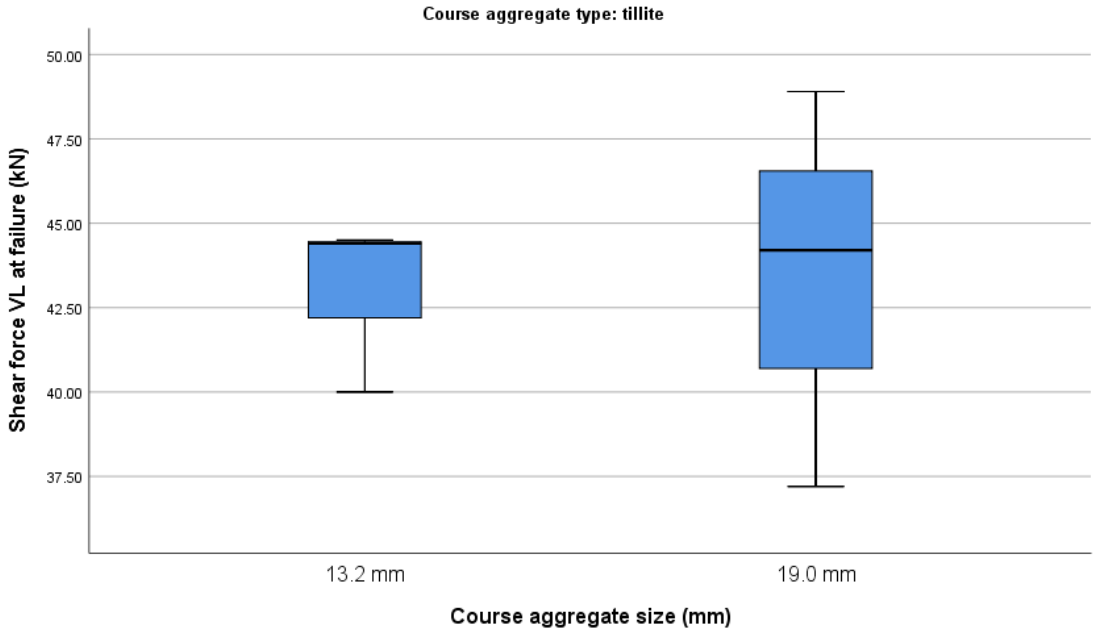


**Figure 5-11: Shear force $V_L$ at failure – tillite coarse aggregate comparison for the two aggregate sizes**

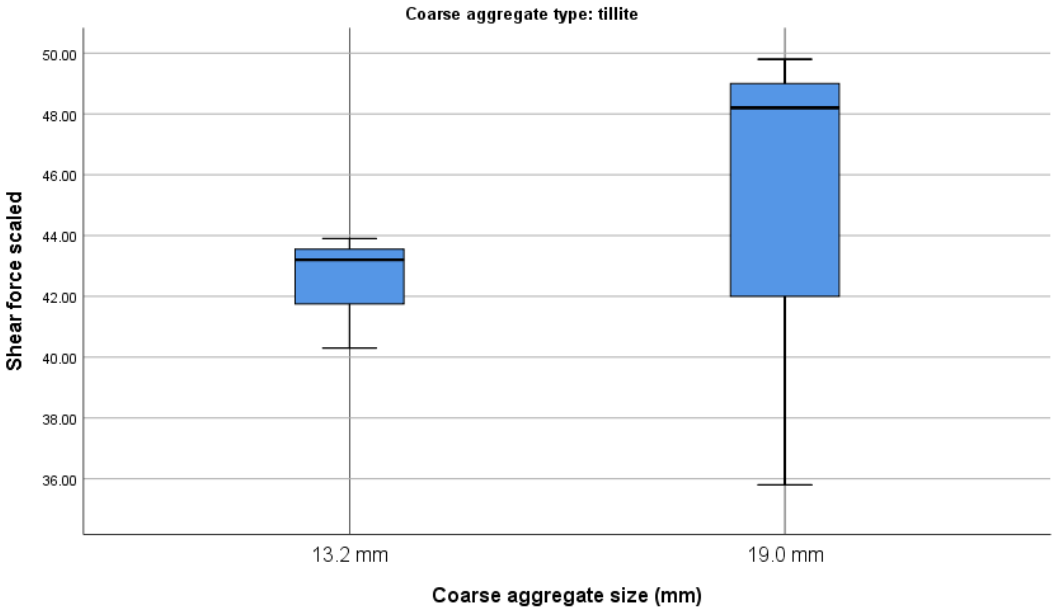


**Figure 5-12: Shear force $V_L$ scaled for targeted cube strengths – tillite coarse aggregate comparison for the two aggregate sizes**

### 5.6.5 Coarse Aggregate Type – Q uartzite

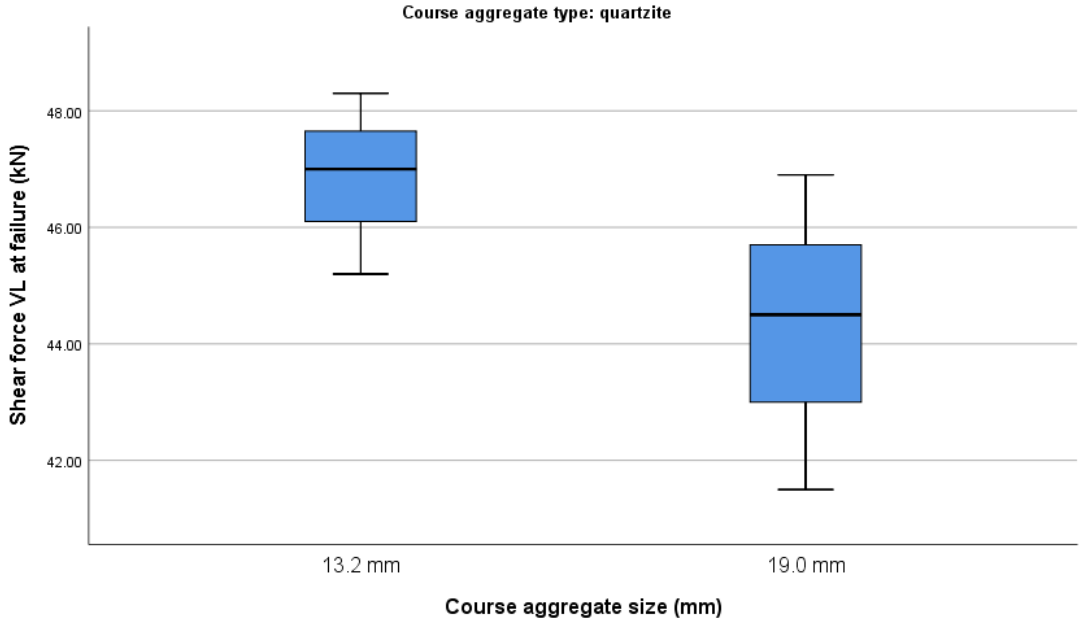


**Figure 5-13: Shear force $V_L$ at failure – quartzite coarse aggregate comparison for the two aggregate sizes**

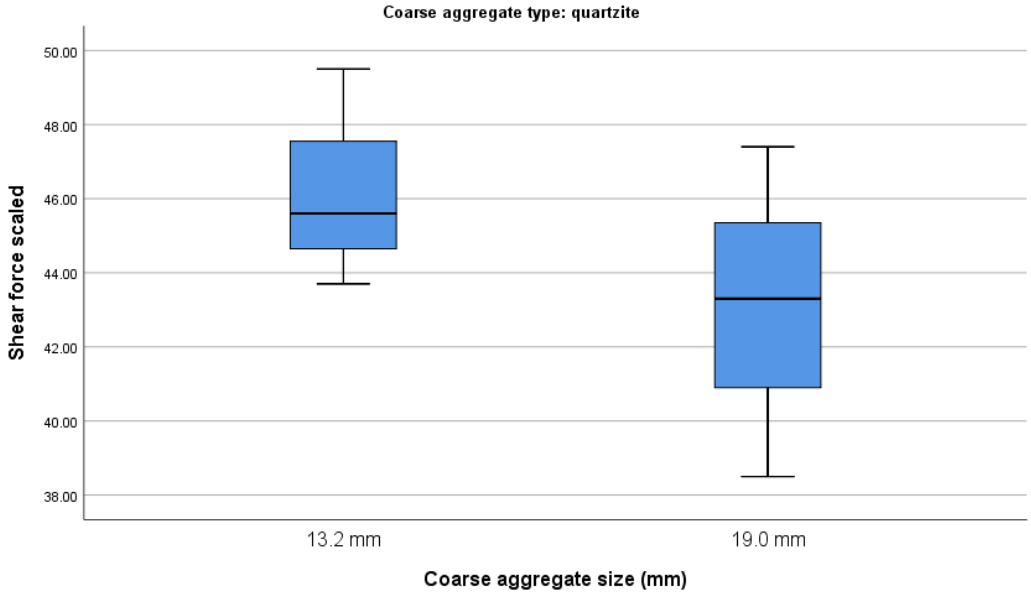


**Figure 5-14: Shear force $V_L$ scaled for targeted cube strengths – quartzite coarse aggregate comparison for the two aggregate sizes**

### 5.6.6 Coarse Aggregate Type – Dolerite

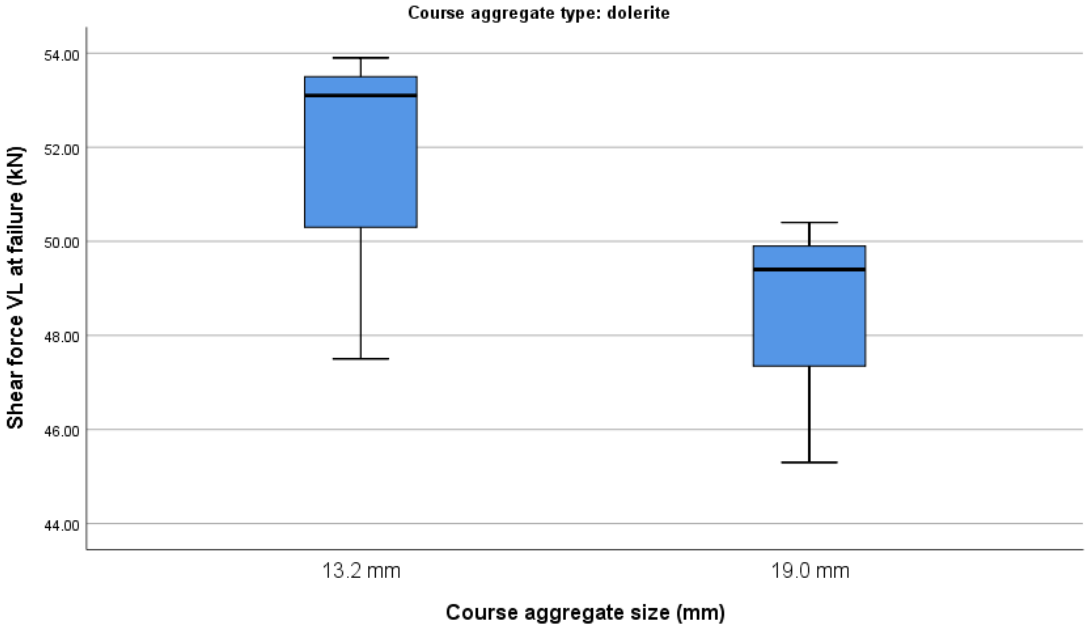


**Figure 5-15: Shear force $V_L$ at failure – dolerite coarse aggregate comparison for the two aggregate sizes**

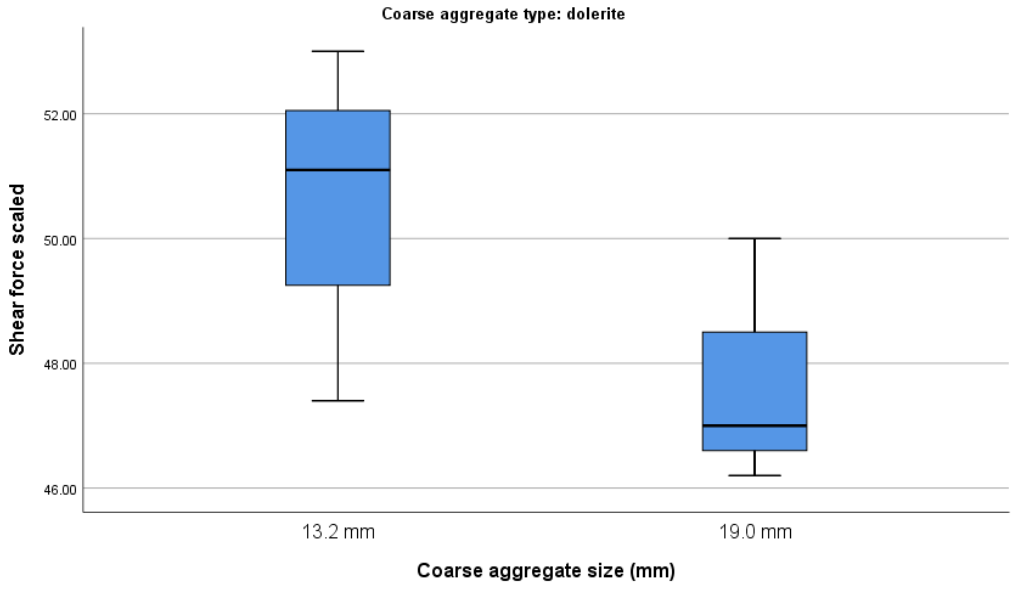


**Figure 5-16: Shear force $V_L$ scaled for targeted cube strengths – dolerite coarse aggregate comparison for the two aggregate sizes**

### 5.6.7 Mean ±1 Standard Deviation (SD) Shear Force

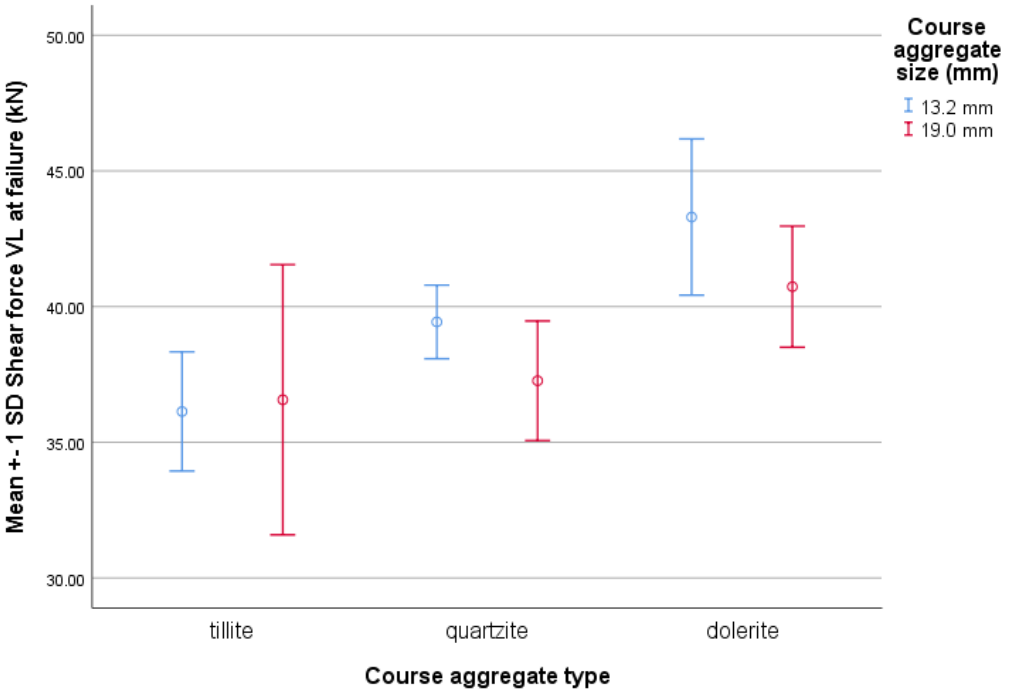


**Figure 5-17: Shear force $V_L$ at failure – mean shear force ± the standard deviation for aggregate size and aggregate type**

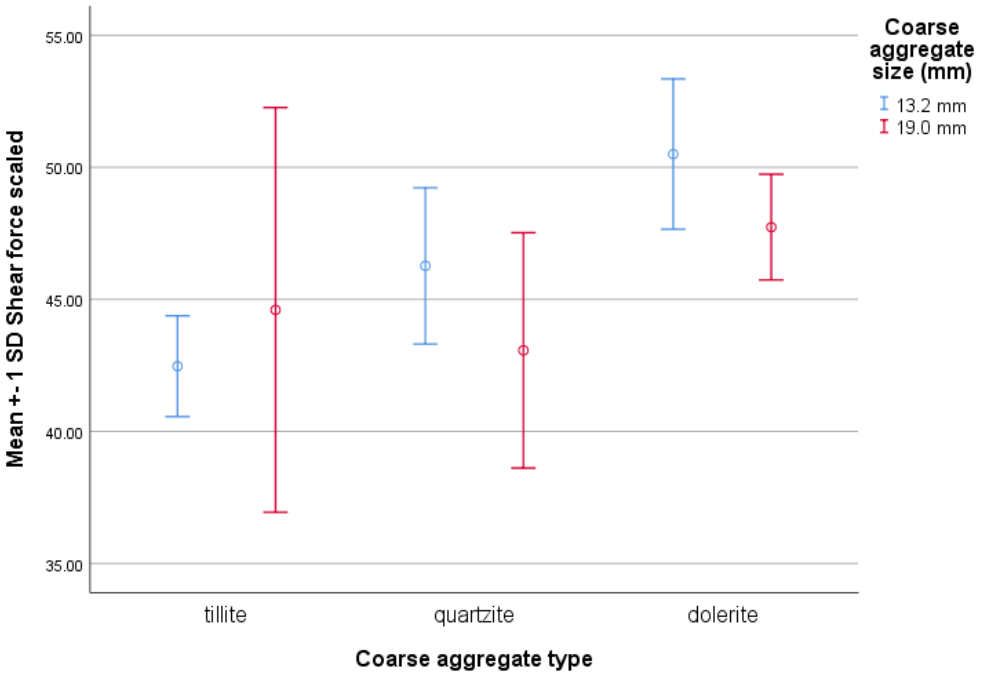


**Figure 5-18: Shear force $V_L$ scaled for targeted cube strengths – mean shear force ± the standard deviation for aggregate size and aggregate type**

## 5.7 Regression Analysis Based on Shear Force at Failure

The statistical method to formulate an equation that best describes the relationship between a dependant variable and an independent variable (or any number of independent variables) is referred to as a regression analysis. The equation is referred to as a regression equation and predicts the dependant variable y if the independent variable x is known.

The results in Table 5-17 to Table 5-21 below indicate the outputs of two regression models. In the first model, Model 1, the independent variable is the shear force at failure and is a function of two independent variables, the coarse aggregate size and the coarse aggregate type. In the second model, Model 2, the independent variable is the shear force at failure and is a function of three independent variables, the coarse aggregate size, the coarse aggregate type and the 28-day concrete cube strength.

**Table 5-17: Regression analysis – models and variables**

| **Variables Entered/Removed[a]** | | | |
|---|---|---|---|
| Model | Variables Entered | Variables Removed | Method |
| 1 | Coarse aggregate size (mm), Coarse aggregate type[b] | . | Enter |
| 2 | 28-day concrete cube strength (MPa)[b] | . | Enter |

a. Dependent Variable: Shear force $V_L$ at failure (kN)

b. All requested variables entered.

**Table 5-18: Regression analysis – model summary**

| **Model Summary** | | | | |
|---|---|---|---|---|
| Model | R | R Square | Adjusted R Square | Std. Error of the Estimate |
| 1 | .699[a] | 0.489 | 0.421 | 3.22601 |
| 2 | .753[b] | 0.566 | 0.473 | 3.07703 |

a. Predictors: (Constant), Coarse aggregate size (mm), Coarse aggregate type

b. Predictors: (Constant), Coarse aggregate size (mm), Coarse aggregate type, 28-day concrete cube strength (MPa)

**Table 5-19: Regression analysis – ANOVA tests of models**

| ANOVA[a] | | | | | | |
|---|---|---|---|---|---|---|
| Model | | Sum of Squares | df | Mean Square | F | Sig. |
| 1 | Regression | 149.533 | 2 | 74.767 | 7.184 | .006[b] |
| | Residual | 156.107 | 15 | 10.407 | | |
| | Total | 305.640 | 17 | | | |
| 2 | Regression | 173.087 | 3 | 57.696 | 6.094 | .007[c] |
| | Residual | 132.553 | 14 | 9.468 | | |
| | Total | 305.640 | 17 | | | |

a. Dependent Variable: Shear force VL at failure (kN)

b. Predictors: (Constant), Coarse aggregate size (mm), Coarse aggregate type

c. Predictors: (Constant), Coarse aggregate size (mm), Coarse aggregate type, 28-day concrete cube strength (MPa)

**Model** – This indicates the number of the model being reported.

Note that there are 2 models that are specified; the first only takes the dependent and independent variables into account, while the second model is adjusted for the predictors.

**Table 5-20: Regression analysis - coefficients**

| Coefficients[a] | | | | | | |
|---|---|---|---|---|---|---|
| Model | | Unstandardized Coefficients | | Standardized Coefficients | t | Sig. |
| | | B | Std. Error | Beta | | |
| 1 | (Constant) | 42.100 | 3.042 | | 13.842 | 0.000 |
| | Coarse aggregate type | 3.367 | 0.931 | 0.667 | 3.615 | 0.003 |
| | Coarse aggregate size (mm) | -1.733 | 1.521 | -0.210 | -1.140 | 0.272 |
| 2 | (Constant) | 35.425 | 5.131 | | 6.904 | 0.000 |
| | Coarse aggregate type | 3.220 | 0.893 | 0.638 | 3.605 | 0.003 |
| | Coarse aggregate size (mm) | -1.554 | 1.455 | -0.189 | -1.068 | 0.304 |
| | 28-day concrete cube strength (MPa) | 0.165 | 0.105 | 0.280 | 1.577 | 0.137 |

a. Dependent Variable: Shear force VL at failure (kN)

**Table 5-21: Regression analysis – excluded variables**

| Excluded Variables[a] | | | | | | |
|---|---|---|---|---|---|---|
| Model | | Beta In | t | Sig. | Partial Correlation | Collinearity Statistics |
| | | | | | | Tolerance |
| 1 | 28-day concrete cube strength (MPa) | .280[b] | 1.577 | 0.137 | 0.388 | 0.983 |

a. Dependent Variable: Shear force VL at failure (kN)

b. Predictors in the Model: (Constant), Coarse aggregate size (mm), Coarse aggregate type

**Model 2** – These are the values for the regression equation for predicting the dependent variable from the independent variable. The regression equation is presented in many different ways, for example:

$$\mathbf{Y_{predicted} = b_0 + b_1*x_1 + b_2*x_2 + b_3*x_3}$$

The column of estimates provides the values for $b_0$, $b_1$, $b_2$ and $b_3$ for this equation.

The equation is written as:

Shear Force = 35.425 + (3.220 × Coarse aggregate type) - (1.554 × Coarse aggregate size) + (0.165 × 28-Day concrete cube strength)

**Example:**

**Aggregate Type** – The coefficient for **aggregate type** is 3.220. This means, for every unit increase in **aggregate type**, a 3.220 unit increase in **Shear Force** value is predicted, holding all other variables constant.

**Aggregate Size** – For every unit increase in **aggregate size**, we **can** expect a -1.554 unit decrease in **Shear Force** value holding all other variables constant.

**Std. Error** – These are the standard errors associated with the coefficients.

**Beta** – These are the standardized coefficients. These are the coefficients that you would obtain if you standardized all of the variables in the regression, including the dependent and all of the independent variables, and ran the regression. By standardizing the variables before running the regression, you have put all of the variables on the same scale, and you can compare the magnitude of the coefficients to see which one has more of an effect. You will also notice that the larger betas are associated with the larger t-values and lower p-values.

**t** and **Sig.** – These are the t-statistics and their associated 2-tailed p-values used in testing whether a given coefficient is significantly different from zero, using an alpha of 0.05:

The coefficient for **Cube Strength** (B = 0.165) is not significantly different from 0 because its p-value is 0.137, which is larger than 0.05. Similarly for **Aggregate Size** B = -1.554 and the p-value = 0.304, which is larger than 0.05.

The coefficient for **Aggregate Type** (B = 3.220) is significantly different from 0 because its p-value is 0.003, which is less than 0.05.

The intercept is also significantly different from 0 at the 0.05 alpha level.

**95% Confidence Limit for B Lower Bound** and **Upper Bound** – These are the 95% confidence intervals for the coefficients. The confidence intervals are related to the p-values such that the coefficient will not be statistically significant if the confidence interval includes 0. These confidence intervals can help you to put the estimate from the coefficient into perspective by seeing how much the value can vary.

## 5.8 Analysis of Shear Failure Loads Based on Aggregate Size and Aggregate Type

### 5.8.1 All Aggregates

**Table 5-22: Shear failure loads and scaled shear failure loads for all beams**

| ALL AGGREGATES | | | | | | | | |
|---|---|---|---|---|---|---|---|---|
| Coarse Aggregate type | | | Actual Force | | | Shear Force $V_L$ Scaled | | |
| Beam no. | Coarse aggregate type | Coarse aggregate size | 28-day concrete cube strength $f_{cu}$ | Point load P at failure | Shear force at failure $V_L = 0.543 \cdot P$ | Scaled 28-day cube strength $f_{scaled}$ | $P_{scaled} = \frac{P}{\sqrt{f_{cu}}} \cdot \frac{\sqrt{f_{scaled}}}{1}$ | Shear force at failure $V_{L\text{-scaled}} = P_{scaled} \cdot 0{,}543$ |
| | | (mm) | (MPa) | (kN) | (kN) | (MPa) | (kN) | (kN) |
| 1 | tillite | 13.2 | 30.8 | 82 | 44.5 | 30 | 80.9 | 43.9 |
| 2 | quartzite | 13.2 | 32.1 | 83.2 | 45.2 | 30 | 80.4 | 43.7 |
| 3 | dolerite | 13.2 | 30.2 | 87.5 | 47.5 | 30 | 87.2 | 47.4 |
| | | | | | | | | |
| 4 | tillite | 19 | 32.3 | 68.5 | 37.2 | 30 | 66.0 | 35.8 |
| 5 | quartzite | 19 | 34.9 | 76.5 | 41.5 | 30 | 70.9 | 38.5 |
| 6 | dolerite | 19 | 34.5 | 92.8 | 50.4 | 30 | 86.5 | 47.0 |
| | | | | | | | | |
| 7 | tillite | 13.2 | 39.4 | 73.6 | 40.0 | 40 | 74.2 | 40.3 |
| 8 | quartzite | 13.2 | 42.6 | 86.6 | 47.0 | 40 | 83.9 | 45.6 |
| 9 | dolerite | 13.2 | 43.1 | 97.7 | 53.1 | 40 | 94.1 | 51.1 |
| | | | | | | | | |
| 10 | tillite | 19 | 41.2 | 90.1 | 48.9 | 40 | 88.8 | 48.2 |
| 11 | quartzite | 19 | 42.2 | 81.9 | 44.5 | 40 | 79.7 | 43.3 |
| 12 | dolerite | 19 | 39 | 91.0 | 49.4 | 40 | 92.2 | 50.0 |
| | | | | | | | | |
| 13 | tillite | 13.2 | 52.8 | 81.7 | 44.4 | 50 | 79.5 | 43.2 |
| 14 | quartzite | 13.2 | 47.6 | 89.0 | 48.3 | 50 | 91.2 | 49.5 |
| 15 | dolerite | 13.2 | 51.7 | 99.2 | 53.9 | 50 | 97.6 | 53.0 |
| | | | | | | | | |
| 16 | tillite | 19 | 39.4 | 81.4 | 44.2 | 50 | 91.7 | 49.8 |
| 17 | quartzite | 19 | 48.9 | 86.3 | 46.9 | 50 | 87.3 | 47.4 |
| 18 | dolerite | 19 | 48.1 | 83.5 | 45.3 | 50 | 85.1 | 46.2 |

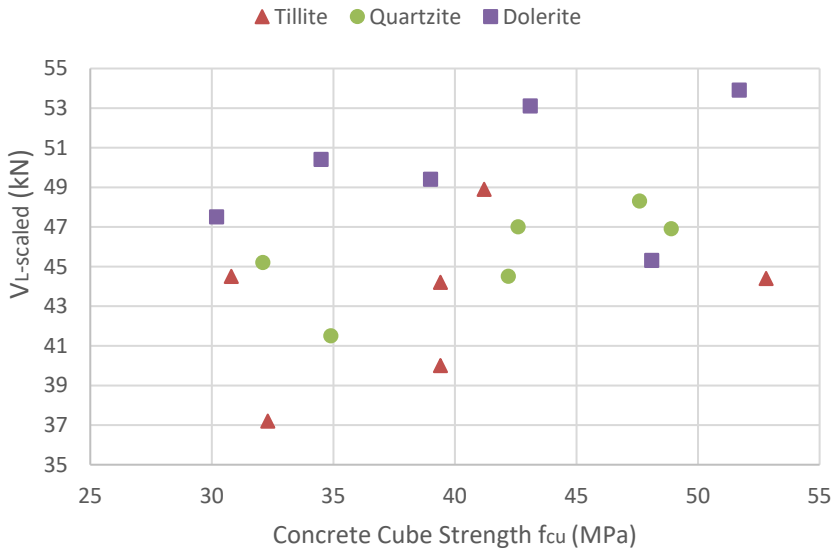


**Figure 5-19: Shear failure load $V_L$ vs concrete cube strength $f_{cu}$ for all beams**

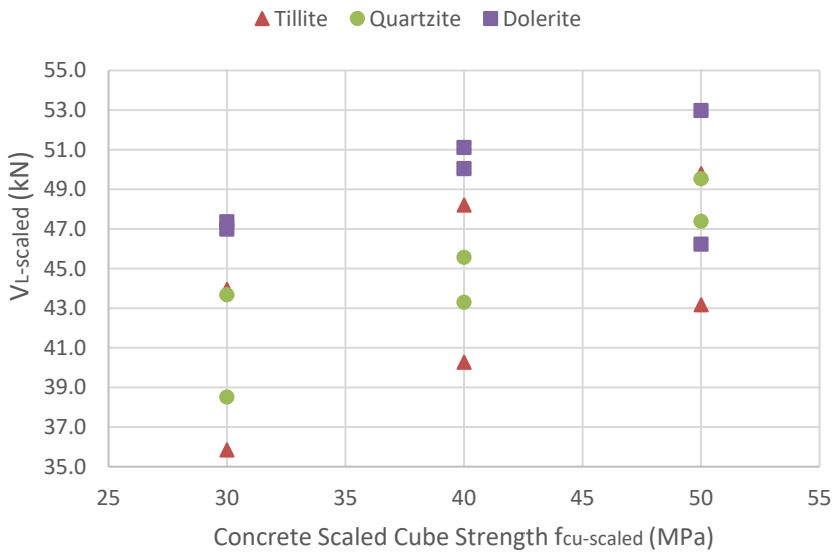


**Figure 5-20: Scaled shear failure load $V_{L\text{-scaled}}$ vs scaled concrete cube strength $f_{cu}$ for all beams**

### 5.8.2 Coarse Aggregate Size (mm) = 13.2 mm

**Table 5-23: Shear failure loads and scaled shear failure loads for beams constructed with 13.2 mm coarse aggregates**

| 13.2 mm max. size continuously graded aggregate | | | | | | | | |
|---|---|---|---|---|---|---|---|---|
| Coarse Aggregate type | | | Actual Force | | | Shear Force $V_L$ Scaled | | |
| Beam no. | Coarse aggregate type | Coarse aggregate size | 28-day concrete cube strength $f_{cu}$ | Point load P at failure | Shear force at failure $V_L = 0.543 \cdot P$ | Scaled 28-day cube strength $f_{scaled}$ | $P_{scaled} = \frac{P}{\sqrt{f_{cu}}} \cdot \frac{\sqrt{f_{scaled}}}{1}$ | Shear force at failure $V_{L\text{-scaled}} = P_{scaled} \cdot 0{,}543$ |
| | | (mm) | (MPa) | (kN) | (kN) | (MPa) | (kN) | (kN) |
| 1 | tillite | 13.2 | 30.8 | 82 | 44.5 | 30 | 80.9 | 43.9 |
| 7 | tillite | 13.2 | 39.4 | 73.6 | 40 | 40 | 74.2 | 40.3 |
| 13 | tillite | 13.2 | 52.8 | 81.7 | 44.4 | 50 | 79.5 | 43.2 |
| | | | | | | | | |
| 2 | quartzite | 13.2 | 32.1 | 83.2 | 45.2 | 30 | 80.4 | 43.7 |
| 8 | quartzite | 13.2 | 42.6 | 86.6 | 47.0 | 40 | 83.9 | 45.6 |
| 14 | quartzite | 13.2 | 47.6 | 89.0 | 48.3 | 50 | 91.2 | 49.5 |
| | | | | | | | | |
| 3 | dolerite | 13.2 | 30.2 | 87.5 | 47.5 | 30 | 87.2 | 47.4 |
| 9 | dolerite | 13.2 | 43.1 | 97.7 | 53.1 | 40 | 94.1 | 51.1 |
| 15 | dolerite | 13.2 | 51.7 | 99.2 | 53.9 | 50 | 97.6 | 53.0 |

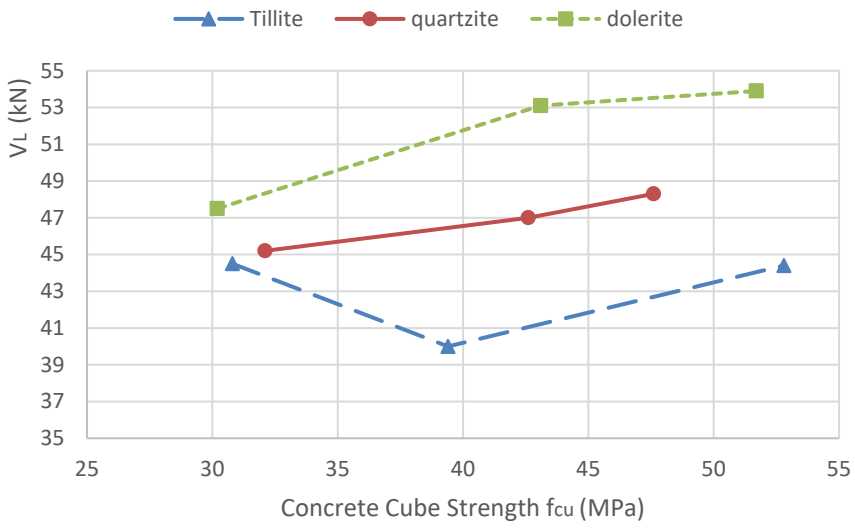


**Figure 5-21: Shear failure load $V_L$ vs concrete cube strength $f_{cu}$ for 13.2 mm coarse aggregate beams**

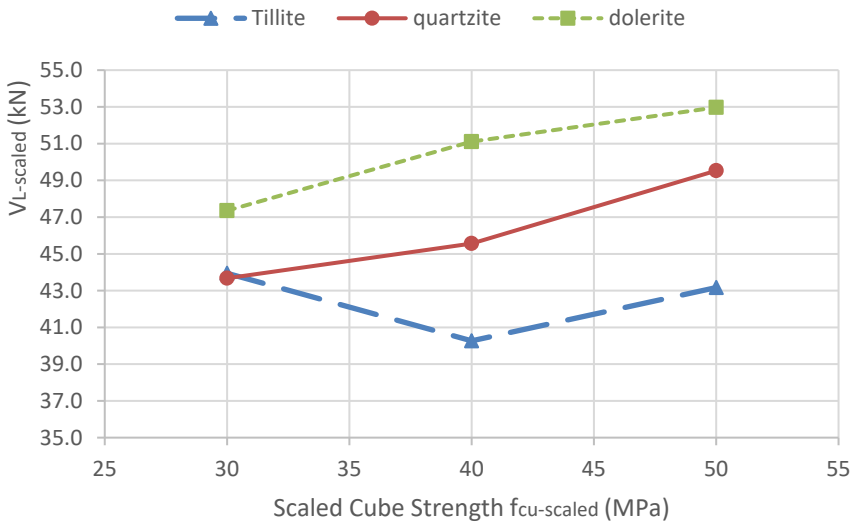


**Figure 5-22: Scaled shear failure load $V_{L\text{-scaled}}$ vs scaled concrete cube strength $f_{cu}$ for 13.2 mm coarse aggregate beams**

### 5.8.3 Coarse Aggregate Size (mm) = 19.0 mm

**Table 5-24: Shear failure loads and scaled shear failure loads for beams constructed with 19 mm coarse aggregates**

| 19 mm max. size continuously graded aggregate | | | | | | | | |
|---|---|---|---|---|---|---|---|---|
| Coarse Aggregate type | | | Actual Force | | | Shear Force $V_L$ Scaled | | |
| Beam no. | Coarse aggregate type | Coarse aggregate size | 28-day concrete cube strength $f_{cu}$ | Point load P at failure | Shear force at failure $V_L$= 0.543·P | Scaled 28-day cube strength $f_{scaled}$ | $P_{scaled} = \frac{P}{\sqrt{f_{cu}}} \cdot \frac{\sqrt{f_{scaled}}}{1}$ | Shear force at failure $V_{L\text{-scaled}} = P_{scaled} \cdot 0{,}543$ |
| | | (mm) | (MPa) | (kN) | (kN) | (MPa) | (kN) | (kN) |
| 4 | tillite | 19 | 32.3 | 68.5 | 37.2 | 30 | 66.0 | 35.8 |
| 10 | tillite | 19 | 41.2 | 90.1 | 48.9 | 40 | 88.8 | 48.2 |
| 16 | tillite | 19 | 39.4 | 81.4 | 44.2 | 50 | 91.7 | 49.8 |
| | | | | | | | | |
| 5 | quartzite | 19 | 34.9 | 76.5 | 41.5 | 30 | 70.9 | 38.5 |
| 11 | quartzite | 19 | 42.2 | 81.9 | 44.5 | 40 | 79.7 | 43.3 |
| 17 | quartzite | 19 | 48.9 | 86.3 | 46.9 | 50 | 87.3 | 47.4 |
| | | | | | | | | |
| 6 | dolerite | 19 | 34.5 | 92.8 | 50.4 | 30 | 86.5 | 47.0 |
| 12 | dolerite | 19 | 39 | 91.0 | 49.4 | 40 | 92.2 | 50.0 |
| 18 | dolerite | 19 | 48.1 | 83.5 | 45.3 | 50 | 85.1 | 46.2 |

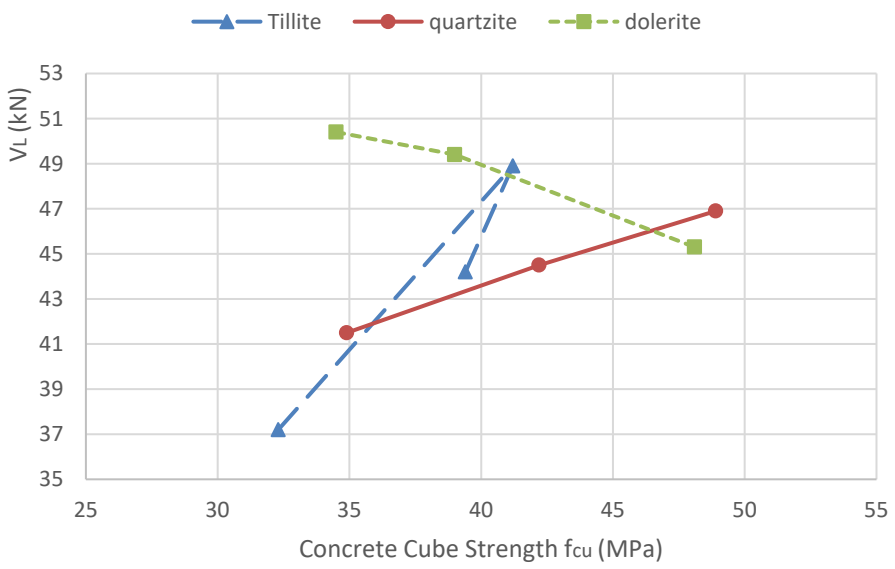


**Figure 5-23: Shear failure load $V_L$ vs concrete cube strength $f_{cu}$ for 19 mm coarse aggregate beams**

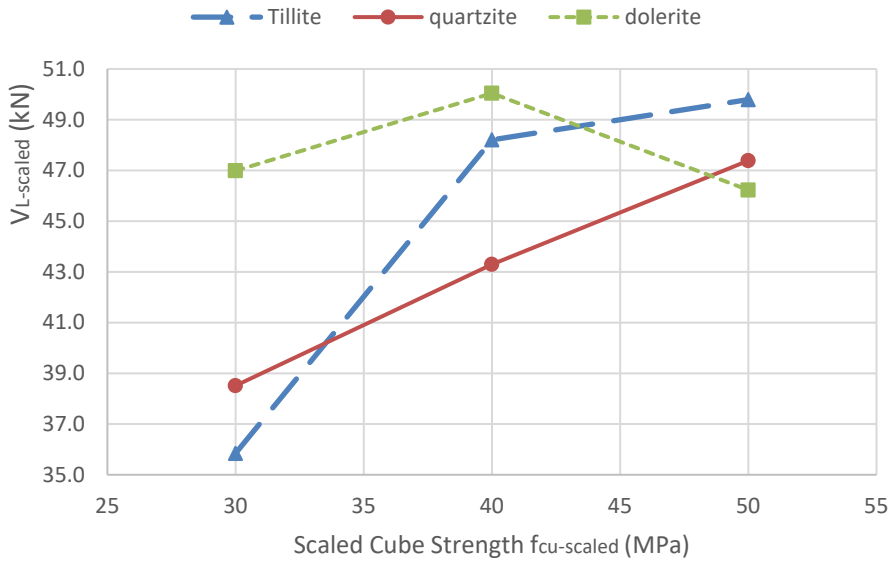


**Figure 5-24: Scaled shear failure load $V_{L\text{-scaled}}$ vs scaled concrete cube strength $f_{cu}$ for 19 mm coarse aggregate beams**

### 5.8.4 Coarse Aggregate Type – Tillite

**Table 5-25: Shear failure loads and scaled shear failure loads for beams constructed with tillite coarse aggregate**

| Tillite | | | | | | | | |
|---|---|---|---|---|---|---|---|---|
| Coarse Aggregate type | | | Actual Force | | | Shear Force $V_L$ Scaled | | |
| Beam no. | Coarse aggregate type | Coarse aggregate size | 28-day concrete cube strength $f_{cu}$ | Point load P at failure | Shear force at failure $V_L = 0.543 \cdot P$ | Scaled 28-day cube strength $f_{scaled}$ | $P_{scaled} = \frac{P}{\sqrt{f_{cu}}} \cdot \frac{\sqrt{f_{scaled}}}{1}$ | Shear force at failure $V_{L\text{-scaled}} = P_{scaled} \cdot 0{,}543$ |
| | | (mm) | (MPa) | (kN) | (kN) | (MPa) | (kN) | (kN) |
| 1 | tillite | 13.2 | 30.8 | 82 | 44.5 | 30 | 80.9 | 43.9 |
| 7 | tillite | 13.2 | 39.4 | 73.6 | 40.0 | 40 | 74.2 | 40.3 |
| 13 | tillite | 13.2 | 52.8 | 81.7 | 44.4 | 50 | 79.5 | 43.2 |
| | | | | | | | | |
| 4 | tillite | 19 | 32.3 | 68.5 | 37.2 | 30 | 66.0 | 35.8 |
| 10 | tillite | 19 | 41.2 | 90.1 | 48.9 | 40 | 88.8 | 48.2 |
| 16 | tillite | 19 | 39.4 | 81.4 | 44.2 | 50 | 91.7 | 49.8 |

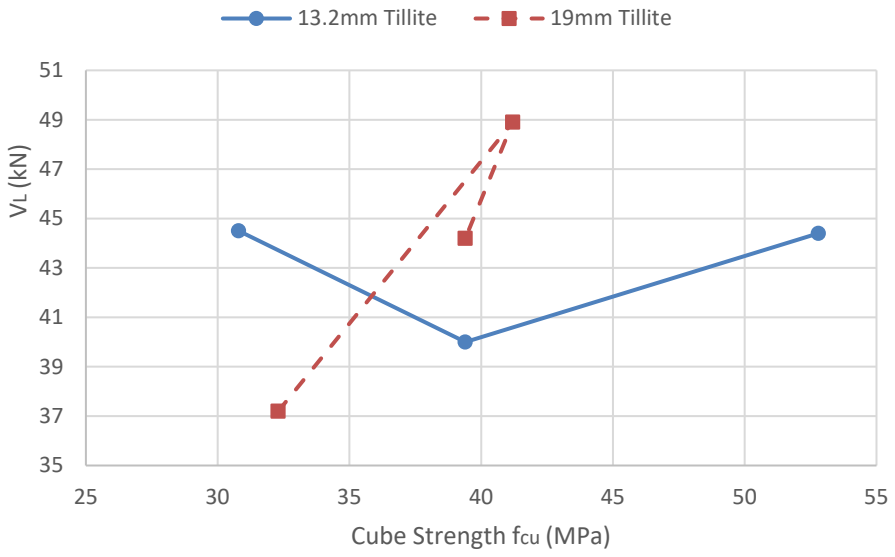


**Figure 5-25: Shear failure load $V_L$ vs concrete cube strength $f_{cu}$ for tillite coarse aggregate beams**

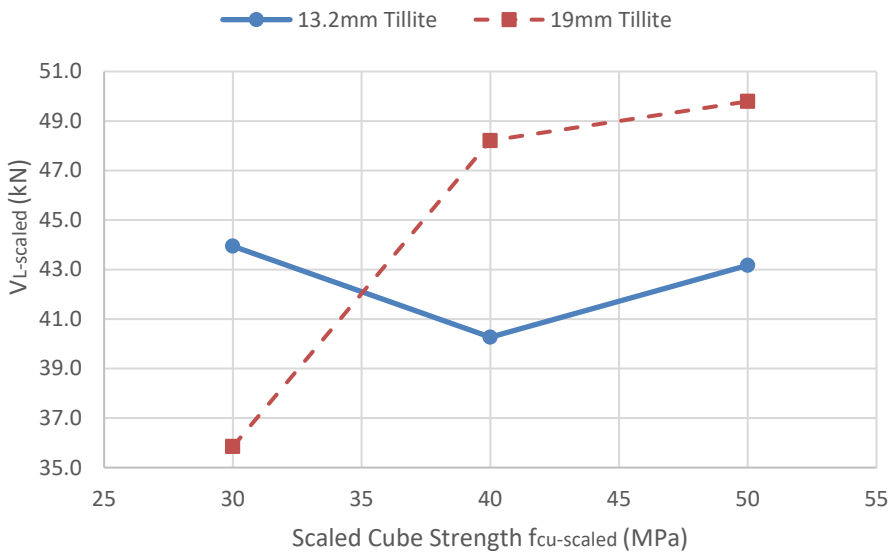


**Figure 5-26: Scaled shear failure load $V_{L\text{-scaled}}$ vs scaled concrete cube strength $f_{cu}$ for tillite coarse aggregate beams**

### 5.8.5 Coarse Aggregate Type – Quartzite

**Table 5-26: Shear failure loads and scaled shear failure loads for beams constructed with quartzite coarse aggregate**

| Quartzite | | | | | | | | |
|---|---|---|---|---|---|---|---|---|
| Coarse Aggregate type | | | Actual Force | | | Shear Force $V_L$ Scaled | | |
| Beam no. | Coarse aggregate type | Coarse aggregate size | 28-day concrete cube strength $f_{cu}$ | Point load P at failure | Shear force at failure $V_L$= 0.543·P | Scaled 28-day cube strength $f_{scaled}$ | $P_{scaled} = \frac{P}{\sqrt{f_{cu}}} \cdot \frac{\sqrt{f_{scaled}}}{1}$ | Shear force at failure $V_{L\text{-scaled}} = P_{scaled} \cdot 0{,}543$ |
| | | (mm) | (MPa) | (kN) | (kN) | (MPa) | (kN) | (kN) |
| 2 | quartzite | 13.2 | 32.1 | 83.2 | 45.2 | 30 | 80.4 | 43.7 |
| 8 | quartzite | 13.2 | 42.6 | 86.6 | 47.0 | 40 | 83.9 | 45.6 |
| 14 | quartzite | 13.2 | 47.6 | 89.0 | 48.3 | 50 | 91.2 | 49.5 |
| | | | | | | | | |
| 5 | quartzite | 19 | 34.9 | 76.5 | 41.5 | 30 | 70.9 | 38.5 |
| 11 | quartzite | 19 | 42.2 | 81.9 | 44.5 | 40 | 79.7 | 43.3 |
| 17 | quartzite | 19 | 48.9 | 86.3 | 46.9 | 50 | 87.3 | 47.4 |

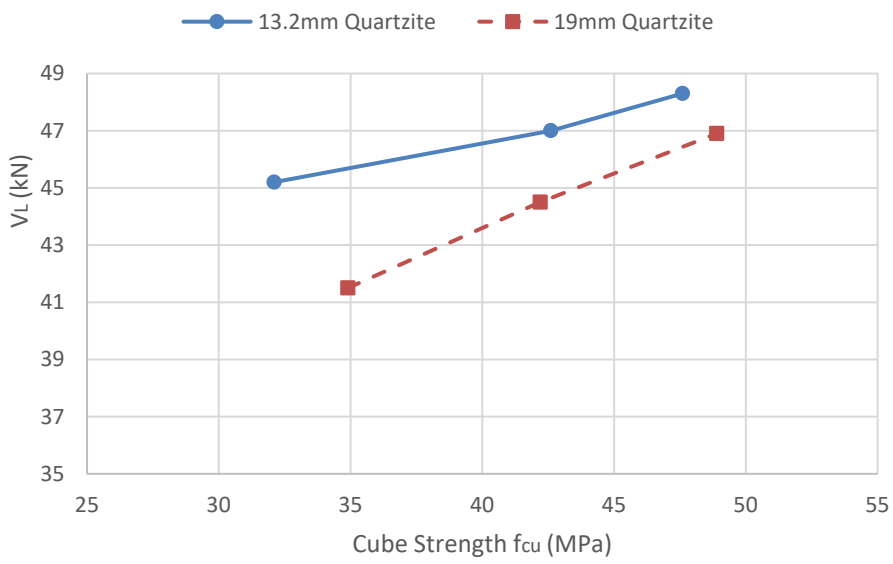


**Figure 5-27: Shear failure load $V_L$ vs concrete cube strength $f_{cu}$ for quartzite coarse aggregate beams**

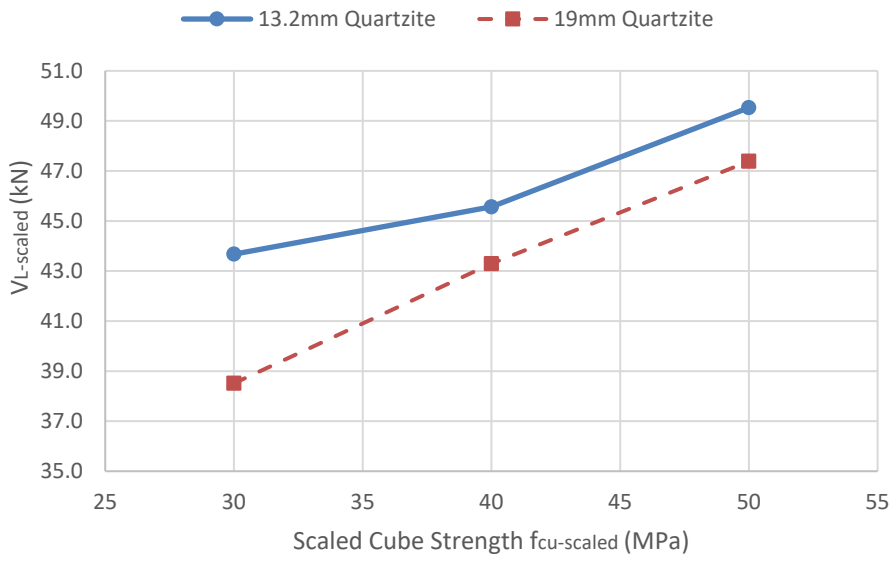


**Figure 5-28: Scaled shear failure load $V_{L\text{-scaled}}$ vs scaled concrete cube strength $f_{cu}$ for quartzite coarse aggregate beams**

### 5.8.6 Coarse Aggregate Type – Dolerite

**Table 5-27: Shear failure loads and scaled shear failure loads for beams constructed with dolerite coarse aggregate**

| Dolerite | | | | | | | | |
|---|---|---|---|---|---|---|---|---|
| Coarse Aggregate type | | | Actual Force | | | Shear Force $V_L$ Scaled | | |
| Beam no. | Coarse aggregate type | Coarse aggregate size | 28-day concrete cube strength $f_{cu}$ | Point load P at failure | Shear force at failure $V_L = 0.543 \cdot P$ | Scaled 28-day cube strength $f_{scaled}$ | $P_{scaled} = \frac{P}{\sqrt{f_{cu}}} \cdot \frac{\sqrt{f_{scaled}}}{1}$ | Shear force at failure $V_{L\text{-scaled}} = P_{scaled} \cdot 0{,}543$ |
| | | (mm) | (MPa) | (kN) | (kN) | (MPa) | (kN) | (kN) |
| 3 | dolerite | 13.2 | 30.2 | 87.5 | 47.5 | 30 | 87.2 | 47.4 |
| 9 | dolerite | 13.2 | 43.1 | 97.7 | 53.1 | 40 | 94.1 | 51.1 |
| 15 | dolerite | 13.2 | 51.7 | 99.2 | 53.9 | 50 | 97.6 | 53.0 |
| | | | | | | | | |
| 6 | dolerite | 19 | 34.5 | 92.8 | 50.4 | 30 | 86.5 | 47.0 |
| 12 | dolerite | 19 | 39 | 91.0 | 49.4 | 40 | 92.2 | 50.0 |
| 18 | dolerite | 19 | 48.1 | 83.5 | 45.3 | 50 | 85.1 | 46.2 |

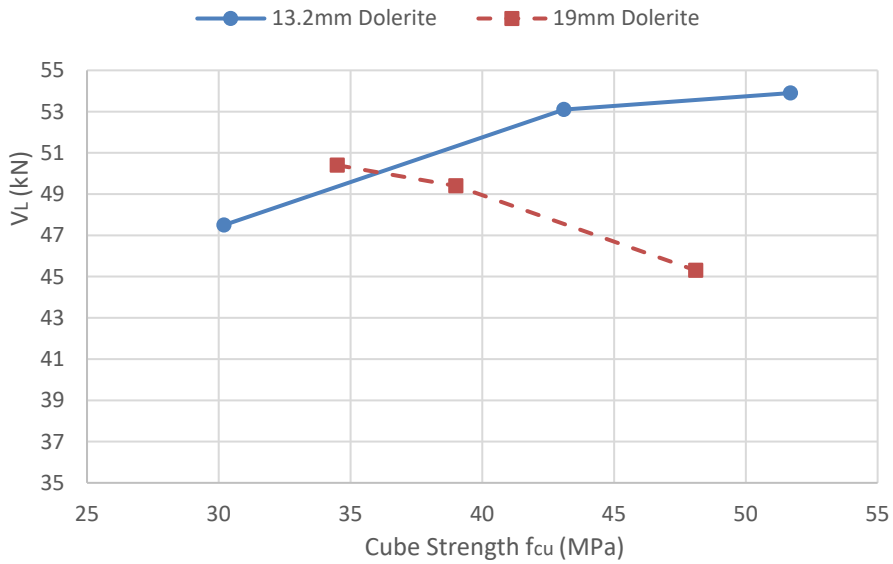


**Figure 5-29: Shear failure load $V_L$ vs concrete cube strength $f_{cu}$ for dolerite coarse aggregate beams**

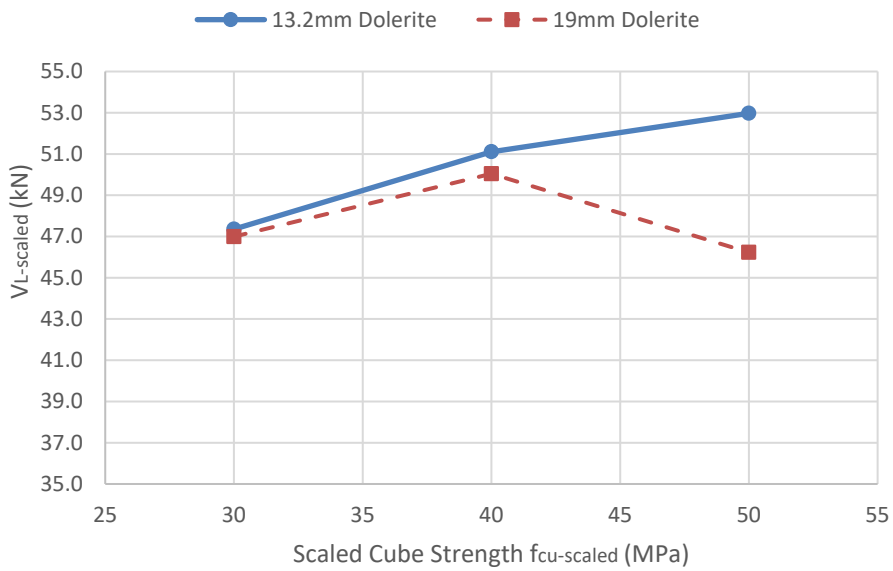


**Figure 5-30: Scaled shear failure load $V_{L\text{-scaled}}$ vs scaled concrete cube strength $f_{cu}$ for dolerite coarse aggregate beams**

## 5.9 Interpretation and Discussion of Results

For the 13.2 mm coarse aggregate it can be inferred from Figure 5-8 that the shear strength of the beam with dolerite aggregate is larger than the shear strength of the beam with quartzite aggregate which in turn is larger than the shear strength of the beam with tillite aggregate. However, from Table 5-12, it is only the difference in shear strength between beams with dolerite aggregate and tilliite aggregate that are statistically significant.

For the 19mm coarse aggregate, the above trend was not as discernible. Figure 5-10 shows that the variation of shear strength with aggregate type was less pronounced for 19mm aggregates, while Table 5-16 shows that the variation in shear strength was statistically insignificant. Therefore it cannot be deduced that the shear strength of beams with 19 mm coarse aggregate differed with aggregate type.

The difference in beam shear strength in beams with different coarse aggregate types may be due to many factors. Differences in mineralogy, homogeneity, particle shape, surface texture, cleavage planes, aggregate crushing value between different coarse aggregates and interfacial transition zone bond strength may give rise to variations in the friction coefficient, smoothness of the shear crack interface, crack width and extent of coarse aggregate fracture. All these factors may, to varying degrees, affect the aggregate interlock strength at the shear crack interface discussed in Section 1.2

The more pronounced variation of beam shear strength with coarse aggregate type for 13.2 mm aggregate as compared to 19.0 mm aggregate can also partly be explained in terms of aggregate interlock at the shear crack interface as discussed in Section 1.2. It can be seen from Figure 1-3 that the protrusion of smaller sized coarse aggregates at the crack interface will be less, thus facilitating easier formation of the shear crack along the surface of the protruding aggregate. Larger coarse aggregate protrusions will be more prone to aggregate fracture and the formation of the shear crack through the fractured aggregate thus reducing aggregate interlock and therefore the shear strength of the beam.

In Figure 5-22 the variation of the shear failure load for the three 13.2 mm coarse aggregate types at 50 MPa concrete is larger than the variation in Figure 5-24 for the three aggregate types and 50 MPa concrete. This lends credence to the argument in the previous paragraph that larger aggregate interlock strength may develop for the smaller coarse aggregate size.

Figure 5-28Figure 3-28 and Figure 5-30 for quartzite and dolerite respectively both show increasing shear strength with increasing concrete strength and smaller coarse aggregate size. On the other hand Figure 5-26 shows the behaviour of tillite to be erratic. Dolerite is a fine grained crystalline igneous rock, quartzite is a metamorphic rock whereas tillite is a non-homogeneous sedimentary rock of glacial origin.

## 5.10 Conclusions from Statistical Analysis

It is concluded from the statistical analysis and discussion of the experimental data that the influence of aggregate type on the shear strength of a reinforced concrete beam without lateral shear reinforcement is statistically significant.

# CHAPTER 6:CONCLUSION, RECOMMENDATIONS AND FUTURE RESEARCH

Based on the literature review it can be concluded that the type and size of coarse aggregate in a reinforced concrete beam without lateral shear reinforcement does influence the shear strength of the beam.

Based on the experimental program and the statistical analysis of the results, for the three aggregate types, and the two aggregate sizes used in the experimental program it can be concluded that the shear strength of a reinforced concrete beam without lateral shear reinforcement,

- is influenced by the coarse aggregate size, and
- is influenced by the type of coarse aggregate for 13.2 mm coarse aggregates.

Since all the beams in this experimental program had a constant cross section, thus eliminating the influence of size effects and other parameters known to influence the shear strength, it is recommended that further research be carried out to determine or clarify:

- The influence of coarse aggregate type on the shear strength of reinforced concrete beams (without transverse shear reinforcement) with deeper and wider cross sections, larger spans and different types of loading.
- The influence or role of fine aggregate type and grading on the shear strength of reinforced concrete beams without transverse shear reinforcement. Since fine aggregate is an integral component of the “cement paste” or “concrete matrix” that the coarse aggregate slides against at the crack interface, it seems reasonable to investigate its influence on shear strength.

# CHAPTER 7:REFERENCES


Addis, B. & Goodman, J., 2009. Chapter 11: Concrete Mix Design. In: G. Owens, ed. *Fulton's Concrete Technology.* 9th ed. Midrand, South Africa: Cement & Concrete Institute, pp. 219-227.

Alexander, M. & Mindess, S., 2005. *Aggregates in concrete.* eBook ed. eBook: Taylor & Francis.

American Concrete Institute (ACI committee 318), 2019. *ACI 318-19 Building code requirement for structural concrete,* Farmington Hills: ACI.

Arezoumandi, M., Drury, J., Volz, J. S. & Khayat, K. H., 2015a. Effect of recycled concrete aggregate replacement level on shear strength of reinforced concrete beams. *ACI Materials Journal,* 112(No. 4, July-August), pp. 559-567.

Arezoumandi, M., Volz, J. S., Ortega, C. A. & Myers, J. J., 2015b. Shear behaviour of high volume fly ash concrete versus conventional concrete: Experimental study. *ASCE Journal of Structural Engineering,* Volume 141(3): B4014006 DOI: 10.1061/(ASCE)ST.1943-541X.0001003.

Bažant, Z. P., 2005. *Scaling of Structural Strength.* 2nd ed. Oxford: Elsevier Butterworth-Heinemann.

Bažant, Z. P. & Planas, J., 1998. *Fracture and size effect in concrete and quasibrittle materials.* Florida: CRC Press.

Bentz, E. C., 2005. Empirical modeling of reinforced concrete shear strength size effects for members without stirrups. *ACI Structural Journal,* 102(2), pp. 232-241.

Bentz, E. C., Vecchio, F. J. & Collins, M. P., 2006. Simplified modified compression field theory for calculating shear strength of reinforced concrete elements. *ACI Structural Journal,* 103(4), pp. 614-624.

Brink, A., Horak, E. & Visser, A., 2003. Imprrovement of aggregate interlock equation for new mechanistic concrete pavement design method. *Journal of the South African Institution of Civil engineering,* 45(2), pp. 2-8.

Campana, S., Ruiz, F. M., Anastasi, A. & Muttoni, A., 2013. Analysis of shear-transfer actions on one-way RC members based on measured cracking pattern and failure kinematics. *Magazine of Concrete Research,* p. 19.

Canadian Standards Association, 2004. *A23.3-04 Design of concrete structures,* Mississauga, Canada: CSA.

CEN, 2004. *BS EN 1992-1-1:2004 : Eurocode 2: Design of concrete structures. Part 1-1 - General rules and rules for buildings,* London: British Standards Institution.

Collins, M. P., Bentz, E. C., Sherwood, E. G. & Xie, L., 2007. An adequate theory for the shear strength of reinforced concrete structures. In: *Morley Symposium on Concrete Plasticity and its Application (23 July 2007).* University of Cambridge: s.n., pp. 75-93.

Emiko, L., Huan, W. T., Thamaraikkannan, V. & Thangayah, T., 2011. Shear transfer in lightweight concrete. *Magaine of Concrete Research,* 63(6), pp. 393-400.

Fenwick, R., 1966. The shear strength of reinforced concrete beams. PhD. University of Canterbury, Christchurch, NewZealand. p. 335.

Gere, J. M. & Goodno, B. J., 2013. *Mechanics of Materials.* 8 SI ed. Stamford, USA: Cengage Learning.

Grieve, G., 2009. Chapter 3: Aggregates for Concrete. In: G. Owens, ed. *Fulton's Concrete Technology.* 9th ed. Midrand, South Africa: Cement & Concrete Institute, pp. 25-61.

Haas, M., 1996. Investigations on shear including the development of a material model for the FE analysis of cracked RC structures. PhD. University of Sheffield.. p. 186.

Hamadi, Y. & Regan, P., 1980. Behaviour in shear of beams with flexural cracks. *Magazine of Concrete Research,* 32(111), pp. 67-78.

Hassan, A. A., Ismail, M. K. & Mayo, J., 2015. Shear behaviour of SCC beams with different coarse-to-fine aggregate ratios and coarse aggregate types. *ASCE Journal of Materials in Civil Engineering,* Volume 27(11): 04015022 DOI: 10.1061/(ASCE)MT.1943-5533.0001276.

International Federation for Structural Concrete (fib), 2013. *fib Model Code for Concrete Structures 2010,* Berlin: Wilhelm Ernst & Sohn.

Joint ASCE-ACI Committee 445 on shear and torsion, 1998 reapproved 2009. ACI 445-R99 (reapproved 2009) Recent approaches to shear design of structural concrete. *ASCE Journal of Structural Engineering,* 124(12), pp. 1375-1415.

Kani, G., 1964. The Riddle of Shear Failure and its Solution. *ACI Journal,* 61(4), pp. 441-468.

Knaack, A. M. & Kurama, Y. C., 2015. Behaviour of reinforced concrete beams with recycled concrete course aggregates. *ASCE Journal of Structural Engineering,* Volume 143(3):B4014009 DOI: 10.1061/(ASCE)ST.1943-541X.0001118.

Kosmatka, S. H., Kerkhoff, B. & Panarese, W. C., 2003. *Design and control of concrete mixtures.* 14th ed. Skokie, Illinois, USA: Portland Cement Association.

Mitchell, D. & Collins, M. P., 1974. Diagonal compression field theory - A rational model for structural concrete in pure torsion. *ACI Journal,* 71(8), pp. 396-408.

Mphonde, A. G., 1988. Aggregate interlock in high strength reinforced concrete beams. *Proceedings of the Institution of Civil Engineers,* Volume 85, pp. 397-413.

Muttoni, A., 1990. Die Anwendbarkeit der Plastizitätstheorie in der Bemessung von Stahlbeton. Dr. sc. techn. Institut für Baustatik und Konstruktion, Eidgenössische Technische Hochschule Zürich (ETH). p. 164.

Muttoni, A. & Ruiz, M. F., 2007. *Shear strength predictions according to the critical shear crack theory and the Swiss code SIA 262 (2003).* [Online] Available at: http://www.researchgate.net/publications/40885070 [Accessed 14 July 2015].

Muttoni, A. & Ruiz, M. F., 2008. Shear Strength of members without transverse reinforcement as function of crititcal shear crack width. *ACI Structural Journal,* 105(March-April 2008), pp. 163-172.

Muttoni, A. & Schwartz, J., 1991. Behaviour of beams and punching in slabs without shear reinforcement. *Proceedings of the IABSE Colloquium,* January, Volume 62, pp. 703-708.

Neville, A., 1995. *Properties of Concrete.* 4th ed. United Kingdom: Longman.

Newman, J., 2003. Chapter 6: Strength and failure of concrete under short-term, cyclic and sustained loading. In: J. Newman & B. Choo, eds. *Advanced Concrete Technology: Concrete Properties.* 1st ed. Great Britain: Butterworth-Heinemann, pp. 6/3-6/36.

Paulay, T. & Loeber, P., 1974. Shear in Reinforced Concrete. In: *American Concrete Institute Special Publication SP-42.* Detroit, MI, USA: American Concrete Institute, p. 1–16..

Presvyri, S. et al., 2019. On the extension of walraven's aggregate interlock model based on laser scanned crack surface. In: *fib Symposium 2019 on Concrete –*

*Innovations in Materials, Design and Structures.* Krakow, Poland, 27-29 May 2019: s.n., pp. 937 - 944.

Raath, B., 2013. Interpretation of test results - what do they mean?. In: Concrete Society of South Africa, ed. *TECON 2013 Specification and Testing of Concrete Seminar.* Durban, 2013. Available at: https://concretesociety.co.za/images/stories/TECON2013/4.Bruce%20Raath.pdf [Accessed 22 Jan 2020 @ 15H26].

Regan, P., 1993. Research on shear? A beneffit to humanity or a waste of time?. *The Strucutrual Engineer,* 71(19), pp. 337-347.

Ritter, W., 1899. The Hennebique construction method (in German, “Die Bauweise Hennebique”). *Schweizerische Bauzeitung,* 33(7), pp. 59-61.

Rodrigues, R. V., 2012. Influence of yielding of flexural reinforcement on shear transfer through cracks. *ICE Magazine of Concrete Research,* 64(9), pp. 751-765.

Roskos, C., White, T. & Michael, B., 2015. Structural performance of self-cementatious fly ash concretes with glass aggregates. *ASCE Journal of structural engineering,* Volume 141(3): B4014010 DOI:10.1061/(ASCE)ST.1943-541X.0001143.

Ruiz, F. M., Muttoni, A. & Sagaseta, J., 2015. Shear Strength of concrete members without transverse reinforcement: A mechanical approach to consistently account for size and strain effects. *Engineering Structures,* Volume 99, pp. 360-372.

Sagaseta, J. & Vollum, R. L., 2011. Influence of aggregate fracture on shear transfer through cracks in reinforced concrete. *ICE Magazine of Concrete Research,* 63(2), pp. 119-137.

Savaris, G. & Pinto, R., 2017. Influence of coarse aggregate on shear resistance of self-consolidating concrete beams. *Ibracon Structures and Materials Journal,* 10(1), pp. 30-52.

Schweizerische Normen-Vereinigung (SNV) (Swiss Association for Standardization), 2013 - corrigenda 2017. *SIA 262:2013 Bauwesen Betonbau (Concrete Structures),* Zurich: Schweizerischer Ingenieur- und Architektenvere (SIA) (Swiss Society of Engineers and Architects).

Sherwood, E. G., Bentz, E. C. & Collins, M. P., 2007. Effect of aggregate size on beam-shear strength of thick slabs. *ACI Structural Journal,* 104(2), pp. 180-190.

SIA, 2003. *Code 262 for Concrete Structures,* Zurich: Swiss Society of Engineers and Architects.

Singh, B. & Chintakindi, S., 2013. An appraisal of dowel action in reinforced concrete beams. *ICE Structures and Buildings,* 166(SB5), pp. 257-267.

Sneed, L. H. & Ramirez, J. A., 2014. Influence of cracking on behaviour and shear strength of reinforced concrete beams. *ACI Structural Jounal,* 111(1), pp. 157-166.

South African National Standard, 2000. *SANS 10100-1:2006 The structural use of concrete. Part 1: Design,* Pretoria: SABS.

South African National Standard, 2006. *SANS 5861-3:2006 Concrete tests. Part 3: Making and curing of test specimens,* Pretoria: SABS.

South African National Standard, 2006. *SANS 5863 : 2006 Concrete tests - Compressive strength of hardened concrete,* Pretoria: SABS.

Talbot, A. N., 1909. *University of Illinois Bulletin. Engineering Experiment Station. Bulletin no. 29,* 6(2), pp. 1-85.

Taylor, H., 1974. The fundamental behaviour of reinforced concrete beams in bending and shear. In: ACI, ed. *Shear in Reinforced Concrete. SP-42..* Detroit, USA: American Concrete Institute, pp. 43-77.

Taylor, R. & Brewer, R., 1963. The effect of the type of aggregate on the diagonal cracking of reinforced concrete beams. *Magazine of Concrete Research,* 15(44), pp. 87-92.

Vecchio, F. J. & Collins, M. P., 1986. The modified compression-field theory for reinforced concrete elements subjected to shear. *ACI Journal,* Volume March-April 1986, pp. 219-231.

Walraven, J. C., 1980. *Aggregate interlock: a theoretical and experimental analysis. PhD. Delft University.*

Walraven, J. & Reinhardt, H., 1981. Theory and experiments on the mechanical behaviour of cracks in plain and reinforced concrete subjected to shear loading. *Heron,* 26(1A), p. 68.

Walraven, J., Vos, E. & Reinhardt, H., 1979. Experiments on shear transfer in cracks in concrete. Part 1. Description of results.. *Delft University of Technology. Stevin Laboratory,* Volume Report 5-79-3, p. 98.

Yang, K.-H. & Ashour, A. F., 2015. Modification factor for shear capacity of lightweigth concrete beams. *ACI Structural Journal,* 112(4), pp. 485-492.

Yang, K. H., Sim, J. I., Choi, B. J. & Lee, E. T., 2011. Effect of aggregate size on shear behaviour of lightweight concrete continuous slender beams. *ACI Materials Journal,* 108(5), pp. 501-509.

Zhang, T., Visintin, P. & Oehlers, D. J., 2015. Shear strength of RC beams with steel stirrups. *ASCE Journal of Structural Engineering,* 04015135(04015135), pp. 1-18.